How to describe and measure spatial configurations and the role of clustering in perceived numerosity

Thesis submitted in accordance with the requirements of the University of Liverpool for the degree of Doctor in Philosophy

by

Martin Guest

Supervisors

Dr Michele Zito

Dr Marco Bertamini

Date: 10th October 2023

Acknowledgements

I would like to thank both my supervisors Dr Michele Zito and Dr Marco Bertamini, for their patience supervising me for the last 8 years. I would also like to thank the Psychology dept. for helping me fund the PhD. I would also like to thank all the members of the visual perception team, that from day one have always seen and treated me as an important part of the team

I dedicate this thesis to my beautiful mum, who I miss every day.

Contents

Abstract

This thesis is concerned with the effect of the geometric distribution of dots, on the numerosity bias. The stimuli most commonly used in numerosity perception are dot patterns, thus we employ a branch of discrete mathematics called graph theory as a way of extracting properties of the dot patterns, that conventional methods in perception cannot capture.

In the 1st research chapter a between participants 2IFC learning task was used, to see if either numerosity of density could be employed to learn a rule. This was part of a joint study, but what is presented here is only the work I conducted. Half the participants were reinforced with low cardinality, the other half high numerosity. Critical trials used clustering as a basis for a density or numerosity strategy, interestingly both strategies would predict opposite results. An independent t test $t(47)=6.370$, $p<0.001$, Cohen's $D=0.92$, showed a significant bias for group membership, and numerosity as the main strategy, hence confirmation of numerosity as a salient dimension in perception.

The 2nd research chapter, presents a series of novel experiments involving the solitaire illusion (SI) and its larger variants, developed exclusively in this work. It was found that when separated, the illusion is sensitive to density. The illusion also survived horizontal displacement at high density in the separate condition. However, this was not seen in the low-density condition. In contrast, during enclosure the illusion remained regardless of cardinality and density. Thus, the mechanisms used for the separate and enclosure are fundamentally different, the illusion needs only enclosure.

The 3rd research chapter, is the first theoretical section where there is an extensive introduction to graph theory. Ten different graph indices were compared to each other and a classical psychometric method of numerosity called the occupancy model. Comparison was done using correlations. It was found, by using the maximum standard for each index, the correlation dataset could be drastically reduced. A PCA was performed and found two groups of strongly

correlated indices were found. One sensitive to clustering, and another sensitive to how information spreads on graphs.

In the final research chapter, we analyse the results of the 4th experiment in the 2nd research using graph theory. Again, this analysis was unique as graph theory allowed the modelling of the SI, as two interacting patterns, on a host graph. We found that the separate\enclosure manipulation has the most dramatic effect on the local clustering coefficient. When split, the inner is the more clustered pattern. However, when modelled on a host graph, where the two patterns can interact, in was the outer pattern that became the more clustered. This result was robust, regardless of cardinality (large variants), and level of random sampling (continuity). I suggest that the SI is also an illusion of clustering, except it is an illusion of clustering between two interacting patterns.

Chapter 1 Introduction

1.1 Introduction

This thesis is about the perception of numerosity, the type of stimuli commonly used in its study and its computational aspects. Numerosity can be described as the non-symbolic perception of number, and I will be using a branch of discrete mathematics called graph theory to study the dot patterns so commonly used as stimuli in this field. I will demonstrate that this approach is different to the current methods employed to model numerosity. For instance convex hull is extensively used in dot density calculations (De Marco & Cutini, 2020; Gebuis & Reynvoet, 2011), the centre of mass has been utilized for predicting dot saliency (Paul et al., 2017) and the occupancy model computes the total area of overlapping regions of influence of occupancy radius o_r (Allik & Tuulmets, 1991). All of these methods are continuous in nature, that is to say that the result computed, can take any value within a given range. In this work, I will use discrete structures called graphs to model dot patterns, and my aim is two-fold. Firstly, this approach lends itself more naturally to the study of numerosity as the dot stimuli used are themselves discrete. Secondly, there exists many different graph indices, hence many different properties of dot patterns may be computed.

1.1.1 Numerosity

It is easy to see a natural relationship between numerosity, mathematics and symbolic numbers. However, this can be misleading. It has been shown that there exists a "number sense" in humans, that is independent of symbols and characterized by a set of underlying properties (Dehaene, 2011). For arrays of four items or lower human observers can process each object as an individual element, and can precisely and rapidly compute its cardinality without the need to count. This ability is called subitizing (Kaufman et al., 1949; Trick & Pylyshyn, 1994). For higher cardinalities, and when counting is not available, humans are able to quickly estimate and compare sets, for the purpose of gauging which has more elements. The latter process is subject

to Weber's law, that is number pairs (4,8) and (8,16) are equivalent in both ratio and complexity for comparison tasks, because of the so-called size effect. However, although pairs (6,8) and (10,12) have the same difference of two, they are not equivalent in complexity, because of the so-called distance effect. The pair (10,12) will be more difficult to compare then the pair (6,8).

Numbers have also special properties in terms of location in space. The number line proceeds naturally from left to right, not because this is an arbitrary choice, but because of a general lateralisation effect. This has been shown in many studies. An interesting paradigm is known as SNARC (Spatial-Numerical Association of Response Codes) (Dehaene et al., 1993). Smaller numbers are identified more quickly on the left, while larger numbers are identified more quickly on the right, consistent with a left to right ordering or mental number line.

The mechanisms that support these processes are not well known, and how they interact is subject to on-going research. However, it is interesting to note that similar phenomena have been found in the animal kingdom, hinting at a shared and ancient system underpinning numerical cognition. For instance 3 day old chickens have demonstrated something similar to the SNARC effect (Rugani et al., 2015). Subitization has been found in guppies (Agrillo et al., 2012) and mosquitofish have demonstrated the ability to discriminate between cardinalities in order to join the bigger social group (Agrillo et al., 2008).

1.1.2 Aims of Thesis

There are four research chapters, the first three are based on three different published papers, thus each have their own introduction sections, that may have some overlap. However, the theme throughout each chapter, will be based on human data collected from comparison tasks. When the term numerosity is employed, it can be taken to refer to numerosity perception. The term cardinality will refer to the number of elements contained in a set, or to an independent variable, when the number contained in a dot pattern is varied. When it is used as the latter, it will be made clear to the reader. The datasets used in this thesis, will be responses

from collected from human studies, and also random dot patterns. I will use the terms dot pattern and dot configuration interchangeably.

It has been shown that there are irrelevant features that can bias numerosity perception. For instance symmetry (Apthorp & Bell, 2015; Maldonado Moscoso et al., 2023), density (Dakin et al., 2011), connectedness (Anobile et al., 2017; He et al., 2009; Kirjakovski & Matsumoto, 2016) and the geometric distribution of dots (Frith & Frith, 1972; Ginsburg, 1980), see Figure 2.1. The latter are two examples of illusions that use the placement of dots to bias numerosity perception. The first is the regular-random illusion RRI (Ginsburg, 1980), which demonstrated that randomly placed dots are perceived as less numerous then a pattern of dots with uniform spacing, even though both patterns have the same number of dots. The second illusion of numerosity is the solitaire illusion SI (Frith & Frith, 1972). In this illusion, there is a striking impression, that when one dot pattern encloses another, the pattern enclosed is perceived as the more numerous. Hence this is the first aim of this thesis, a full investigation into how and why dot placement can bias numerosity.

The methods employed, in this thesis, is heavily reliant on graph theory, and to a lesser extent machine learning; a PCA analysis is employed in chapter 4. I aim to show that the former approach is novel and will benefit researchers in the field. Graph theory, at its most basic level is concerned with connections between elements, and although the concept of connectedness has been studied in numerosity, in terms of actual lines connecting dots (He et al., 2009, 2009), and Kaniza-type illusionary contours (Kirjakovski & Matsumoto, 2016). I will show that these approaches are fundamentally different to the methods employed in this thesis. For instance, only a subset of dots will be connected and only in pairs, using either method. In contrast graph indices are applied to all dots uniformly in a configuration. In addition, after reading chapter 4, you the reader, will see that the only indices that can be computed, using traditional connectedness approaches, is the number of connected components. Again, in contrast many indices can be computed on fully defined graphs.

Also, when investigating dot placement, there is a problem with using convex hull and density calculations. This is because there is limited information one can extract from just the hull and the associated cardinality of the dot configuration. As an example, convex hull only uses a subset of dots from a dot configuration, this is the set that forms the hull. Density calculations tend to use some form of hull, divided into the cardinality of the configuration. Hence, an unlimited number of dot configurations will give similar results when computing either property. This is because there is little information extracted on the geometric distribution of the dots within the hull, from either of these methods.

This leads to the second aim of the thesis, that is to demonstrate the advantages of using graph theory to study dot configurations. Many different indices can be employed when a dot pattern is defined as a graph, hence many different properties, of the underlying dot pattern can be computed. This also has an added benefit of controlling for different properties in experiments, such as groupings or clustering, other than cardinality and convex hull.

As the placement of dots change, in any dot configuration, there will be a corresponding change in the underlying patterns properties. As neighbouring dots either come closer together, or are pushed further apart, clustering, at both a dot level, and at a pattern level will be affected. Hence, the reader will find clustering will be a prominent feature through this thesis. This was not the purpose at the start of this work, moreover it emerged naturally as the predominant effect, by its unusual effectiveness to describe different phenomena studied.

2. Definitions Used in Thesis

Chapter 4 explains graph theory extensively. However, I believe it to be beneficial to define the important terms and concepts used here, that will be important in the rest of the thesis.

1. 2.1 Graph theory

Graph theory is a branch of mathematics that is concerned with objects, called either nodes, or vertices and the binary relations that exist between them, called edges. The notation for a graph G is typically $G(V, E)$, where V is the set of vertices\nodes, and E the set of all edges. As an approach, graph theory is flexible for instance it can be used to model friendships on a social network. In this example the nodes are people and the edges represent whether any two people are friends. In addition, the edges represent something non-physical, whether or not a friendship exists between any two people. However, edges can also represent physical connections such bonds between atoms within a molecule, or routing problems to avoid road traffic jams.

Its discovery is a classic example of its flexibility in practise. In 1736, the great mathematician Leonard Euler (1707 – 1783), considered the seven bridges of Konigsberg that connect 4 different land masses, Figure 1.1a.

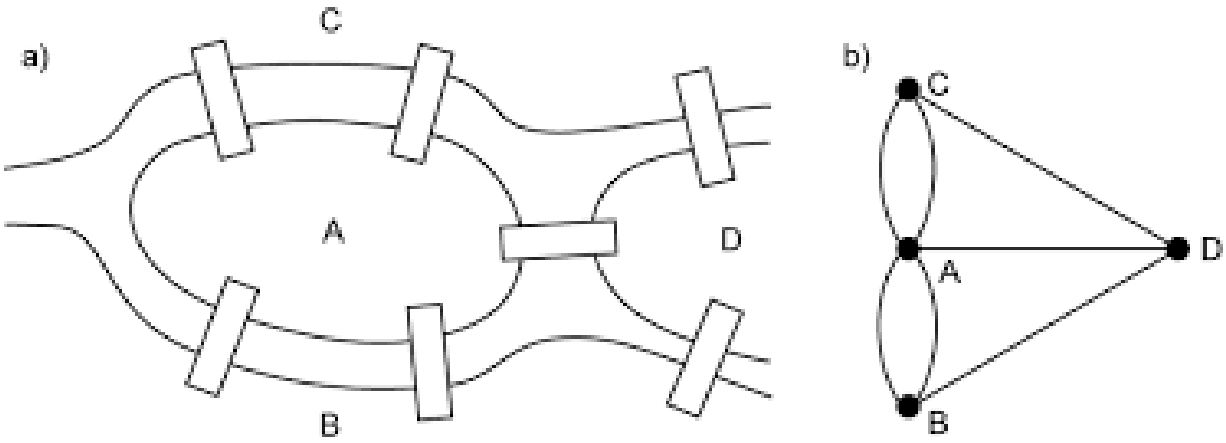

Figure 1.1: A schematic of the bridges of Konigsberg (a), and its representation as a graph on the right (b). Here the land masses are nodes and the bridges are represented as edges on a graph.

Euler asked whether it would be possible to walk across all seven bridges once, and finish on the same land mass where one started, now called a Eulerian circuit in his honour. He also considered a simpler problem, whether it was possible to walk across all seven bridges just once, without the constraint of finishing on the same land mass one started, this is now called a Eulerian path.

In tackling this conundrum, Euler was able to represent the problem more abstractly Figure 1.1b. He let the land masses be the nodes, and the bridges connecting land masses be the edges. Euler realised that, except at the start and endpoints of the walk. When one enters a land mass by a bridge, one has to leave the land mass by another bridge. Thus, the connections or bridges each land mass has, would need to be an even number. In modern terms we call this the degree of each node, see section 4.1.2. We can see clearly from Figure 1.1b, that each node or land mass has an odd number of edges\bridges. Therefore, Euler was able to conclude that it is immaterial as which land mass one starts, there exists no Eulerian circuit or path to the Konigsberg bridges problem. This type of analysis marks the beginning of graph theory.

1.2.2 Random Geometric Graphs

Random geometric graphs, are a type of graph that is concerned with random sets of point configurations (Penrose, 2003). Accompanying such graphs is a connectivity distance d, which in 2D configurations, is the Euclidean distance between two points. The notation for this type of graph is $G_d(V, E)$, where the meaning of V and E is the same as a graph described in section 1.2.1. It is the parameter d that determines if any two nodes will be connected by an edge. If we let d_{ij} be the distance between two nodes v_i and v_j, and $d_{ij} \leq d$ is a true statement, then an edge exists between v_i and v_j.

The connectivity distance is an important concept in this thesis, I will show that there is a relationship between the connectivity distance of random geometric graphs, and the occupancy radius of the occupancy model (Allïk & Tuulmets, 1991), see section 4.1.3. Also, as this investigation is about the effect of the geometric distribution of dots, on numerosity perception, the connectivity distance gives graphs the geometric component needed in order to study this phenomenon. This is not normally the case with graphs, we can see from Figure 1.1b, we are free to draw the graph of the Konigsberg problem anyway the reader pleases, the important properties are the numbers of nodes, and the edges connecting them.

1.3 Summary of Research Chapters

The research chapters can be split into two different approaches, experimental and theoretical. The experimental chapters are chapters 2 and chapter 3, and are based on data collected from human studies. The theoretical chapters are 4 and 5, where graph theory is used, extensively. Chapter 5 uses data from experiment 4, chapter 3 for a novel interpretation of the results.

1.3.1 Chapter 2

This is the first experimental chapter, and is based on a published joint study that compared human and animal data (Bertamini et al., 2018). However, the chapter in this thesis presents only the human data, and nothing from the animal study. The motivation for this chapter came from role of numerosity, as a salient dimension in human perception.

I used a between-participants 2IFC learning task. Given a choice between two dot patterns of 20 and 40 dots, one group of participants was trained to select the 20-dot pattern, the second group was trained to select the 40-dot pattern, this was achieved by a giving a correct response. After achieving a threshold value, intermingled were critical trials. In these trails two patterns, both of cardinality 30 were used. The only difference between the two critical patterns, was that one had a minimum spacing of 5 dot radii between a dot and any of its neighbours. The second critical pattern had minimum spacing of 2 radii, that is dots could not overlap. If numerosity was the strategy employed in the training phase, then group 20 should pick the 2r pattern, and the group 40 should choose the 5r pattern. This is a direct consequence of the regular random illusion. However, density was also a valid strategy, as minimum spacing between the 40-dot pattern and the 2r critical trial pattern were similar. Likewise, the 20-dot pattern and the 5r critical trials had similar minimum spacing. Thus, a density strategy would produce the opposite effect.

A t-test showed conclusively that the predominant strategy was cardinality. Some participants mentioned the work "density", in a post debrief when asked which strategy was employed. However, this did not correlate with the response data. I believe that density was used and an alternative word for cardinality, that is there were more or less dots packed into a given space. I therefore postulate that numerosity is a salient dimension in human perception.

1.3.2 Chapter 3

This chapter is based on the following published paper (Bertamini et al., 2022). What I present is my own work. The motivation behind, this chapter was that the occupancy model predicts the opposite outcome, to the observed bias seen in the solitaire illusion SI (Agrillo et al., 2016; Frith & Frith, 1972). The results of this chapter are split over 4 experiments. All four experiments used the solitaire illusion SI, and a linear version we called BAR.

Frith & Frith (1972), postulate that the bias seen in SI was driven by the continuity of an enclosed pattern, called the inner pattern in this thesis, as opposed to the well-ordered groupings of the enclosing pattern, referred to as outer in the thesis.

I tested this assertion by first splitting (horizontal displacement) the illusion into its constituent parts (inner, outer), and also increasing the size of the SI into larger variants. This approach is experimentally novel, and has never been done before by any other researcher. It also allowed to test the hypothesis that is the continuity of the inner pattern, and high ordered sub-units of the outer pattern (Frith & Frith, 1972), drive the illusion.

In the first experiment, the illusion persisted in both the enclosed and the split condition. This showed that not only does the illusion survive being split, but it also proved that the large variants are also valid solitaire illusions. Binomial tests showed the bias towards the inner was strongly significant regardless of displacement.

The second experiment was a repeat of the first experiment, with the exception that a concave hull was drawn around each of the inner and outer shapes. The reasoning behind this, was to emphasize the greater area that outer extends into, compared to the inner. A concave hull

was used, as a convex hull would have entered the space occupied by the other shape when in the enclosed condition. The illusion remained regardless of the concave hull. A binomial test again showed a strongly significant bias towards the inner in both the enclosure and split condition. Hence the larger area of the outer, does not affect the SI.

The third experiment was a repeat of the first experiment, except both the inner and outer shapes were randomly sampled down to 50% of the original configuration. This directly tested the assumption of the Frith & Frith (1972), that it was the continuity of the inner that drove it to be perceived as the more numerous. In the enclosure condition, the illusion remained strong. However, in the split condition the bias toward the inner was much reduced. A binomial analysis showed a strongly significant bias towards the inner pattern. This was not the in case in the split condition, where the binomial test was only just significant.

The fourth experiment was repeat of the first experiment except both the inner and outer were randomly sampled down to 10% of the original condition. I also had to use larger variants of the SI and BAR to keep the cardinality of each pattern out of the subitizing range. The illusion was slightly reduced, but still strong in the enclosed position. In the split condition the illusion was not present. This was backed up by a binomial test, which showed a strongly significant bias towards the inner in the enclosed position, and an effect of no better than chance in the split condition.

Due to the independent and dependent variables all being either binary or categorical, I decided to implement a general mixed linear model. I used analysis of deviance with a type III (Wald) test because the type 3 Wald test allows you to assess the significance of individual independent variables in the presence of other variables in the model. This is particularly useful when you have multiple predictors, as we did split\enclosure, colour pair and cardinality. Also, this type of analysis helps to determine which variables are contributing significantly to the model's explanatory power. It was sensitive enough to show that there was a statistically significant effect in experiment 4, from cardinality. That is the bias for the inner increased with

increasing the cardinality of both illusions (SI, BAR). The reason for this is difficult to explain, however this could lay the foundation for future work.

1.3.3 Chapter 4

This chapter is based on the published work, (Guest et al., 2022), and what I present is my own work. In this chapter I introduce graph theory and investigate the occupancy model further by comparing it to 10 different graph indices. The datasets used where 1000 dot patterns for the following cardinalities $n = (22, 28, 34, 40)$. First, I state the relationship between the occupancy radius o_r of the occupancy model, and the connectivity distance d; $2o_r = d$. This relationship is important, as it enables the occupancy model to be directly compared with RGG analysis.

Secondly a full correlational analysis between indices was conducted, across the full range of d. The resulting datasets were huge in dimension, however the use of discrete heatmaps aided in extracting persistent groupings of highly correlated indices. Persistent meaning, that the correlation lasted over a wide range of d. Two such groupings stood out, which I named the cluster and spread group, as one group seemed to contain indices sensitive to clustering, the other to how information can spread on network.

However, most graph indices have threshold values, and some are only computable over a small range of d (connected components). The effect of this was at many values of d, data from these indices was pathologically distributed (non-normal), and thus gave artificially high correlation values, with other similarly pathologically distributed indices, see Figure 4.11.

As a way of attempting to reduce the complexity of the datasets, and avoid pathological distributions, we used for each index m the value of d that gave the maximum standard deviation for each index, at each cardinality $\sigma_m(n, d)$. The correlational analysis was then repeated on the resulting datasets, were the two groupings of strongly clustered was displayed on the same heat map. This result was seen regardless of what cardinality was used.

I followed this up with a PCA analysis on datasets $\sigma_m(n, d)$, and PCA confirmed the correlational analysis, in that it found two components. The members of which matched the cluster and spread groups of the correlational analysis.

I believe this work is useful to researchers in the field. Occupancy is computationally difficult to compute. However, the results from the analysis, in this work, can allow researchers to swap OC for more computational lightweight alternatives. The reduction in the dimensions of the data, from using only $\sigma_m(n, d)$, can also serve as a guide on what value of d is most sensitive to variation for any given indices

1.3.4 Chapter 5

This is the final research chapter, and in it I apply graph theory to the SI as a way of modelling interaction between the outer and inner pattern, while in the enclosed condition. The experiments of chapter 3 clearly show that enclosure is vital for the illusion, and the processes involved in comparing numerosity are different for the split condition. For instance, in the split condition, density has a significant effect on numerosity bias, this is not seen in the enclosure condition. Thus, something happens during enclosure to drive the illusion. I could not find, in the literature, any instance where an attempt was made to model the interaction between the inner and outer shapes, during enclosure.

Graph theory, is built on binary relations between vertices\nodes. Therefore, modelling for interaction between the inner and outer shapes during enclosure, is a straight-forward process. I allow edges to exist between dots regardless of whether they a member of the inner or outer shape. The only criteria used is the criteria of an RGG, that is the Euclidean distance between a dot and its neighbour. Also, certain graph indices can be computed down to node level, for instance total degree, eigenvector centrality and local clustering. Hence, all three of these of these indices can be computed then partitioned into inner\outer while interaction is or is not present.

It was found that interaction, on the original SI, has a reversal effect on clustering, when compared to no interaction. That is to say, treated as separate shapes the inner is always the most clustered pattern. This was unintuitive, because of the groupings of outer pattern. However, when interaction was allowed, the reversal was true and the outer was the most clustered pattern. This reversal from interaction, was not seen with indices total degree and eigenvector vector centrality.

This was repeated on the data from experiment 4 chapter 3, and the same reversal in clustering was seen when interaction between shapes was allowed. I speculate that the solitaire illusion is also an illusion of clustering, but an illusion of two interacting patterns, were the pattern enclosed is perceived as the least clustered, and hence the more numerous.

2 The effect of clustering on perceived quantity

2.1 Introduction

Perception of numerosity is affected by a number of biases in relation to visual properties of the image. In particular, there are known effects of the size of the elements (Ginsburg & Nicholls, 1988; Hurewitz et al., 2006; Tokita & Ishiguchi, 2010), the regularity of the pattern (Frith & Frith, 1972) the spacing of elements (Ginsburg, 1976, 1991), and the area of the configuration (Dakin et al., 2011; Hurewitz et al., 2006; Tokita & Ishiguchi, 2010).

2.1.1 Density

Density affects perceived numerosity, and density can be manipulated in terms of inter-stimulus distance. In comparative studies an explanation for density effects comes from optimal foraging models. Uller et al., (2013), presented 10-month old infants with sets of edible items (cookies), one densely arranged and the other sparsely arranged, infants chose the denser set. Stevens et al., (2007) tested cotton-top tamarins (Saguinus oedipus) and marmosets (Callithrix jacchus). They confirmed a preference for densely arranged items relative to the same amount of food sparsely arranged for cotton-top tamarins.

Parrish et al., (2017) studied the density bias in capuchin monkeys (Cebus apella) and rhesus monkeys (Macaca mulatta). There was a density bias in capuchin monkeys and to a lesser extent in rhesus monkeys. Interestingly, Parrish et al. (2017) analyzed how this density bias was related to an illusion of numerosity known as the Solitaire illusion (Frith & Frith, 1972). They did not find evidence for a link.

The name of the Solitaire illusion derives from the board game "Peg Solitaire", and the configuration is shown in Figure 2.1. Frith & Frith (1972), suggested the illusion was due to the continuity of the inner compared to the ordered subunits of the outer. On the surface, the effect seems consistent with the density bias, however recently it has been shown that neither ordered subunits, nor continuity of the inner pattern is needed. Instead it seems to be driven by

enclosure, see (Guest et al., 2022), and chapter 4. However, paradoxically the OC predicts the outer pattern to be the more numerous, the opposite of the regular-random illusion. See chapter 5 for a fuller investigation into this.

Early work on the role of extent on numerosity was conducted by Ponzo using the, now famous, Ponzo illusion (Ponzo, 1928). The two illusion are place side-by-side in Figure 2.1. If the region with black elements is perceived as larger, this may be the driving factor in the Solitaire illusion. To study density and clustering on their own it is, therefore, essential to control overall area.

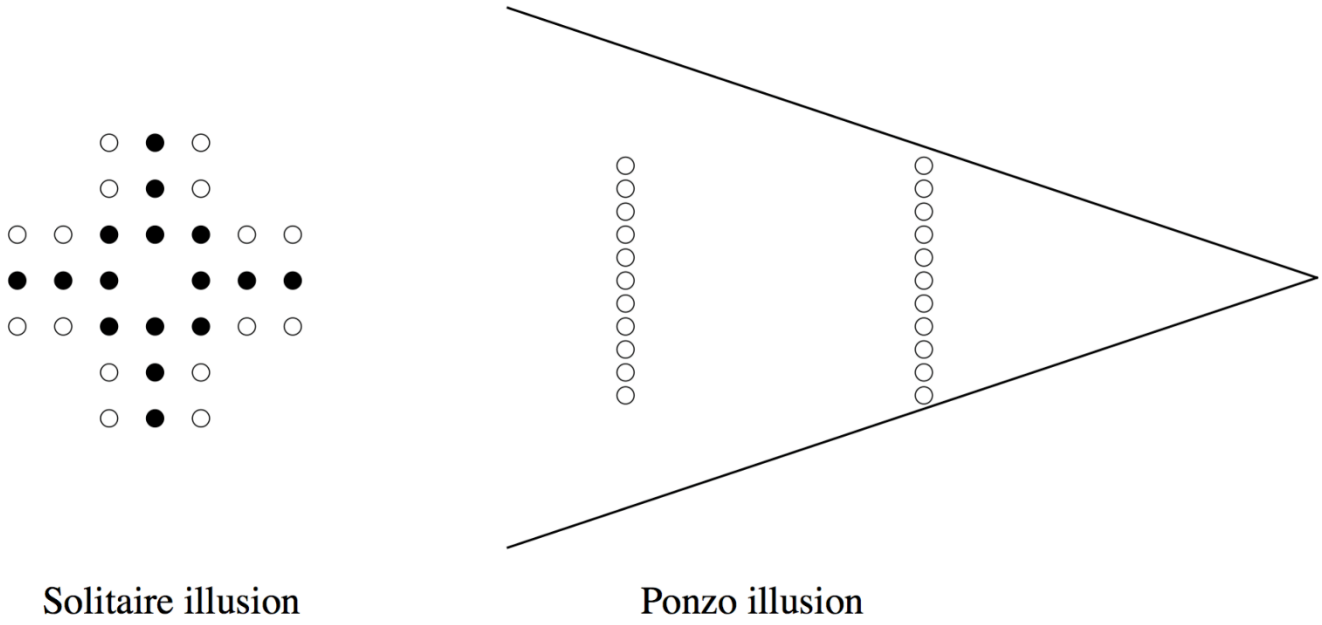

Figure 2.1. On the left, most people judge the black elements as more numerous than the white elements. The spatial distribution of elements matches the example in Frith and Frith (1972). On the right, most people judge the elements nearer the apex as more numerous. The distribution of elements is based on the example in Ponzo (1928) also reproduced in Vicario (2011).

Although there is a compelling body of evidence for the existence of a sense of number, it is necessary to understand how perceptual systems achieve this estimation. In this context it is useful to study cues that bias numerosity estimation. There have already been cues mentioned earlier in the introduction, such as size, spacing and density. The regular-random numerosity illusion and the Solitaire illusion are also examples of properties of the configuration that bias perceived numerosity.

2.1.2 Numerosity as a salient dimension

If approximate numerosity is perceived for any large sets of visual elements, do individuals spontaneously use differences in cardinality to discriminate and classify stimuli? Cantlon and Brannon (2007) asked the question whether individuals spontaneously represent the numerical attributes of their environments. They tested rhesus monkeys and compared the influence of number to that of shape, colour, and area on a matching task with more than one correct answer: there was a numerical match and a non-numerical match (based on colour, area or shape). The results were clear: all monkeys based their decisions on the difference in cardinality. A similar conclusion applies to human infants. In a more recent review, Ferrigno & Cantlon, (2017) concluded that non-verbal numerical reasoning about physical objects is the first type of numerical cognition that emerges in human development. Moreover, human adults are more sensitive to cardinality than to density or area. Cicchini et al., (2016) found that when stimuli varied in density, area and cardinality, observers reacted with greater sensitivity to changes in cardinality relative to the other dimensions. Not only humans and other animals can estimate numbers, but they seem to use the number as an important dimension in the environment.

3.1.3 The approximate number system and normalization

In a critique against the mainstream view, Gebuis et al., (2016) have argued that cardinality is estimated by a sensory-integration system that compares stimuli by integrating different sensory cues related to changes in number. However, proponents of the approximate number system are aware that irrelevant properties of the stimulus affect perceived numerosity. They argue that the necessary normalization stage may not be perfect (Dehaene et al., 1993), and that interference may also exist after numerosity has been computed, at the decision or response stage (Inglis & Gilmore, 2013).

Estimation of cardinality has to rely on spatial properties of the patterns. More regular patterns, with less clustering of the elements, are overestimated relative to less regular patterns. These clustering effects may highlight the way the numerosity perception works. For instance, is

it a by-product of computations carried out by an ancient and shared system. If so the role of clustering should be robust across individuals, groups and even different species.

An alternative view is that the approximate number system achieves normalization and is unaffected by correlations between cardinality and other cues. There are effects of irrelevant cues, such as clustering, but they are separate from cardinality estimation per se. Based on this view the role of irrelevant cues on cardinality judgments should not be robust across individuals, groups and different species. It is therefore necessary to study the effect of regularity and clustering in people and in other species to compare and analyse the similarities and differences.

2.2 The procedure

This a human study, however the procedure has been developed in the study of animal behaviour. In a first phase individuals are reinforced when they select one of a pair of stimuli. In the case of cardinality some individuals are reinforced when they select the higher cardinality and other individuals are reinforced when they select the lower cardinality. For human observers the reinforcement is a "Correct" message presented after the choice was performed. In a second phase of the procedure individuals have to choose between a pair of novel stimuli. Here the cardinality was the same in the pair of stimuli but there was a difference in the type of configuration. I used configurations with more or less clustering, by means of a minimum inter-dot distance constraint similar to that used by Valsecchi et al. (2013). Therefore, if individuals could estimate cardinality independently from clustering there should not be any preference, but if they perceived a difference in cardinality due to clustering they would be guided by that variable.

A similar approach has already been used to study numerosity with humans and monkeys, see experiment 2 in Beran, (2006). In that study he compared humans to four rhesus monkeys and used dot configurations that varied in regularity. However, following the type of stimuli used in the original work on the regular-random illusion (Ginsburg, 1980) the regular

configuration was a perfect square matrix. There was evidence that both humans and monkeys experienced the regular-random illusion, but with some individual differences. Different methodology provided different results, including some cases where monkeys had preference for the less regular configuration (Experiment 1).

Agrillo et al., (2014) tested capuchin monkeys, rhesus monkeys and chimpanzees, using the Solitaire illusion. Overall there was no or weak evidence of the configuration affecting perceived numerosity in these species using this illusion. Parrish et al., (2016) further studied the solitaire illusion in children and capuchin monkeys. There was some evidence that the monkeys perceived the illusion, although there were large individual differences. Interestingly, similar large individual differences were present also in the young children. Parrish et al. (2016) conclude that perhaps experience plays a role in shaping the emergence of the Solitaire illusion.

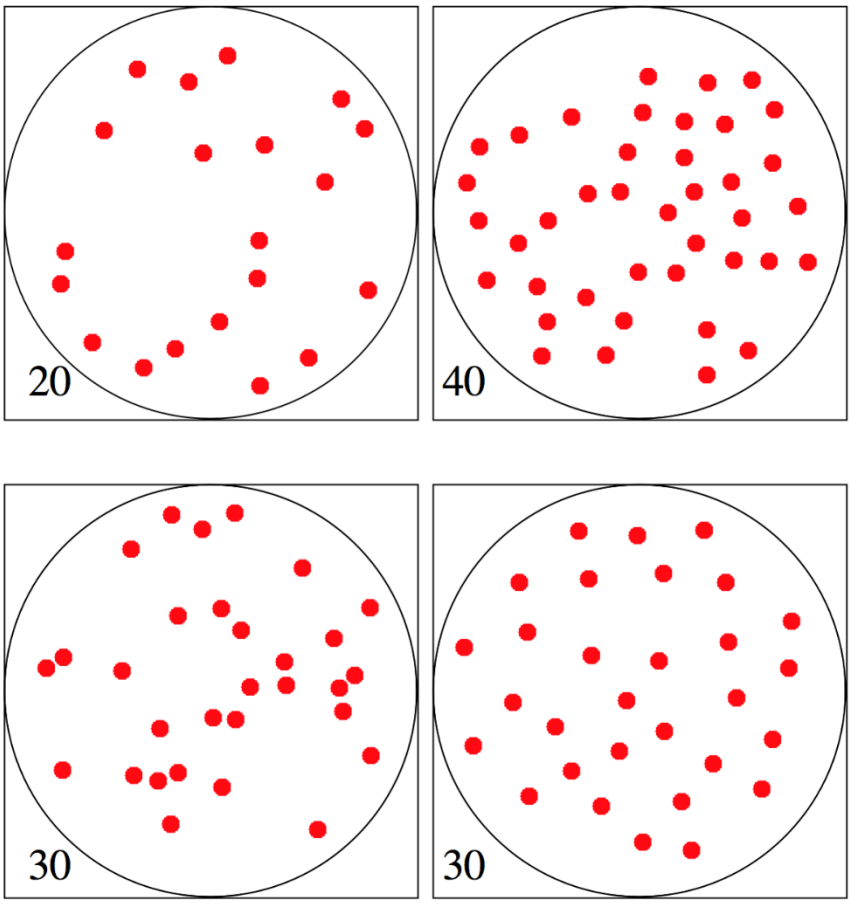

Figure 2.2. The first pair of stimuli is an example of stimuli used during training. Cardinality was always 20 in one pattern and 40 in the other. The dot had a radius of 10 pixels. The minimum inter element distance was 3.6 times the radius (36 pixels). The second pair of stimuli are examples of stimuli used in the experimental phase. Cardinality was always 30 dots, however they differed in clustering. One pattern has a minimum inter element distance of 2.1 radii or 21 pixels (left example), and the other a minimum of 5.1 radii or 51 pixels (right example). The choice was such that for 2.1 radii elements could be close but without touching.

2.3 Experiment

I tested human adults using the modified reinforcement task. Participants, naïve to the purpose of the study, were presented with two images of red dots. They were told to start by selecting either stimulus, and that they would receive feedback as to whether it was correct. Images were presented sequentially so that observers could look at the centre of the screen and to control amount of time per image. Participants were assigned to either the condition in which the 20 dots stimulus was the correct choice or the condition in which the 40 dots stimulus was the correct choice, by participant number. Odd numbered participants were in the 20-dot condition, even numbered participants were in the 40-dot condition.

The feedback is expected to lead individuals to use a rule. After they reached a criterion, the training phase was followed by an experimental phase. New stimuli were interleaved with the original stimuli. All stimuli in the new pairs had 30 dots, but the two images differed in the minimum inter-element distance (MD). In one the minimum distance was smaller than the original, in the other it was greater than the original. Therefore, the test stimuli did not differ in density (over the whole area) but they differed in amount of clustering. Based on the regular-random numerosity illusion, one would predict that stimuli with higher values of MD would be perceived as more numerous. This prediction is related to occupancy, which increases with higher values of minimum inter-element distance.

It is important to analyse which rules participants could use. An obvious choice is cardinality; it is easy to perceive a difference and estimate which set has more dots (20 or 40). However, cardinality was confounded with density as dots were always within the same circular

area. There is a debate in the literature on whether judgments of cardinality and density are based on the same mechanism (Anobile et al., 2015; Tibber et al., 2012).

Density can increase the clustering of elements. Therefore, effective strategies were available based on density or clustering. For clustering the prediction for the choice between the test stimuli is the opposite than what is predicted by occupancy (see Figure 2.3). There are, therefore, two different predictions one based on occupancy (a cue to cardinality) and one based on clustering.

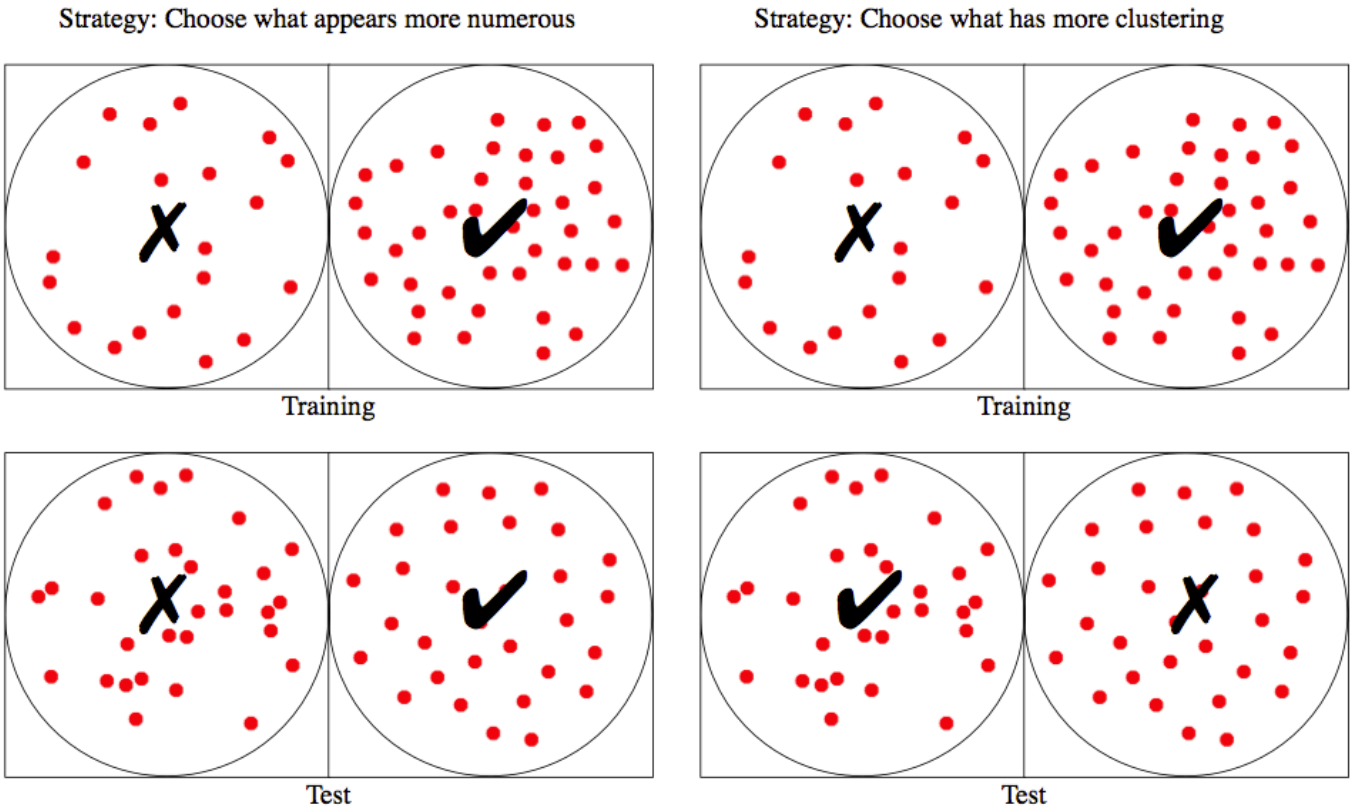

Figure 2.3. A strategy based on estimated cardinality predicts that when reinforced for N=40, for test stimuli there will be a preference for the one with more spacing (MD=51). A strategy based on clustering, or element proximity, predicts that when reinforced for N=40, for test stimuli there will be a preference for the one with less spacing (MD=21). For a quantification of these variables see Supplementary analysis.

2.3.1 Methods

Participants. Forty-eight psychology students took part in the study (30 female and 18 males). They were naïve with respect to the purpose of the study. Participants were alternatively (odd or even) assigned to two conditions, one in which low cardinality was the correct answer

(N=24), and one in which high cardinality was the correct answer (N=24). The study had local ethics approval by the Ethics committee (IPHS-1516-SMc-199) and was conducted in accordance with the Declaration of Helsinki (Revised 2008).

Materials. The procedure, including stimulus generation, was controlled by a Python program using the PsychoPy libraries (v1.80) (Peirce, 2009). The computer was a HP EliteDesk 800 G1, with a Dell 17 inch CRT monitor and 60Hz refresh rate. Each red dot was a circle of radius 10 pixels. Dots were placed inside a circular region of radius 200 pixels, and presented on a white background.

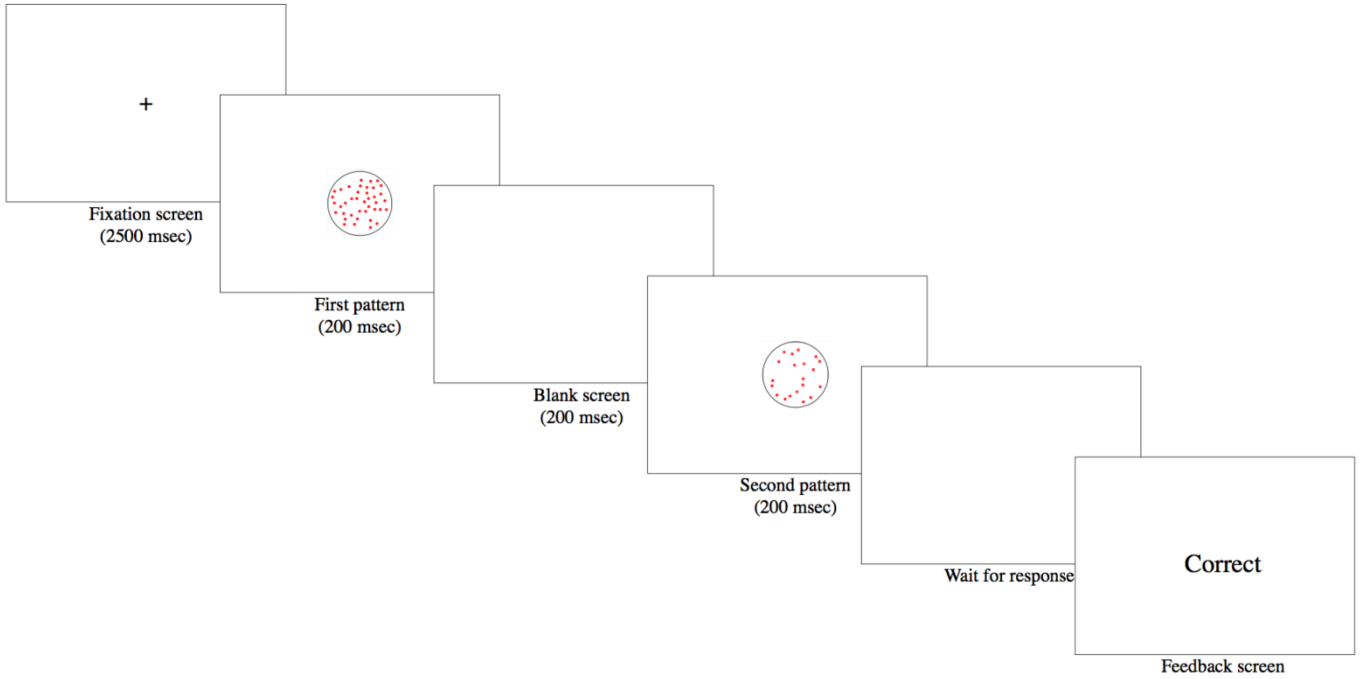

Figure 2.4. An illustration of the structure of a trial. The fixation was followed by two patterns, shown sequentially for 200 ms each, and by a blank screen. After a response was produced there was a feedback.

Procedure. Observers were seated at approximately 80 cm from the monitor in quiet room. On each trial there was a fixation cross for 2500 ms, followed by two patterns. Each pattern was on the screen for 200 ms and there was a 200 ms blank screen between them (Figure 2.4).

Participants were informed that there was a right and a wrong answer, but they would have to use trial and error to work out the correct response. They could choose the first pattern

by pressing the "a" key on the keyboard, or the second pattern by pressing the "l" key. Correct answers were followed by the word "Correct" displayed on the screen. There was no feedback for incorrect answers. The experiment had two phases.

Training Phase: Each participant completed a minimum of 20 trials and after that the phase stopped based on accuracy. The criterion to complete the training was 75% accuracy. The experiment would then move on to the next phase.

Experimental phase: To the participant there was no indication of any change in the procedure, but in the experimental phase new test stimuli were interleaved with the training stimuli. The length of the experimental phase was fixed at 36 trials. Of these 24 were identical to the training phase (pairs of stimuli with 20 and 40 dots) and included feedback. The other 12 trials had a pair of stimuli with 30 dots. The difference between the two patterns was the minimum inter-element distance (MD). One pattern has a minimum inter element distance of 2.1 radii (21 pixels), and the other of 5.1 radii (51 pixels). For 2.1 radii elements could be close but without touching. No feedback was provided on these trials. The computer stored responses for all trials.

At the end of the experiment, participants were asked to select what best described the strategy they employed. Choices were: Greater number of dots, Fewer dots, Dots were more dense, Dots were less dense, Other. I refer to the first two choices as Numerosity Strategy and the next two as Density Strategy. This was followed by a debrief: Participants described, in their own words, what strategy they had used.

The local clustering coefficient was computed using the python library Networkx (Hagberg et al., 2008), and occupancy was computed using the algorithm outlined in chapter 2.

2.3.2 Results

2.3.2.1 Experimental Results

Every individual tested reached the criterion. The number of trials necessary to reach it varied between 20 and 99. There were always 12 test pairs and therefore the main analysis is on responses to these stimuli. If participants choose randomly then you would expect equal number of responses to the MD=21 (clustered) and MD=51 (dispersed) stimuli. I tested two possible biases with two independent t-tests. Clustered and dispersed stimuli were chosen 52% and 48% of the times respectively and this difference was not significant ($t(47)=0.417$, $p=0.678$, Cohen's $D=0.06$). With respect to selecting the type of clustering depending on training, the prediction based on the illusion was supported by the data (69%, $t(47)=6.370$, $p<0.001$, Cohen's $D=0.92$).

Results support the hypothesis that most people responded to the test stimuli on the basis of which pattern appeared more or less numerous (Figure 2.5). In the test stimuli cardinality was the same (N=30), but perceived numerosity was influenced by spacing. This result therefore also supports the occupancy model of perceived numerosity.

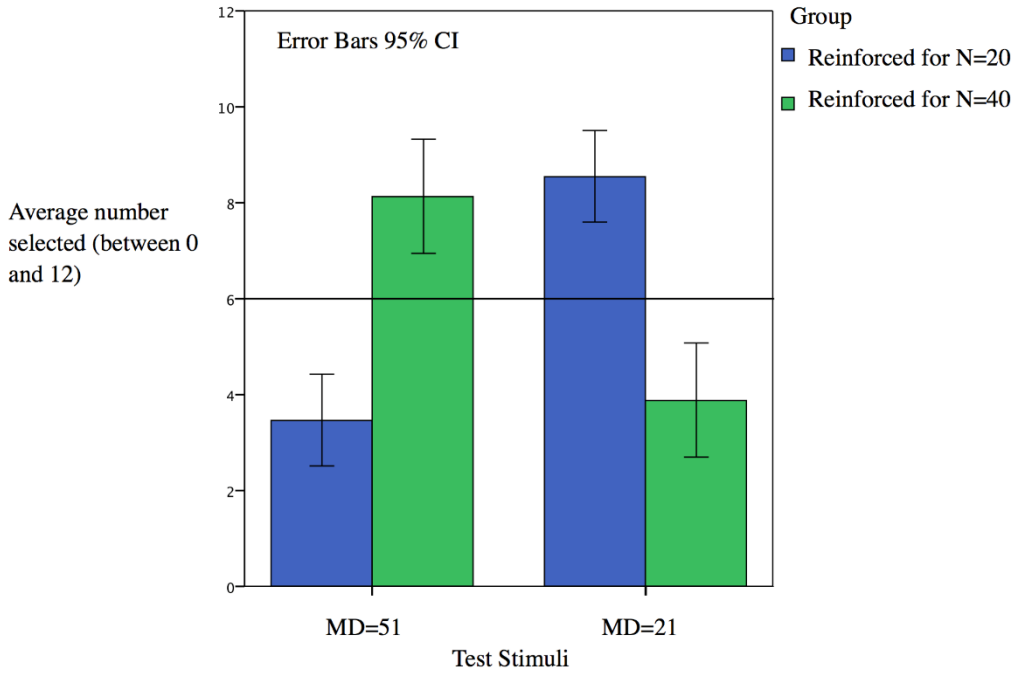

Figure 2.5. The average number of times that each type of test stimulus was selected. For each participant this number can be between 0 and 12. Blue and green bars are the two groups with different reinforcement and therefore the data are from different individuals. The Horizontal line indicates no effect.

Although the aggregate data suggest strong support for the idea that cardinality was the more important aspect of the stimuli and that observers used a strategy based on cardinality, there were some exceptions. Figure 2.6 shows the data for all individuals.

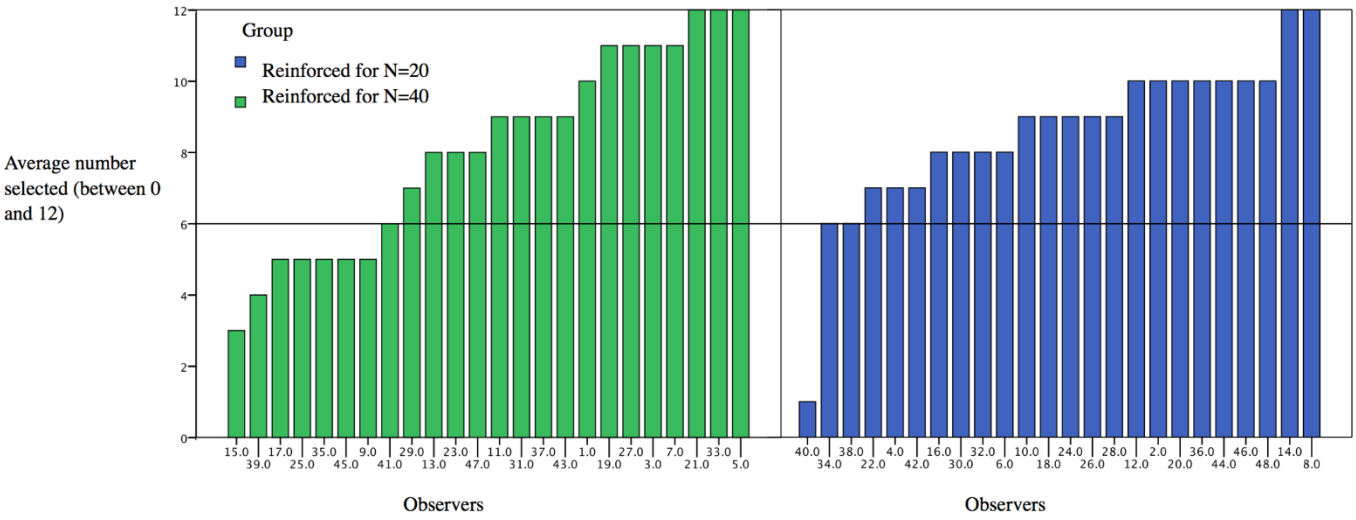

Figure 2.6. How often the test stimulus predicted by a choice based on cardinality was selected by each observer. For each participant this number can be between 0 and 12, but it is the selection of the clustered stimulus for the group reinforced with N=20 and the dispersed stimulus for the other group. Anything above 6 fits the prediction. Anything below suggests a different strategy. Blue and green bars are the two groups with different reinforcement and therefore the data are from different individuals.

2.3.2.2 Strategy Used

Participants had to report whether they used one of three possible strategies: numerosity, density or other. Out of 48, 34 said that they had used numerosity, 11 said they had used density and 3 said other. The graphs of Figure 2.7, however, do not show any direct relationship between this answer and the results. This is surprising but there may be an ambiguity of the terms. Some people may have used density as a word to refer to numerosity. The interview gave us a chance to understand the strategy. Ignoring those who displayed no strategy (6 choices either way out of 12) there were 8 participants who responded in a direction inconsistent with the majority, and inconsistent with a strategy based on occupancy. However, interviews did not highlight any pattern common to all 8. One mentioned number of dots, four said they started using number but then switched to density, one mentioned dot spacing and two did not made

any comments. The spacing of the dots was mentioned by other participants, although again they may have been referring to density in general rather than clustering.

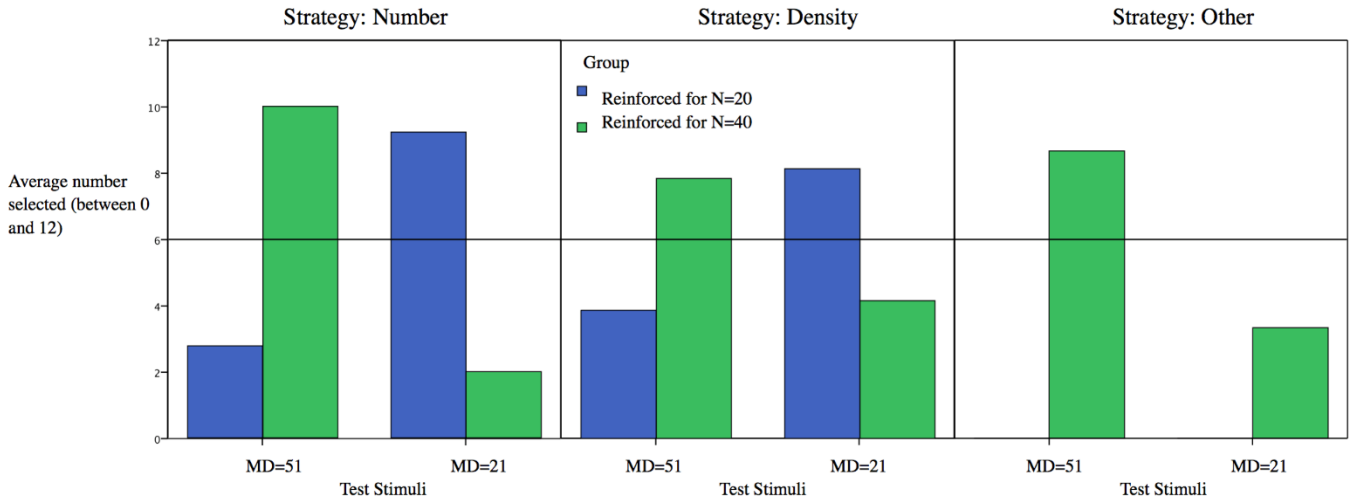

Figure 2.7. The same information in Figure 2.7 is replotted by dividing participants in three groups based on the strategy they reported at the end of the study.

Overall, Experiment 1 confirmed that human adults quickly develop a rule to select images based on difference in numerosity. A clear majority also reported this as part of the post-study debrief. For the test stimuli again, a clear majority selected the more or less spaced stimulus as predicted by the occupancy model of numerosity.

2.3 General Discussion

During training the configurations had 20 or 40 elements, and density and clustering covaried with numerosity. Either the dimension numerosity or the dimension clustering could be used to perform the task. Test trials presented configurations with 30 elements, but one had a larger inter-element distance than the other. Most human observers adopted a strategy based on numerosity, and chose the low clustering test image (when reinforced with 40 elements) or the high clustering test image (when reinforced with 20 elements). In the verbal description of the strategy they mentioned both numerosity and density, but not clustering.

This reinforces the prediction made by the occupancy model, that a pattern with greater spacing between its elements will be perceived as the more numerous. Likewise, a pattern that is more clustered, will be perceived as less numerous. Hence the mechanism used must be either the same or similar to that which produces the regular random illusion.

The question at the end of experiment, gave each participant a chance at selecting which strategy they had used. The choices were numerosity, density, other. There was also a debrief where the participant verbally explained the strategy they had. The responses they gave it not correspond with the choices they made during the experiment. This may be due to a mis-interpretation of the word "density", that can be used in way that actually means dot number. For example, more or less dots confined in a given space. In summary, evidence was found that numerosity is a salient property of dot patterns, and can be used to develop a response strategy.

3 What the Solitaire Illusion tells us about perception of numerosity

3.1 Introduction

Human observers can estimate the cardinality of a set of visual elements by means of a process that is fast and does not rely on symbols or counting. This type of numerosity estimation is shared with other non-human species see chapter 3.

The estimation process may not be relevant for small cardinalities or very high-density displays. This is because below 5 the cardinality is available directly, a process that has been called subitisation (Kaufman et al., 1949). At the other extreme, configurations with high density become texturised, and in that case observers may estimate cardinality on the basis of density, or spatial frequencies (Anobile et al., 2015; Cicchini et al., 2016; Dakin et al., 2011).

It is known that some irrelevant features of the stimulus can bias judgments of cardinality. Perceived numerosity is higher for smaller elements (Ginsburg & Nicholls, 1988; Shuman & Spelke, 2006), more regular patterns (Ginsburg, 1976, 1991), and for larger areas of the configuration (Dakin et al., 2011; Poom et al., 2019; Tokita & Ishiguchi, 2010; Vos et al., 1988). When two configurations are presented in sequence, the second tends to be perceived as more numerous (van den Berg et al., 2017). With respect to the spatial arrangement of the elements, its role is illustrated by two illusions. The Regular-Random numerosity illusion (Ginsburg, 1976, 1980), and the Solitaire illusion (Frith & Frith, 1972). They are presented in Figure 3.1 and I will refer to them as RRI and SI.

The RRI shows that as dots cluster together, their contribution to the overall perceived numerosity of a dot pattern starts to diminish. When two or more dots came close together, the overlap in their area of influence could explain the reduced contribution to numerosity. This concept has been developed and led to the occupancy model (Vos et al., 1988; Allïk and Tuulmets, 1991). Although it is difficult to know the precise size of the area of influence, Allik and Tuulmets (1991) speculated that it would depend on the properties of the dot pattern being analysed. However, the occupancy model or more generally the importance of spacing between

dots and clustering have been supported by empirical studies (Allik & Raidvee, 2021; Bertamini et al., 2016; Valsecchi et al., 2013).

In this study I focus on the SI, introduced in 1972 by Frith and Frith (1972). The name comes from a table top game played with pegs. The configuration shown in Figure 3.1 and has 16 black elements and 16 white elements. For most observers it appears that the inner group of elements is more numerous. This illusion is very robust to changes in stimuli and paradigm. For example, (Agrillo et al., 2016) used blue and yellow items. They also used a direct estimation task with random pegs positions for blue and yellow, and found an underestimation of 76% of outer elements compared to the inner elements. In this study I systematically investigate which mechanisms govern the SI by eliminating some of the contextual factors one at a time. To do so, in four different stimulus manipulations, the aim was to destroy the illusion on perceived numerosity.

Valsecchi et al. (2013) found a strong effect of clustering on perceived numerosity, in line with the RRI and as predicted by the occupancy model. The methodology used constrained the minimum distance between randomly located elements. In addition, they also discovered another strong effect, a reduced perceived numerosity for patterns presented in the periphery compared to central vision. In theory this may be relevant for the SI as the outside group is underestimated.

However, the SI works for extended presentation, allowing the participant to inspect every region with multiple fixations.

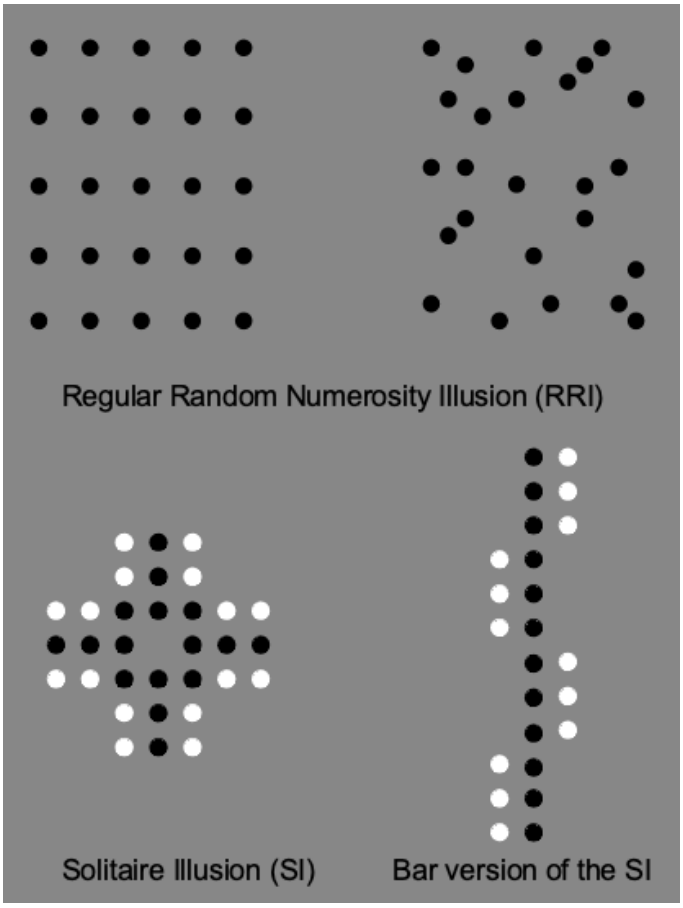

Figure 3.2. Top row: In the Regular-Random Numerosity Illusion the elements that form a regular array (left) appear to be more numerous (Ginsburg, 1976). Bottom row: In the original Solitaire illusion the inner set of elements (black) appear more numerous than the outer set. Frith and Frith (1972) tested also a version of the SI with elements placed along a line (bar version). People tend to perceive more elements for the bar (shown in black).

It is important to study the SI because the effect is strong and easy to demonstrate, and because we do not currently have a good explanation for it. There is also some evidence that it is an illusion specific to adult humans, because it does not work in chimpanzees, rhesus or capuchin monkeys (Agrillo et al., 2014; Parrish et al., 2019) in dogs (Looke et al., 2020), and in children under the age of four (Parrish et al., 2016). Although a recent report found some evidence of the SI in fish (Miletto Petrazzini et al., 2018). A summary of the findings using the two versions of the illusion and different populations are shown in Table 3.1.

Table 3.1: A summary of the experimental studies on the Solitaire illusion, listed in chronological order.

Authors	Year	Version	Participants	Result
Frith & Frith	1972	S B	Ha Hc	yes
Agrillo et al.	2014	S	Ha Ch Rh Ca	only in Ha
Parrish et al.	2016	S	Hc Ca	weak
Agrillo et al.	2016	S	Ha	yes

Miletto Petrazzini et al.	2018	S	Gu	weak
Parrish et al.	2019	S B	Ha Ca Rh	only in Ha
Lõoke et al.	2020	B	Do	no
Pecunioso & Agrillo	2021	S	Ha	yes

Version: S=Standard B=Bar
Participants: Ha= Human adults Hc= Human children Ch=Chimpanzees Rh=Rhesus Ca=Capuchin Gu=Guppies Do=Dogs

Frith and Frith (1972) described the SI as a result of grouping and Gestalt factors. The inner group is stronger because all its elements are contiguous, and thus form a better Gestalt. More recently, Poom et al. (2019) confirmed that perceived numerosity decreases with number of groups, independently by how the groups were created (e.g., colour, motion). The SI may therefore depend on the fact that the outer elements are separated into subsets.

However, there are reasons that make the SI effect counterintuitive. As we have seen in the case of the RRI, strong Gestalt (a regular grid) can lead to overestimation. Moreover, elements that form clusters (grouping by proximity) lead to underestimation, as shown in many studies (e.g., Bertamini et al., 2016; Valsecchi et al., 2013). This is the opposite of what happens in the SI. Because elements are placed on a grid with fixed cells, if we take the outer configuration on its own, these elements are farther apart than the elements in the inner group. Average distance is also higher for the outer group of elements. Similarly, if we were to apply the occupancy model, to the SI, then if the region of influence is large enough to create overlap despite the grid, then more overlap will be present for the inner set of elements (more contiguity). Again, this leads to a prediction that is the opposite of what is observed, see section 5.2.

Grouping can also be manipulated by connecting elements. He et al. (2009) and Franconeri, Bemis, and Alvarez (2009) used randomly distributed dots, but some pairs were joined. Connected patterns are perceived as less numerous than unconnected patterns. Even symmetry may increase strength of grouping between elements and reduce perceived numerosity

(Apthorp & Bell, 2015). In general, the SI seems inconsistent with these findings because the elements grouped in a regular and compact region appear more numerous.

Equally counterintuitive is the role of area, as we have seen larger areas lead to a bias towards larger perceived numerosity (e.g., Poom et al., 2019). One simple way to measure the area of a set of elements in the plane is by computing the area of the convex hull. In the case of the SI the convex hull is larger for the outer elements than for the inner elements in the SI. Despite this it is the inner group that is perceived as more numerous. Note that the convex hull measures objective size; it is also known that perceived (subjective) size can affect numerosity, as illustrated in the context of the Ponzo illusion (Ponzo, 1928), the horizontal vertical illusion (Pecunioso et al., 2020) or in terms of changes of perceived size after adaptation (Zimmermann & Fink, 2016).

In a more recent study, Pecunioso & Agrillo, (2021) were interested in the role of expertise, and compared musicians to non musicians. They predicted that musical expertise would reduce the illusion. They found no effect of expertise in experiment 1 (forced choice), and some evidence in favour of their hypothesis in experiment 2 (absolute number estimation). What is most relevant here is that in their experiment 2 they presented the dots from the SI in the standard configuration, or as isolated patterns. The outside set of elements were overestimated compared to the inner set even when presented in isolation. This supports the hypothesis that the SI is a robust effect that does not requires enclosure. However, this study relied on absolute cardinality judgments, which can be biased by many factors. Indeed, only when using absolute judgments there was a difference between musicians and non musicians. Moreover, observers were in general closer to the correct estimation for the outer configuration of the dots. Here we have subgroups of just two dots, which may be perceived by subitization.

In summary, if we accept that both spatial proximity of the elements and total area bias responses in the direction of greater perceived numerosity, than some other factor must operate in the case of the SI that is strong enough to overpower these and lead to the opposite outcome.

In this study, I started with the original SI configuration and manipulated two properties: overall cardinality, and enclosure. First, we note that each of the outer subsets of the original SI pattern has only two elements, or four if we consider the quadrants (Figure 3.1). These values are within the subitizing range. The comparison is therefore between a value that has to be estimated (inner set), and the sum of values each of which could be subitized (outer sets). To test the hypothesis that the SI is specific to the original configuration of 32 elements (16 in the inner and 16 in the outer sets) I increased the number of elements while keeping the overall structure. This was achieved by treating each original element as a cell and filling the cell with either 1 element (original version), 4 or 9 elements. Therefore, we have Solitaire configurations with 16+16, 64+64, and 144+144 elements. A similar manipulation for the Bar version of the SI creates configurations with 12+12, 48+48, and 108+108 elements.

The second manipulation is a direct test of the importance of having one set enclosed within the other set. Therefore, taking the two configurations and then displacing them horizontally, so that there is no overlap, as shown in Figures 3.2 (original Solitaire version) and 3.3 (Bar version). I report results of four experiments in which the basic design was the same, but the appearance of the stimuli changed as follows: Exp 1) change in total cardinality and separation; Exp 2) same as Exp 1 but with lines that form closed polygons; Exp 3) degradation of the groups (50%reduction in dot density/cardinality); Exp 4) degradation of the groups (90%reduction in dot density/cardinality). To anticipate the results, the basic effect of a bias in favour the inner group of elements turned out to be remarkably strong and general.

3.2 Experiment 1.

This experiment tests the role of cardinality and of enclosure of the Solitaire illusion. Using the original version (16+16 elements) as well as versions of the illusions with much larger total number of elements by increasing the number of elements in each cell. Also usage of both the original configuration that took the name from the Solitaire game, and a version with a line

of elements that had already been introduced by Frith and Frith (1972), and used also by Parrish et al. (2019).

Given the novelty of the experimental design, it was not possible to conduct an a priori power analysis based on the size of similar effects in the literature. There was 20 subjects (for a total of 1920 trials). The main hypotheses concerned the factors Separation and cardinality and their interaction (2 x 3). However, for subsequent Experiments I report a power analysis based on the data collected in Experiment 1.

3.2.1 Methods

Participants.

Twenty individuals participated (age range 19 to 50, with 7 males). All participants had normal or corrected-to-normal vision, and none reported colour blindness. The study was approved by the Health and Life Sciences Committee on Research Ethics (Psychology, Health and Society) and conducted in accordance with the Declaration of Helsinki (revised 2008). Participants were naive with respect to the hypotheses.

Design.

The factors were the Illusion version (the original Solitaire illusion or the Bar version), Separation (whether the inner and outer patterns were separated on the screen), Colour (red/green or blue/yellow) for the inner and outer pattern (for example if the colours were red/green the inner elements could be red or green) and cardinality (1, 4, 9 cell size). This 2 x 2 x 4 x 3 design has 48 unique stimuli. Each observer was shown each stimulus twice, giving a total of 96 trials, which were split into two blocks for the two colours (red/green and blue/yellow). Block order was counter-balanced between participants.

Stimuli and Procedure.

The experiment was conducted in a dark room, using a mac (Intel i5 processor, 8 Gb of RAM running Mac OS version 10.11.16). All stimuli were generated using PsychoPy version

1.84.2 (Peirce, 2009), and presented using an Apple studio 20-inch monitor, with resolution 1152x870 (75Hz). Each colour was adjusted to have similar luminance (25.20 cd/m2). The standard RGB (sRGB) values were as follows. Yellow: 0.7, 0.7, 0.5; blue: 0.565, 0.565, 1.0; red: 1.0, 0.5375, 0.5375; green: 0.5, 0.77, 0.5. Distance from the screen was 57cm, and it was controlled with a chinrest.

If we treat each dot in the original illusion as a cell, and replaced it with either 4 dots, or 9 dots. The size and spacing between dots remained the same. Hence, turning the Solitaire illusion containing 16 dots for the inner and outer pattern, into two larger versions containing 64 and 144 dots. The cardinalities are labelled as 1, 4 and 9 because each cell had either 1, 4 or 9 elements. Repeated the same procedure enables increases the cardinality for the bar version of the illusion.

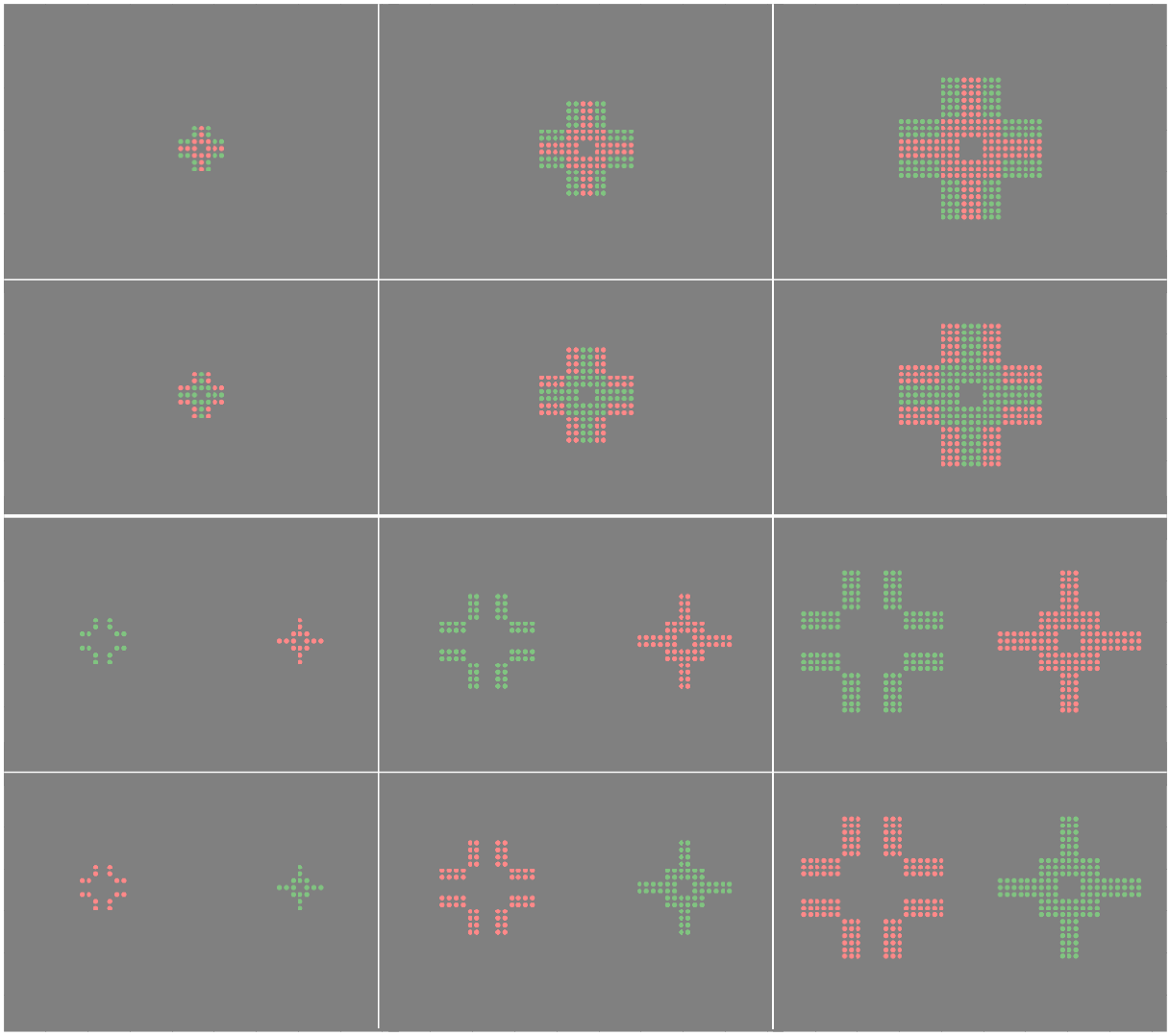

Figure 3.2: Top half: The original Solitaire illusion has 16 elements for the inner and outer sets, the middle column has 64 for each set and the last column has 144 elements per set. Bottom half: the same stimuli presented as separate groups. The examples shown have green-inner and red-outer colours, and the opposite arrangement underneath. For another set of stimuli, not shown here, the colours were blue and yellow.

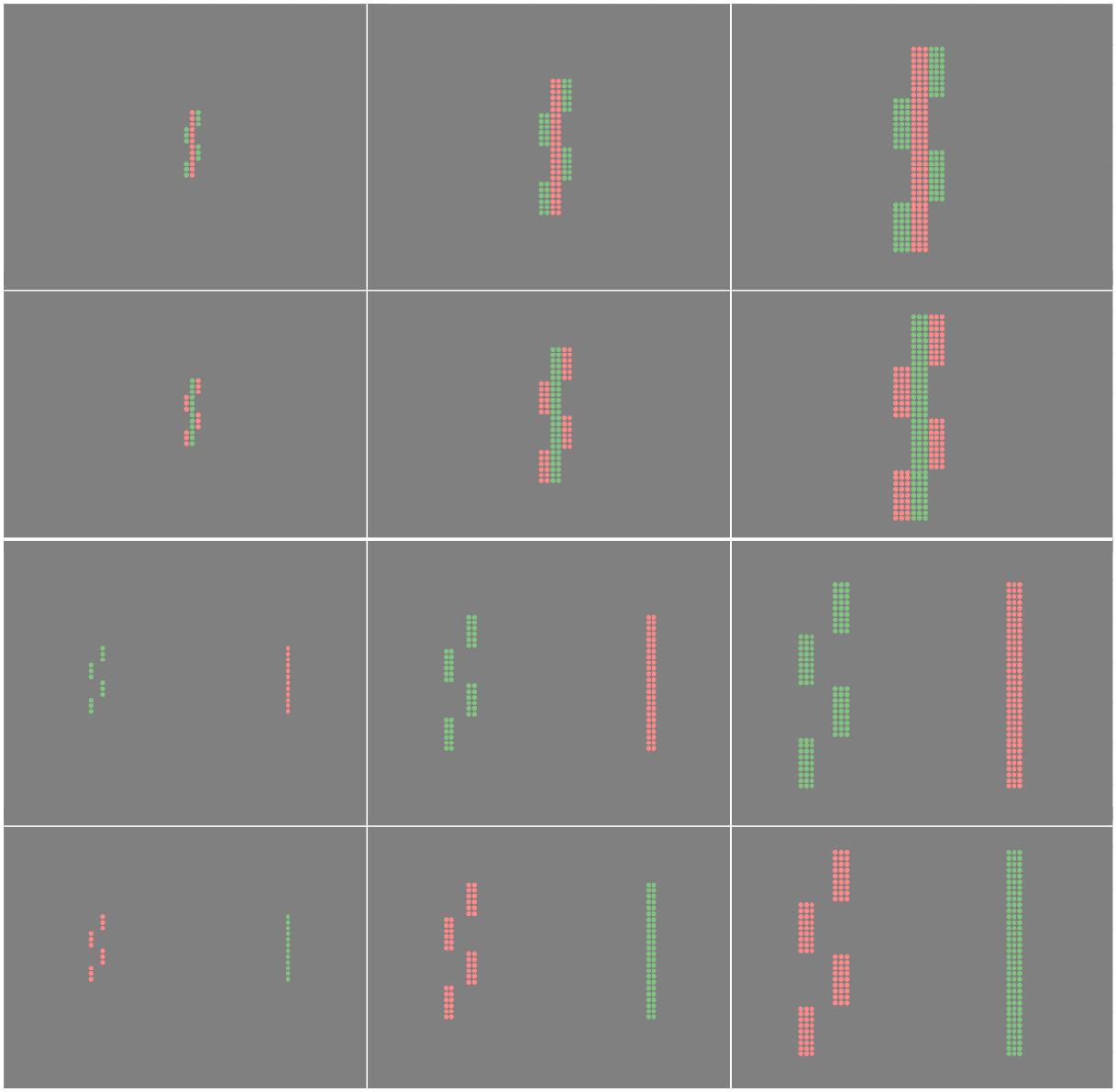

Figure 3.3: Top half: For the bar version of the illusion the numbers of elements in each of the three columns are 12, 48 and 108. Bottom half: stimuli for the bar version of the Solitaire illusion presented as separate groups. The examples shown have green-inner and red-outer colours, and the opposite arrangement. For another set of stimuli, not shown here, the colours were blue and yellow.

Participants were told that they would see two sets of dots with two different colours. Sometimes the sets would be in the centre of the screen, sometimes that would be separated. The task was to choose which colour set appeared to have more dots.

Stimuli were presented on the screen for two seconds. Only after the stimulus disappeared the participants could enter a response. The keys 'a' and 'l' were mapped to the two colours in such a way that participants could press 'a' to judge that the red colour dots were more

numerous and the 'l' to judge that the green colour dots were more numerous. Similarly, the same two keys were used for the blue/yellow stimuli. Raw data from all studies as well as example images are available online: https://osf.io/9utzx/.

3.2.2 Data analysis

Data analysis was performed using R Version 3.5.3 (R Core Team, 2021). Data were analysed by means of a generalized logit-linear mixed model for binomially distributed outcomes (GLMM) suitable for analysing complex datasets with repeated or grouped observations (Bolker et al., 2009; Schielzeth et al., 2020). Also an omnibus test based on type-III Wald chi-square with the *anova* function from the *car* package, was performed (Weisberg & Fox, 2011).
For all experiments, included in the model was the Illusion version (Solitaire vs Bar), Separation (original or separated inner and outer patterns), cardinality (1, 4, 9 cell size) and also Colour (red inner/green outer, blue inner/yellow outer, red outer/green inner, blue outer/yellow inner) as a within subject factors. Moreover, block Order was included as a between subject factors. The dependent variable was the number of times the inner pattern was selected as having more dots. The participant, the Colour pairing and the block Order were entered as random effects. By doing so, it is assumed a by-subject variation in the intercept for each colour pair and block order combination.

As an estimate of the effect size, a calculation of the semi-partial coefficients of determination, also known as part R^2, was performed, by means of the partR2 package (Stoffel et al., 2021). As suggested by Stoffel, part R^2 for main effects and interactions were calculated separately and part R^2 for the main effects were estimated after excluding the interaction from the model. The package does not calculate the part R^2 for effects who are included in the random effects, so the coefficient for Colour pairing and the block Order was not reported.

3.2.3 Results and discussion

The analysis of deviance with the Type III Wald chi-square tests showed a significant

main effect of Separation (χ^2= 64.748, df= 1, p< 0.001, part R^2= 0.036, C.I.= 0.031 – 0.069), and Cardinality (χ^2= 6.437, df= 2, p= 0.040, part R^2= 0.001, C.I.= 0.001 – 0.033). Among the interactions, Separation:Illusion (χ^2= 20.631, df= 1 , p< 0.001, part R^2= 0.012, C.I.= 0.007 – 0.047), and Separation:Cardinality (χ^2= 6.627, df= 2, p= 0.036, part R^2= 0.008, C.I.= 0.004 – 0.043) were also significant. All other effects were not significant. Table 3.2 summarizes the results of the Wald test for experiment 1.

Table 3.2: Analysis of Deviance Table (Type III Wald chi-square tests) for Experiment 1 with part R2 for each term in the model. Model marginal R2 = 0.067, C.I = [0.057 – 0.149].

	χ^2	DF	p(>χ^2)	part R^2	R^2CI
(Intercept)	9.893	1	0.002		
Separation	64.748	1	0.000	0.036	0.031 – 0.069
Illusion	0.143	1	0.706	0.001	0.001 – 0-032
Cardinality	6.437	2	0.040	0.001	0.001 – 0.033
Colour	0.561	3	0.905		
Order	0.204	1	0.652		
Separation:Illusion	20.631	1	0.000	0.012	0.007 – 0.047
Separation:Cardinality	6.627	2	0.036	0.008	0.004 – 0.043
Illusion:Cardinality	3.675	2	0.159	0.003	0.001 – 0-038
Separation:Illusion:Cardinality	3.302	2	0.192	0.007	0.004 – 0.094

The analysis above does not directly test whether the response level is above chance. Although this may seem obvious from Figure 3.4, it was decided to add an exact binomial test on the proportions. To avoid multiple tests, only the test for the Separate condition is reported. Number of responses inner was 734 out of a total of 960 trials, p < 0.001. The alternative hypothesis was that the probability of success is not equal to 0.5 (95% confidence interval: 0.736 to 0.791). On an individual basis, proportions were above chance for 19 out of 20 subjects.

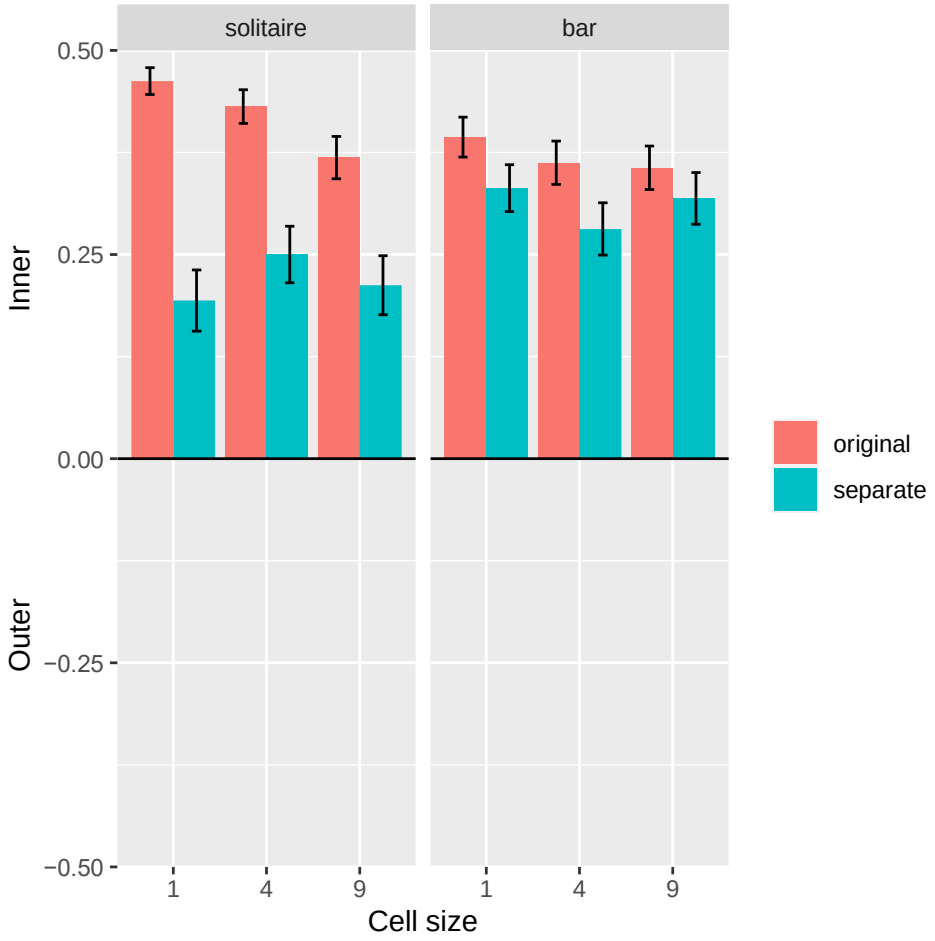

Figure 3.4: Proportion of responses for the two versions of the illusion (Solitaire and Bar). The chance level (50%) has been shifted to correspond to zero. Cell size is the number of elements in each of the cells, leading to a total of 16+16, 64+64, and 144+144 elements (Solitaire version) and 12+12, 48+48, and 108+108 (Bar version). The two colours are for the original combined configuration and the presentation of the two sets as separate groups. Error bars are ± 1 SE of the mean.

The results confirm the presence of the illusion, the inner set of elements tends to appear more numerous in the original configuration and in the bar version of the SI. The key feature of the SI is the arrangement of the two sets, one inside the other. Therefore, it was expected that a separation of the two would have a large effect. Indeed, based on the literature one could predict a reversal of the effect given that the outer configuration occupies a larger area. This did not happen in the data collected. The illusion survived the separation of the two groups, but the effect was reduced at least for the original Solitaire version (an interaction illusion and separation).

The main motivation for Experiment 1 was a test of the role of cardinality. I wanted to test whether the SI would still be present with large sets of elements, and in particular when none

of the subsets are within subitizing range. The results demonstrate that the illusion is not specific to the set size of the original configuration. In the original configuration the outer elements formed groups of two or three, which is within the subitization range, however the effect is present also when the smaller groups include sets of elements well above subitazation range. Overall, the SI reveals itself as robust to various manipulations (differences in colour, cardinality, separation of the groups).

3.3 Experiment 2

Frith and Frith (1972) pointed to the importance of perceptual grouping in the SI. It therefore can be reasoned that adding information about grouping may therefore directly affect the illusion. In Experiment 2 the same stimuli, was used, and the same procedure as in Experiment 1, with the only addition of two lines. These lines connected the elements of a group as shown in Figure 3.5. The lines corresponded to the concave hull of each of the two colour sets and were of the same colour.

I predicted that by emphasising the area would reduce the SI and produce instead an effect in line with the role of area: greater perceived numerosity for the larger area (outer group).

Power analysis. To define the sample size of Experiment 2, a power analysis was performed based on Experiment 1. The simulation-based power analyses was performed with the packages mixedpower (Kumle et al., 2021) and simr (Green et al., 2016) in R. The estimation of effects was conducted based on the data from Experiment 1. One thousand simulations, were performed, for sample cardinalities from 14 to 20 participants. Already with 14 participants the power for the Separation factor was close to 100% while the Cardinality reached 80% and their interaction 50%.

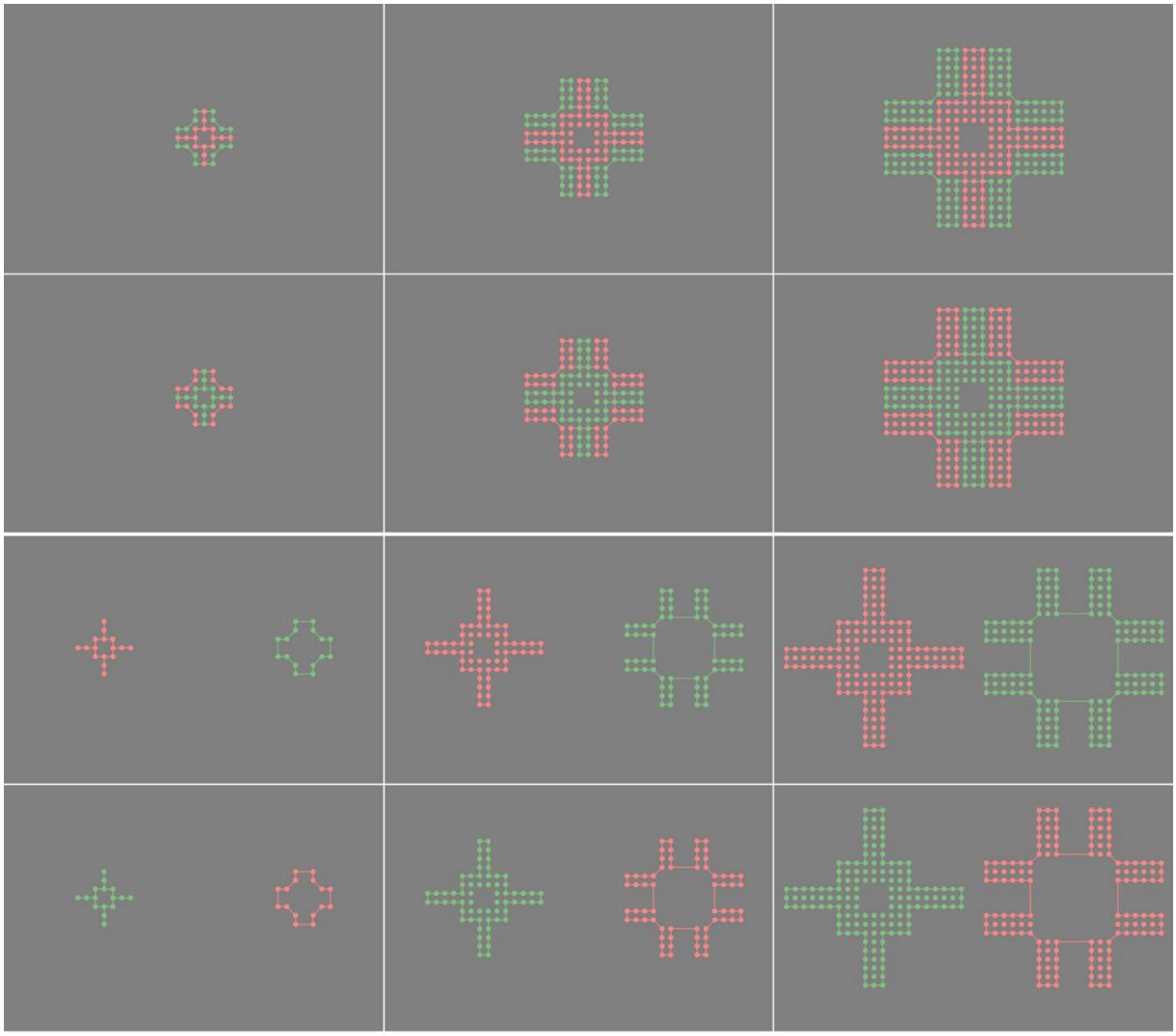

Figure 3.5: Stimuli for Experiment 2 were the same as those of Experiment 1 except for the thin lines that create closed polygons (I increased thickness by a factor of three to make them more visible in the figure). Here the stimuli can be compared to those in Figure 3.2.

3.3.1 Methods

Participants.

Fourteen individuals participated (age range 21 to 38, 3 males). All participants had normal or corrected-to-normal vision, and none reported any colour blindness. The study was approved by the Health and Life Sciences Committee on Research Ethics (Psychology, Health and Society) and conducted in accordance with the Declaration of Helsinki (revised 2008). Participants were naive with respect to the hypotheses

Design

The design was the same as that of Experiment 1. The factors were the configuration (the original Solitaire illusion or the Bar version), separation (whether the inner and outer

patterns were separated on the screen), colour (red/green or blue/yellow), colour for the inner and outer pattern (for example if the colours were red/green the inner elements could be red or green) and Cardinality (1, 4, 9 cell size). Each observer was shown a total of 96 trials.

Stimuli and Procedure

The stimuli were the same as in Experiment 1 except for the addition of lines that created two polygons, one for each colour. The procedure was the same as in Experiment 1.

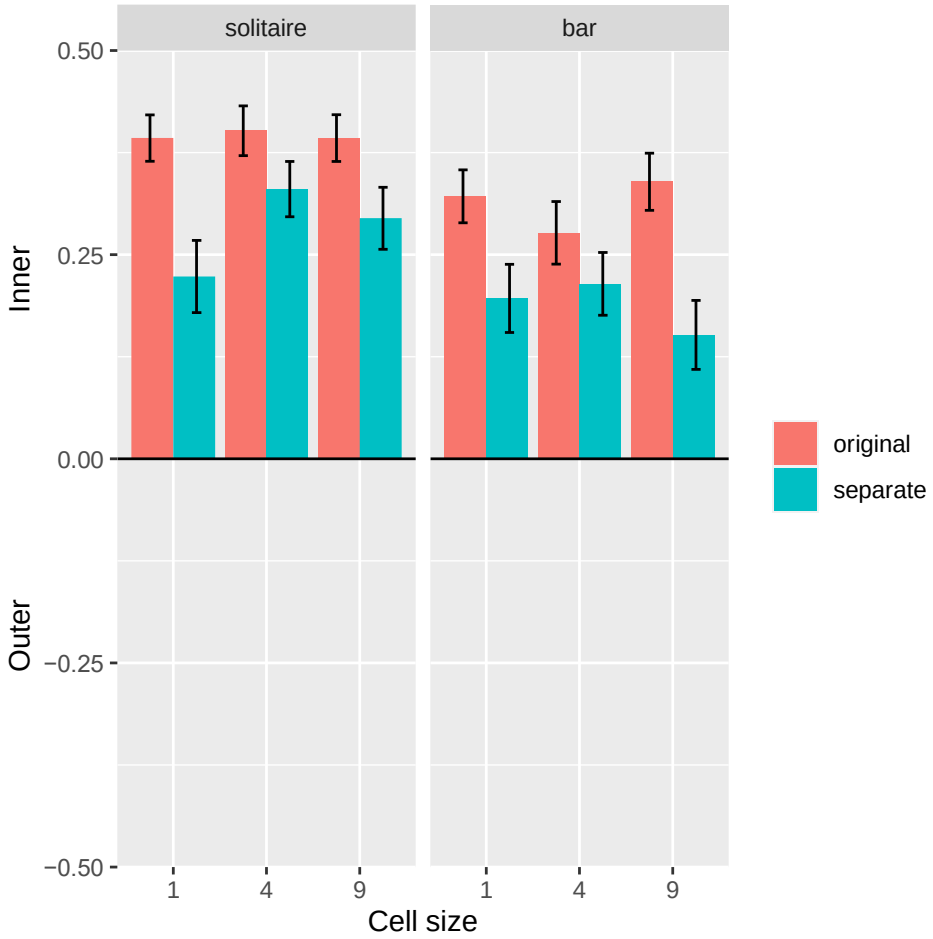

Figure 3.6: Proportion of responses for the two versions of the illusion (Solitaire and Bar). The chance level (50%) has been shifted to correspond to zero. Cell size is the number of elements in each of the cells, leading to a total of 16+16, 64+64, and 144+144 elements (Solitaire version) and 12+12, 48+48, and 108+108 (Bar version). The two colours are for the original combined configuration and the presentation of the two sets as separate groups. Error bars are ± 1 SE of the mean.

3.3.2 Results and Discussion.

The results of Experiment 2 are consistent with those of Experiment 1. Confirmation of the existence of the illusion for both the original and the bar version. Also, the illusion persists

for larger cardinalities, and that it is reduced but not eliminated when the two sets of elements are shown as separate groups.

The novelty of Experiment 2 was the presence of lines that would surround the elements and highlight the two groups of different colours. It was hypothesised that this may increase the effect of overall area, and also bind together the outer elements. If these lines had changed the strength of the grouping, making them more similar to each other, this should reduce the effect, and if it highlighted the areas, at least in the separate condition, it should reverse the effect. This did not happen. Overall, a preference for the inner pattern was present in all conditions.

The analysis of deviance with the Type III Wald chi-square tests showed a significant main effect of Separation (χ^2= 33.719, df= 1, p< 0.001, part R^2= 0.031, C.I.= 0.015 – 0.093), Illusion (χ^2= 20.056, df= 1, p< 0.001, part R^2= 0.018, C.I.= 0.002 – 0.082), and Order (χ^2= 6.693, df= 1, p= 0.01). All interactions were not significant. Table 3.3 summarizes the results of the Wald test for experiment 2.

Table 3.3: Analysis of Deviance Table (Type III Wald chi-square tests) for Experiment 2 with part R2 for each term in the model. Model marginal R2 = 0.120, C.I = [0.088 – 0.206].

	χ2	DF	p(>χ^2)	part R^2	R^2CI
(Intercept)	0.089	1	0.765		
Separation	33.719	1	0.000	0.031	0.015 – 0.093
Illusion	20.056	1	0.000	0.018	0.002 – 0-082
Cardinality	0.716	2	0.699	0.001	0.000 – 0.067
Colour	1.787	3	0.618		
Order	6.693	1	0.010		
Separation:Illusion	0.212	1	0.645	0.001	0.000 – 0.042
Separation:Cardinality	2.535	2	0.282	0.002	0.000 – 0.042
Illusion:Cardinality	2.049	2	0.359	0.002	0.000 – 0-042
Separation:Illusion:Cardinality	1.496	2	0.473	0.001	0.000 – 0.100

As for Experiment 1, I report an exact binomial test for the Separate condition. Number of responses inner was 494 out of a total of 672 trials, $p < 0.001$. The alternative hypothesis was that the probability of success is not equal to 0.5 (95% confidence interval: 0.735 to 0.768). On an individual basis, proportions were above chance for 9 out of 14 subjects.

Experiment 2 confirmed an illusion, but now it is stronger in the original than the bar version. This may be because the lines joining the elements interfered more with the Bar stimuli. Separation was again significant, confirming that this manipulation reduces (but does not eliminate) the illusion.

3.4 Experiment 3

We have seen in Experiments 1 and 2 that dots placed within a regular array form a configuration that leads to a perceived difference in cardinality in favour of the inner pattern. This illusion is robust and extends to large cardinalities and even to cases when the two sets (the inner and the outer) are presented side by side.

The critical factor seems to be that one group form a central more compact set, either a cross or a bar, and this is the group that appears more numerous. In Experiment 3 the role of the regularity of the array, was tested. To destroy the perception of a regular matrix, the configurations generated according to the same process as in Experiment1, were used but randomly sampled, so that only a proportion of the elements to keep (50%) and deleted the others. Examples of stimuli are shown in Figure 3.7, there is a degree of randomness in the configurations although it is still easy to see that one group is more central and one more peripheral.

Power analysis. Since the rationale of the experiment was to interfere with the illusion by degrading the stimulus, it was expected a reduction in the strength of the illusion and thus an overall reduction in the effects of the factors. The estimation was conducted based on the data from

Experiment 1. To ensure that there was sufficient power to test the effect of the factors of interest (Separation and Cardinality) the effects sizes of Separation, Cardinality and their interaction were reduced by 25%. One thousand simulations for sample Cardinlity from 14 to 20 participants, was performed. Already with 14 participants the power for the Separation factor was over 90%. The Cardinality reached 90% for n = 17, while their interaction for n = 20. Thus, the same sample size as Experiment 1 (20), was chosen.

3.4.1 Methods

Participants

Twenty individuals participated (age range 18 to 38, 9 males). All participants had normal or corrected-to-normal vision, and none reported any colour blindness. The study was approved by the Health and Life Sciences Committee on Research Ethics (Psychology, Health and Society) and conducted in accordance with the Declaration of Helsinki (revised 2008). Participants were naive with respect to the hypotheses.

Design

The design was the same as that if Experiment 3 except that the stimuli were different.

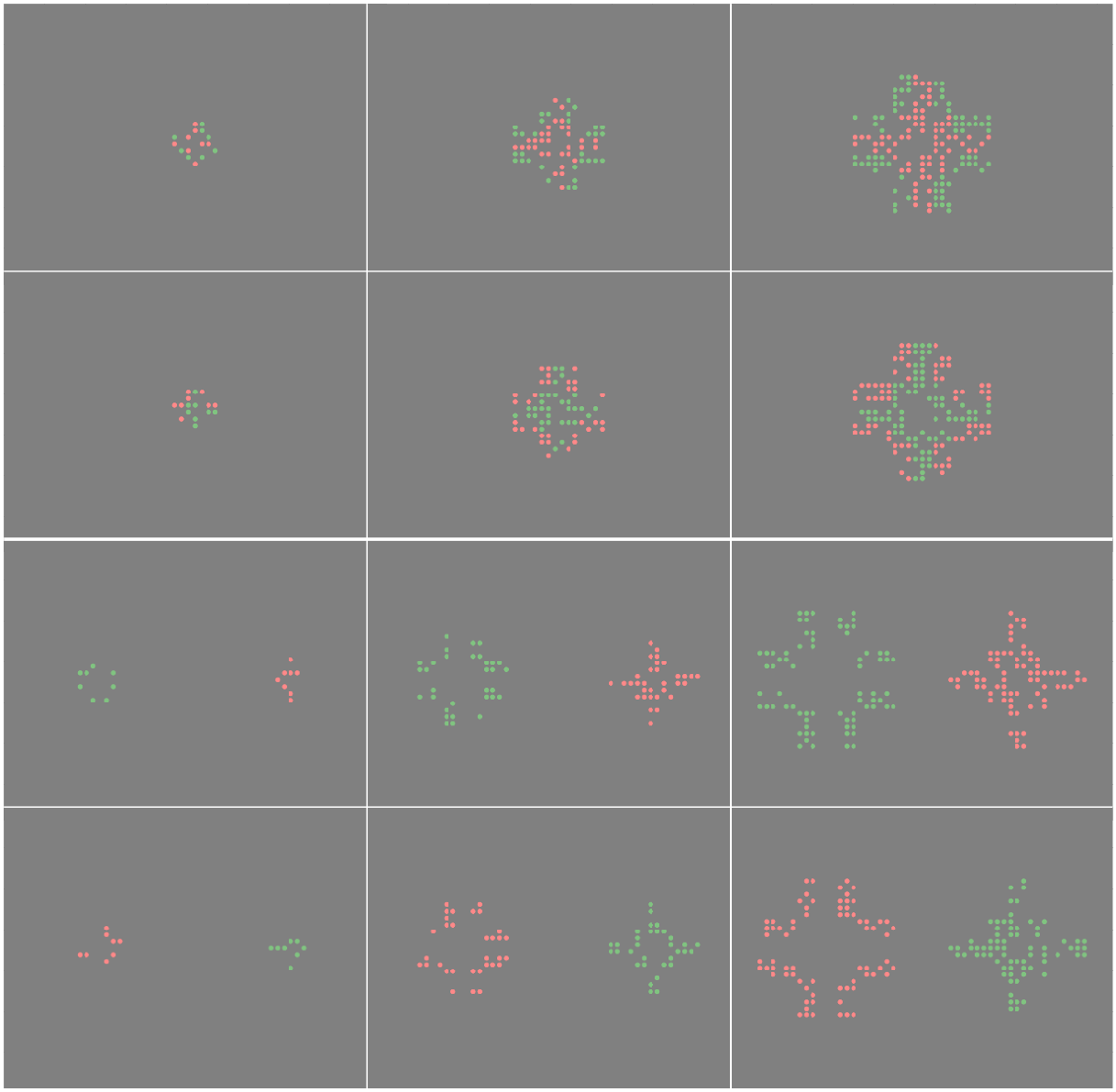

Figure 3.7: Stimuli for Experiment 3 were generated starting from configurations like those of Experiment 1. Patterns were created, and then a random sample of 50% of the elements were kept and the rest deleted. Therefore, unlike Experiment 1, no exact stimulus was ever presented to the participants twice. Here examples of stimuli can be compared to those in Figure 3.2.

Stimuli and Procedure

The procedure was the same as for the previous experiments.

Stimuli was the same as previously except that only some of the elements were visible. The regular configurations were reduced to just 50% of the full array. This sampling was done randomly using the computer random number generator.

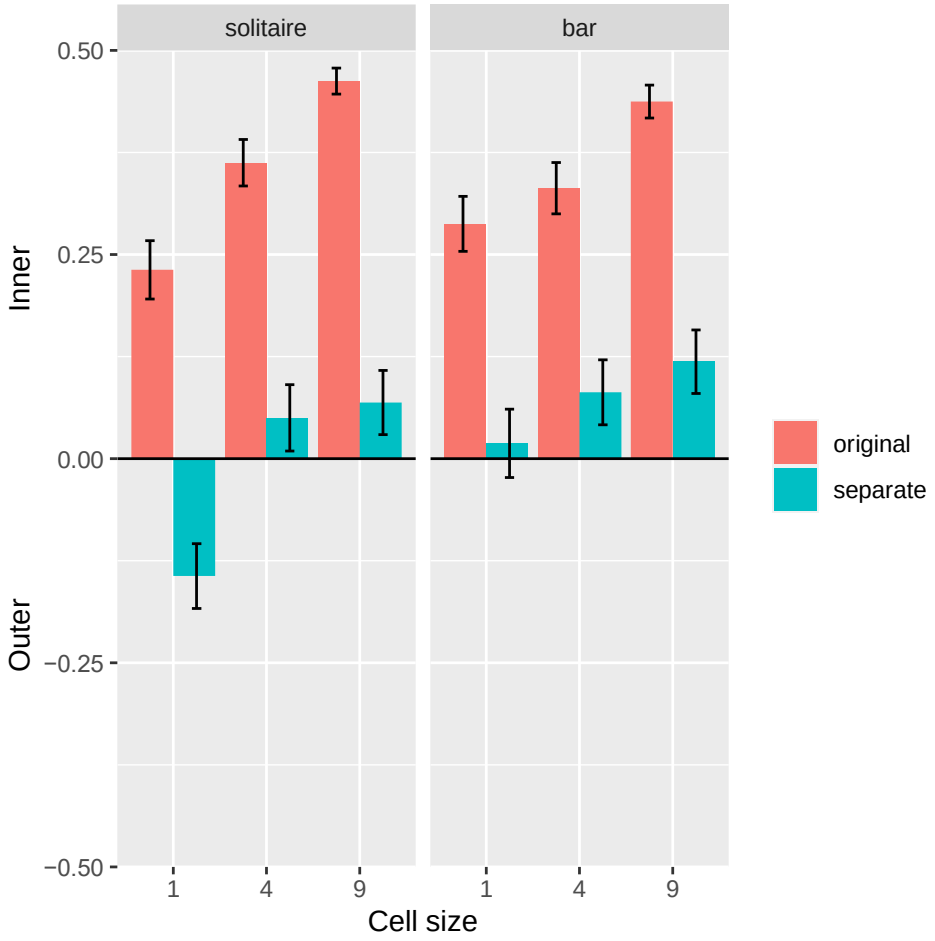

Figure 3.8: Proportion of responses for the two versions of the illusion (Solitaire and Bar). Cell size is the number of elements in each of the cells. The two colours are for the original combined configuration and the presentation of the two sets as separate groups. Error bars are ± 1 SE of the mean.

3.4.2 Results and discussion

The analysis of deviance with the Type III Wald chi-square tests for the memory score showed a significant main effect of Separation (χ2= 203.860, df= 1, p< 0.001, part R2= 0.138, C.I.= 0.111 – 0.187), and Cardinality (χ2= 58.410, df= 2, p= 0.01, part R2= 0.036, C.I.= 0.006 – 0.095). Among the interactions, Separation:Cardinality (χ2= 13.769, df= 2 , p= 0.001, part R2= 0.049, C.I.= 0.010 – 0.119), and Illusion:Cardinality (χ2= 6.322, df= 2, p= 0.042, part R2= 0.005, C.I.= 0.000 – 0.080) were also significant. All other effects were not significant. Table 3.4 summarizes the results of the Wald test for experiment 3.

Table 3.4: Analysis of Deviance Table (Type III Wald chi-square tests) for Experiment 3 with part R2 for each term in the model. Model marginal R2 = 0.208, C.I = [0.188 – 0.306].

	$\chi 2$	DF	$p(>\chi^2)$	part R^2	R^2CI
(Intercept)	7.227	1	0.007		
Separation	203.860	1	0.000	0.138	0.111 – 0.187
Illusion	0.546	1	0.460	0.003	0.000 – 0-066
Cardinality	58.410	2	0.000	0.036	0.006 – 0.095
Colour	0.779	3	0.854		
Order	0.611	1	0.434		
Separation:Illusion	3.761	1	0.052	0.003	0.000 – 0.078
Separation:Cardinality	13.769	2	0.001	0.049	0.010 – 0.187
Illusion:Cardinality	6.322	2	0.042	0.005	0.000 – 0-080
Separation:Illusion:Cardinality	0.358	2	0.836	0.004	0.000 – 0.126

As for Experiment1, I report an exact binomial test for the Separate condition. Number of responses inner was 511 out of a total of 960 trials, $p < 0.049$. The alternative hypothesis was that the probability of success is not equal to 0.5 (95% confidence interval: 0.500 to 0.564). Here the effect is extremely weak, and very different from Experiment 1 and 2. On an individual basis, proportions were above chance for 5 out of 20 subjects.

3.5 Experiment 4

Experiment 3 tested the role of the regularity of the array. Removing 50% of the elements did not destroy the preference for the inner group. In Experiment 4 only 10% of the elements. Examples of stimuli are shown in Figure 3.9. Because of the reduction in number of elements the starting configurations had larger cardinalities, this was achieved by increasing the number of elements in each cell from the original 1, 4 & 9 to 9, 16 and 25. The 10% did not always produce a whole number, therefore each number was rounded up to the nearest whole number, hence the final cardinalities were 15, 26, 40 for SI, and 11, 20, 30 for the Bar version of

SI. Note how we are now having stimuli much more similar to those used in the RRI (see Figure 3.1).

Power analysis. As in Experiment 3, a priori power calculation based on the data collected in Experiment 1, was performed. In this case, it was expected an even greater reduction in effect size, the observed effects sizes of Separation, Cardinality and their interaction were reduced by 50%. As before, one thousand simulations for sample cardinality from 14 to 20 participants, was performed. Once again, with 14 participants the power for the Separation factor was over 90%. The Cardinality reached 90% for n = 18, while their interaction for n = 20 reached a power above 80%. Therefore, the same sample size of Experiment 1, was used.

3.5.1 Methods

Participants

Twenty individuals participated (age range 18 to 36, 3 males). All participants had normal or corrected-to-normal vision, and none reported any colour blindness. The study was approved by the Health and Life Sciences Committee on Research Ethics (Psychology, Health and Society) and conducted in accordance with the Declaration of Helsinki (revised 2008). Participants were naive with respect to the hypotheses.

Design

The design was the same as that if Experiment 4 except that the stimuli were different. The number of elements in each cell (before sampling) was increased from the original 1, 4 & 9 to 9, 16 and 25.

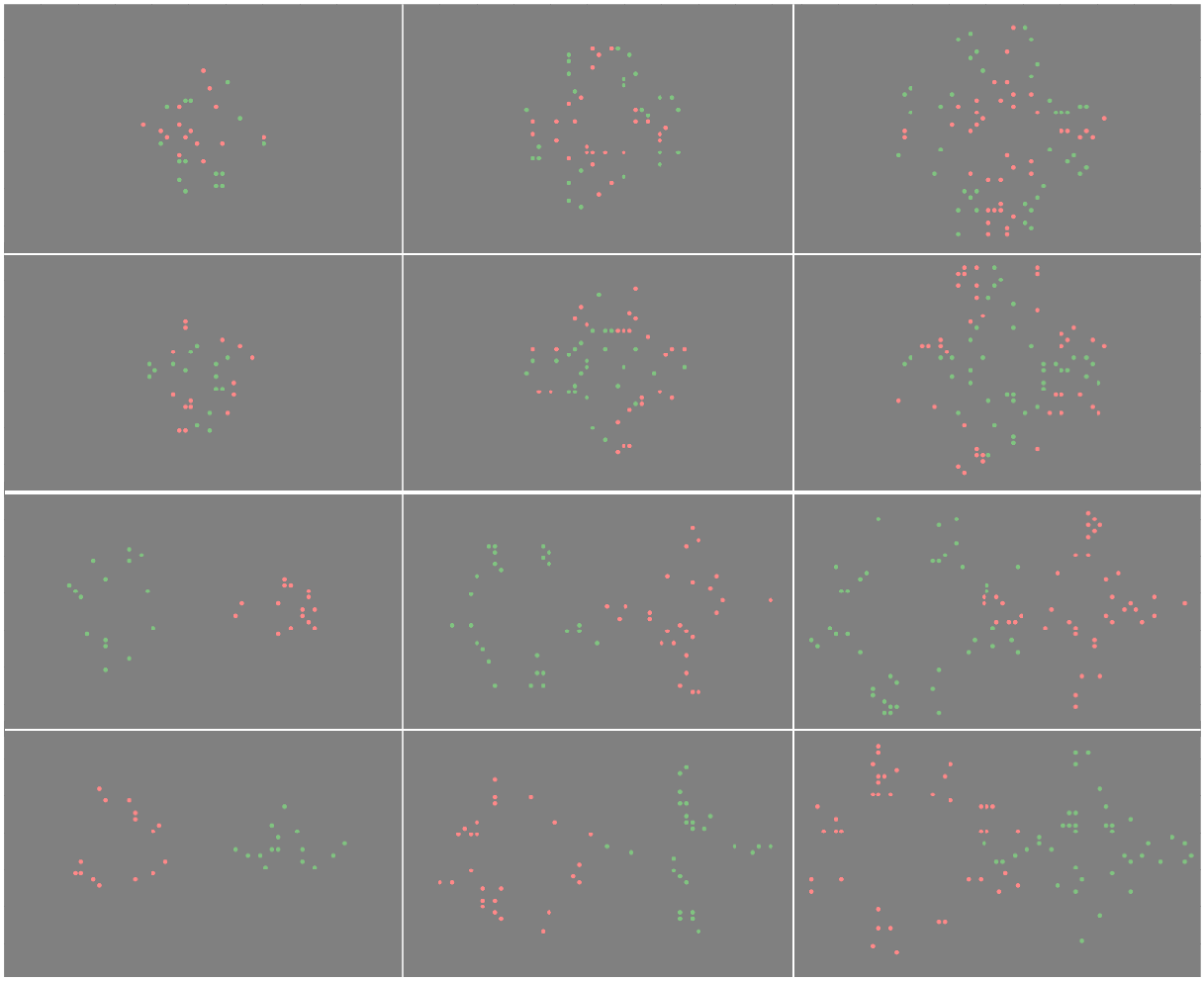

Figure 3.9: Stimuli for Experiment 4. Configurations with high number of elements were created, and then a random sample of 10% of these elements were kept and the rest deleted. Here examples of stimuli can be compared to those in Figure 3.2 and in Figure 3.7.

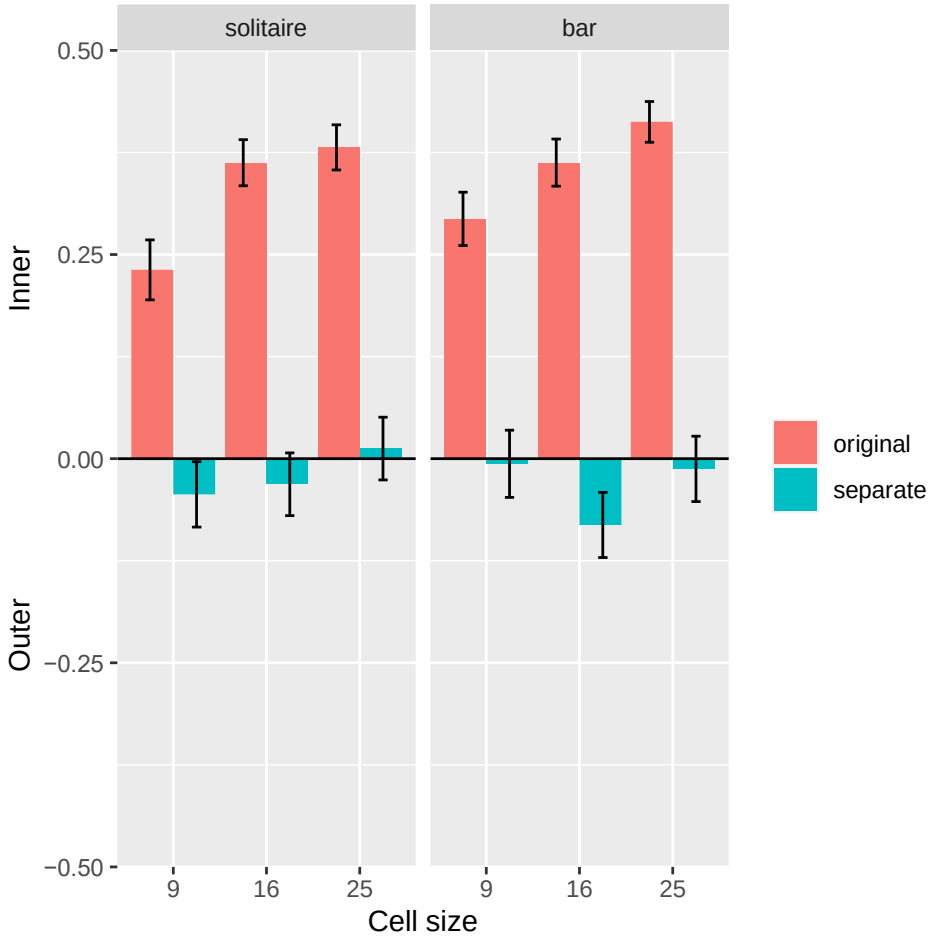

Figure 3.10: Proportion of responses for the two versions of the illusion (Solitaire and Bar). Cell size is the number of elements in each of the cells. The two colours are for the original combined configuration and the presentation of the two sets as separate groups. Error bars are ± 1 SE of the mean.

3.5.2 Results and discussion

The analysis of deviance with the Type III Wald chi-square tests showed a significant main effect of Separation (χ^2= 267.227, df= 1, p< 0.001, part R^2= 0.158, C.I.= 0.127 – 0.184), and Cardinality (χ^2= 16.317, df= 2, p= 0.01, part R^2= 0.008, C.I.= 0.000 – 0.042). Among the interactions, Separation:Cardinality (χ^2= 14.142, df= 2 , p= 0.001, part R^2= 0.019, C.I.= 0.009 – 0.071) was significant. All other effects were not significant. Table 3.5 summarizes the results of the Wald test for experiment 4.

As before, separation reduces the effect, now the illusion has disappeared. When the illusion is present (original configuration) the strength of the illusion increases with cardinality for both Solitaire and Bar version.

Table 3.5: Analysis of Deviance Table (Type III Wald chi-square tests) for Experiment 4 with part R2 for each term in the model. Model marginal R2 = 0.184, C.I = [0.159 – 0.214].

	$\chi 2$	DF	p($>\chi^2$)	part R^2	R^2CI
(Intercept)	7.227	1	0.007		
Separation	203.860	1	0.000	0.158	0.127 – 0.184
Illusion	0.546	1	0.460	0.000	0.000 – 0-036
Cardinality	58.410	2	0.000	0.008	0.000 – 0.042
Colour	0.779	3	0.854		
Order	0.611	1	0.434		
Separation:Illusion	3.761	1	0.052	0.001	0.000 – 0.055
Separation:Cardinality	13.769	2	0.001	0.019	0.000 – 0.071
Illusion:Cardinality	6.322	2	0.042	0.000	0.000 – 0-054
Separation:Illusion:Cardinality	0.358	2	0.836	0.001	0.000 – 0.038

As for all other experiments, I report an exact binomial test for the Separate condition. Number of responses inner was 454 out of a total of 960 trials, $p < 0.100$. The alternative hypothesis was that the probability of success is not equal to 0.5 (95% confidence interval: 0.441 to 0.505). Therefore, for this condition there is no evidence that people are more likely to select inner or outer. On an individual basis, proportions were above chance for 4 and below chance for 6 subjects out of 20.

3.6 General Discussion

The Solitaire illusion is an interesting and surprising effect. For most observers there is a strong bias to perceive a difference in cardinality between two sets of elements based on their configuration (Frith & Frith, 1972). In the original configuration the outer set, which is the one perceived as less numerous, is split into subsets of few elements. Specifically, the 16 elements are

divided into 8 groups of two. Also, modification of the pattern to include higher cardinalities, to avoid that any of the subsets would fall within the subitizing range. In all experiments both the original configuration (Solitaire) and the version with a line of dots (Bar) as illustrated in Figure 3.1, was used.

Also, four colour combinations, red inside/green outside, green inside/red outside, blue insider/yellow outside, yellow inside/blue outside, was used. It was found that colour had no effect. Note only colours similar in luminance and contrast, was used. It is known that low contrast disks appear higher in cardinality when intermingled with the high contrast ones (Lei & Reeves, 2018).

Table 3.6 is a summary of the results from four experiments. In Experiment 1, it was found that the illusion exists also at high cardinalities, although it was slightly reduced for the Solitaire version as cardinality increased. The story was quite different in Experiment 3 and 4, where the elements appeared as clouds and not fixed within a rigid alignment grid. Here the illusion was still present (as long as the two groups were not separated) but the strength increased with cardinality. This could be due to the fact that at low cardinality the inner/outer separation is partly lost for sampled displays, while with high cardinality the inner/outer separation becomes easier to see (see Figures 3.7 and 3.9).

Table 3.6. A list of the four experiments and main findings.

Experiment	Main factors	Results
Exp 1	Version	The illusion generalises to large cardinalities, well above subitization. It also survives the separation of the two groups:
	Cardinality	1, 4, 9
	Separation	SI together: 92%, separate: 72% Bar together: 87%, separate: 81%
Exp 2	Version	As for Exp 1, there is an illusion in all conditions
	Cardinality	1, 4, 9
		SI together: 89%, separate: 78%
	Separation	Bar together: 81%, separate: 69%
Exp 3	Version	Only 50% of the elements are shown. The illusion is weaker, especially in the separate condition, and it increases with cardinality:

	Cardinality	1, 4, 9
	Separation	SI together: 85%, separate: 57% Bar together: 85%, separate: 57%
Exp 4	Version	Only 10% of the elements are shown. The illusion is absent in the separate condition, when present it increases with cardinality:
	Cardinality	9, 16, 25
	Separation	SI together: 85%, separate: 57% Bar together: 85, separate: 57%

Another important feature of the SI is the enclosure of the inner set by the outer. This was already observed by Frith and Frith (1972) using the bar version of the illusion, but with limited data. Their observers made a single response and were then divided between those who had experienced the illusion and those who did not. For a configuration similar to the one used here (12+12 elements, as shown in Figure 3.1) 12 out of 13 adult observers chose the inner group as more numerous, but only 7 out of 13 did so for the divided version. Therefore, it was expected that placing the two side by side (horizontal translation) would have a large effect.

The separation of the groups could eliminate or reverse the illusion because when separated it is clearer that one set spreads over a larger area (Dakin, 2011; Tokita & Ishiguchi, 2010). Contrary to this prediction, in Experiments 1 and 2 the illusion survived the separation of the two groups, although the effect was reduced. This result is consistent with what recently reported by Pecunioso and Agrillo, (2021). They used the original version of the SI and presented it in the standard configuration and also as separate groups (inner and outer subsets, each with 16 elements). The task was different from what had been used, as observers had to report verbally an estimate of the number of dots. Despite the difference in tasks, it is clear in both studies that the SI is not completely eliminated by the separation, suggestion that the key factor is the distribution of the elements.

The SI, was eliminated only when the elements were made to appear as clouds of elements. This was achieved in Experiments 3 and 4 by starting with the original configurations and then removing randomly 50% (Experiment 3) or 90% (Experiment 4) of the elements.

However, in no case was a reversal of the effect seen. The manipulation necessary to destroy the illusion in Experiments 3 and 4 also weakened grouping and Gestalt factors such as continuity (Frith and Frith, 1972) and clustering (Valsecchi, 2013). When enclosure is present, however, the illusory effect wins out over grouping (Experiment 1) and continuity (Experiment 2), and even when enclosure is weak (Experiments 3 and 4) dispersion over a larger area (causing overestimation) is countered by a possible effect of central location of the elements (causing underestimation). These two effects may then cancel each other out leading to no overall bias.

In the introduction it was mentioned that at high densities, patterns behave differently because individual items are no longer discernible as separate items. The switching point can depend on various factors, but is around 1 dots/deg^2 (Anobile et al., 2016). In Experiment 1 and 2, relative to a square enclosing region, densities ranged between 1 and 1.79 dots/deg^2. The case is special because of the regularity of the pattern. It is a question that will require further work, regularity could increase the perception of a uniform texture, or do the opposite, and allow elements to remain separate items (for the role of regularity on crowding see Sayim et al., (2010). In Experiment 3 and 4 density was lower because of sampling (between 0.54 and 0.89 for Exp 3, between 0.16 and 0.26 for Exp 4).

We have seen that the central location is therefore the key factor in the SI, but why? One possibility was noted already in the introduction, a decrease in perceived numerosity in the visual periphery (Valsecchi et al., 2013). It has been suggested that in the periphery elements can become harder to identify and segment from each other, in line with the phenomenon of crowding. However, the relationship between numerosity and crowding is far from clear (Anobile et al., 2016; Chakravarthi & Bertamini, 2020). It should also be noted that in all experiments there was no control fixation and eye movements. In other words, the central region remains a central region, and has higher density, because of its location, not position in the visual field.

In the original study, Frith and Frith (1972) pointed out that Gestalt factors are important for the illusion. Perhaps grouping is related to figure-ground organisation, and elements in the foreground become more influential in cardinality judgments. The problem, as we have seen, is that other Gestalt factors, such as brightness (Ross & Burr, 2010), or grouping by connectedness (Franconeri et al., 2009), lead to the opposite effect (a reduction in perceived numerosity).

In conclusion, despite the fact that the original illusion may have been noticed serendipitously, looking at a board game (Frith & Frith, 1972), the underlying phenomenon is strong and general. Alignment is not important, any time a set appears *inside* another, or is more centrally located, the estimation of cardinality is biased in its favour.

4 On the usefulness of graph-theoretic properties in the study of perceived numerosity

4.1 Introduction

Humans and other animals can estimate the quantity of a set of visual elements. This ability has been called the number sense (Cantlon, Platt & Brannon, 2009; Dehaene, 2011). However, estimations can be systematically biased by visual properties, such as size and clustering of the elements. Many studies have investigated the effect of visual properties of 2D configurations of elements on perceived numerosity. In this chapter, I focus on various indices from graph theory and their relevance for the perception of numerosity. I will start with a review of the numerosity literature and an introduction to the relevant aspects of graph theory. Then I will report a series of analyses. This analysis identifies two main groups of measures; one sensitive to presence of local clustering of elements, the other more sensitive to density.

4.1.1 Perception of Numerosity

The capacity to estimate the difference in quantity or numerosity between two sets of elements without the use of counting or symbolic representation, is an important ability present in humans and in other species (Dehaene, 2011; Neider, 2019). There are two separate mechanisms. For small sets ($N<5$), the precise number is rapidly determined without the need to individually attend to each item ((Kaufman et al., 1949; Trick & Pylyshyn, 1994). For larger sets, when counting or immediate apprehension of quantity is not possible, a different mechanism allows numerosity estimation (Burr & Ross, 2008; Dehaene, 1992; Izard & Dehaene, 2008). This mechanism has been postulated as the approximate number system (ANS), and is believed to be responsible for non-symbolic representation of large numerosities (Dehaene, 2011). Also not precise, it is used in basic operations such as estimation, subtraction and comparison (Cantlon & Brannon, 2007). A feature of the ANS is that with increasing difference in numerosity between two configurations, the task of choosing the larger set becomes easier: the distance effect.

Furthermore, if the size of both sets increases, the task of extracting the larger set becomes harder: the size effect. Hence, the most important parameter is the ratio of the two numerosities, in accordance with Weber's law.

Studies of the ANS in humans and non-human animals have found converging results. For instance, mosquitofish can discriminate between social groups if the ratio in group size is at least 1:2 (Agrillo et al., 2008). In non-human primates, numerosity performance decreases when the numerical distance between sets becomes smaller (Barnard et al., 2013). When it is difficult to process separate elements within dense patterns, they are perceived as texture and the properties of the estimation process change (Anobile et al., 2014, 2015).

It is well-known that several properties of the stimuli affect perceived numerosity. In particular, the geometric configuration of the elements biases judgements of numerosity. There is evidence of this in two phenomena: the solitaire illusion (Frith & Frith, 1972) and the regular-random numerosity illusion (Ginsburg, 1976; Ginsburg, 1980), see Figure 4.1. For the solitaire illusion, a regular pattern of black and white dots (similar to the pieces in the game of peg solitaire) leads to a striking impression that the dots in the centre are more numerous, Figure 4.1 A. For the regular-random effect, the elements that are spaced evenly are perceived as more numerous than the randomly distributed elements Figure 4.1 B. In both cases, and also in more generic configurations, it is the groupings or clustering of the items that influences perceived numerosity (Allik & Tuulmets, 1991; Bertamini et al., 2016; Cousins & Ginsburg, 1983; Im et al., 2016).

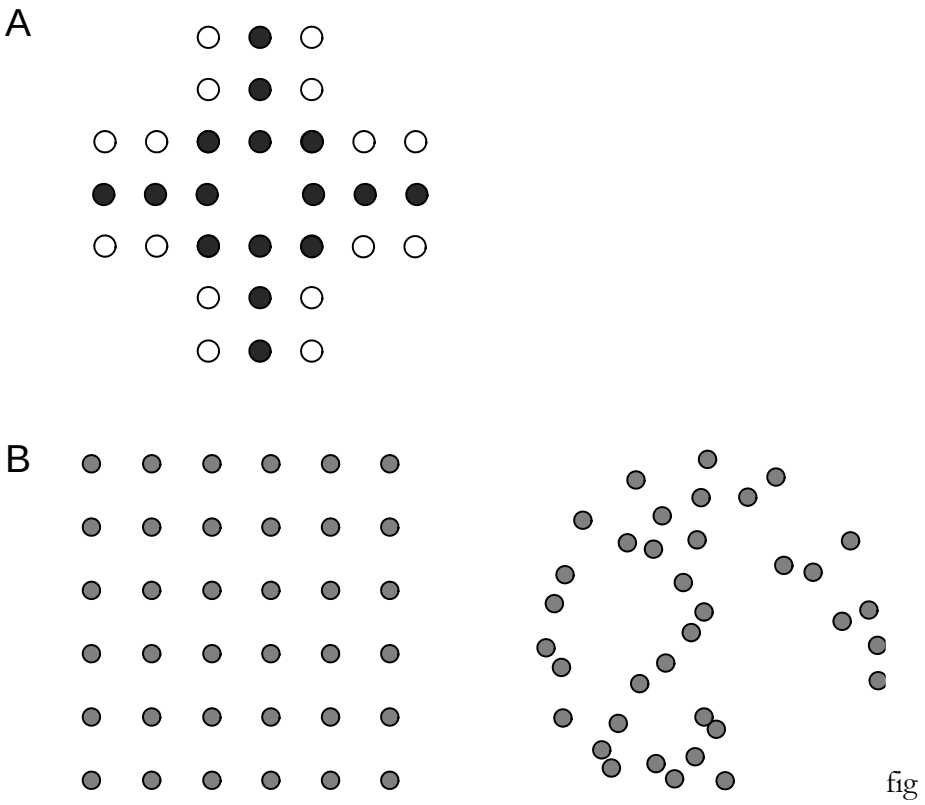

Figure 4.1. A. Solitaire illusion. People perceive that there are more black than white dots (Frith & Frith, 1972). B. Regular-Random Numerosity Illusion. A regular configuration of dots (on the left) is perceived as more numerous than the random configuration on the right. Both configurations have the same number of dots (Ginsburg, 1976).

The observation that grouping leads to underestimation led to the occupancy model (Allik et al., 1991; Allïk & Tuulmets, 1991). According to this model, each element is surrounded by a region of influence whose effect decays with the distance to the element (Burgess & Barlow, 1983). If two or more elements are close together, then their respective regions of influence will overlap, and their combined contribution to the perceived numerosity diminishes. Allïk and Tuulmets (1991) approximated these regions by circles of fixed radius r. If two elements are at a distance smaller than $2r$, then the circles of influence will overlap and their combined area, or occupancy value, will decrease. The model predicts that configurations with a greater occupancy value will be perceived to have greater numerosity.

Both the Solitaire illusion and the Regular-Random Numerosity illusion show the importance of configuration. Frith and Frith (1972) already explicitly mentioned grouping and Gestalt formation. Proximity has a key role in grouping (Kubovy & Wagemans, 1995), and asits

is known that the occupancy model provides a measure based on proximity. Proximity may also lead to crowding, as a possible cause of underestimation (Chakravarthi & Bertamini, 2020; Valsecchi et al, 2016). Not everything, however, can be reduced to proximity. For the Solitaire illusion in Figure 4.1A, the average distance between elements is greater for the white than for the black dots, and yet the black dots are judged as more numerous. This is the opposite of the effect of average distance in the Regular-Random Numerosity illusion. Another curious and unexplained effect occurs when the convex hull is computed. The area is larger for the white compared to the black dots in the Solitaire illusion Figure 4.1A. Therefore, although in the general case the larger area leads to an increase in perceived numerosity (Hurewitz, et al., 2006), in the case of this particular configuration there is the opposite effect. The SI and its variants, are studied more closely in chapter 5.

4.1.2 Graph theory

Graph Theory is a branch of Mathematics that dates back to, at least, Euler (1707-1783) and the famous Königsberg bridges problem (which Euler proved to have no solution), see introduction. Its main object of study are collections of objects, modelled as dots, points, or vertices, and the relationships between these elements, usually represented as edges (lines connecting pairs of points). In this thesis, the term vertex or dot interchangeably, and edge for the line connecting two vertices. I present some graph-theoretic numerical measures that could be useful to capture properties of dot configurations, and therefore also help explain numerosity judgements. I report a correlation analysis between pairs of these measures and between these measures and occupancy because the latter is known as an effective model for perception of numerosity.

A graph G can be defined as a finite structure formed by a non-empty set of vertices $\{v_1, v_2, \dots, v_n\}$ and a set of edges connecting pairs of vertices. Let $G(V, E)$ denote a

graph with vertex set V and edge set E. If v_i, v_j is an edge, denoted as e_{ij}, then both vertices in e_{ij} are said to be adjacent with each other, Figure 4.2.

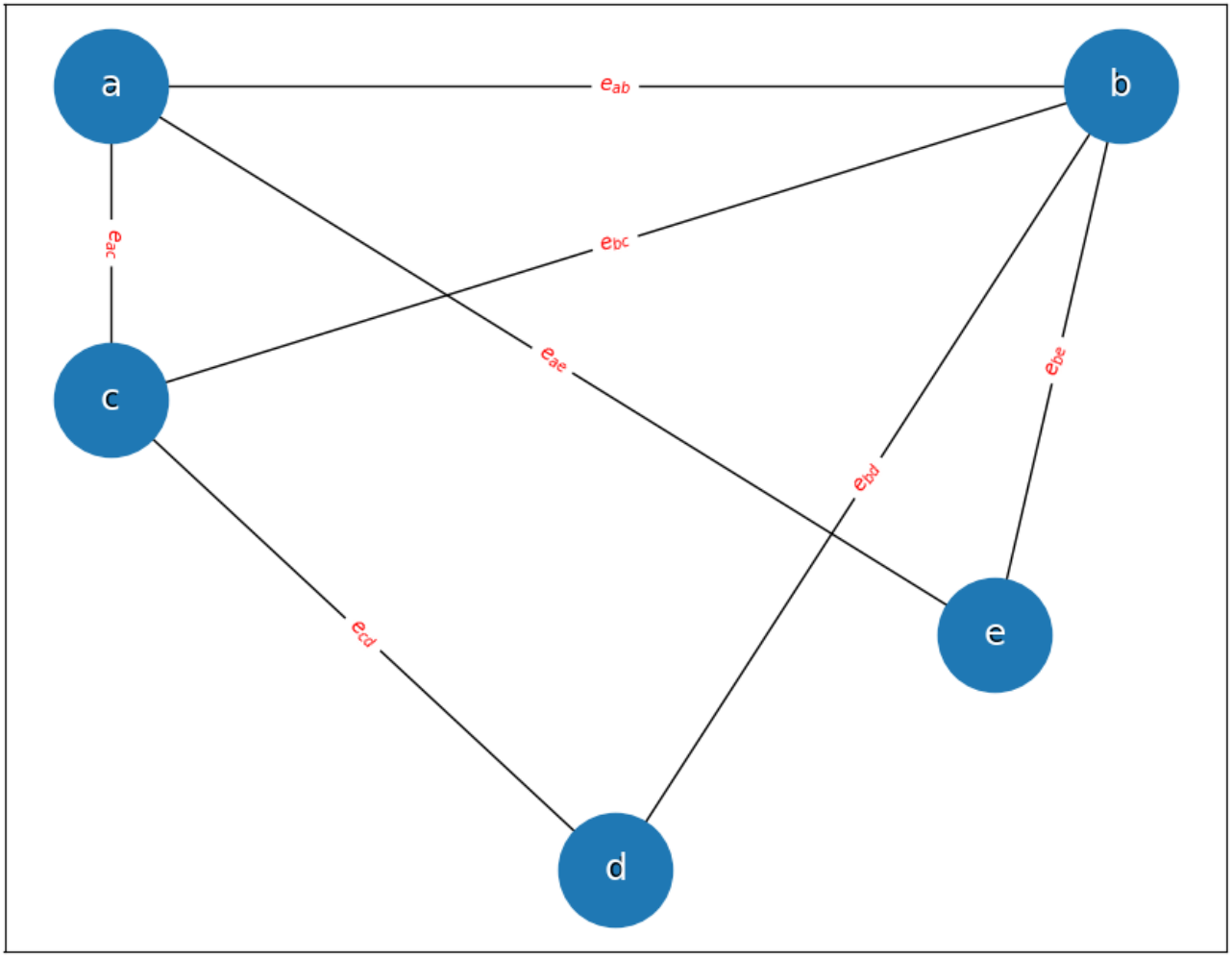

Figure 4.2: Graphical representation of a simple graph, with 5 vertices and 7 edges. Vertices are labelled a, …, e, edges are labelled e_{ij} where i and j are the vertices incident on that edge. The vertices can represent any object, the edges represent some binary relationship between vertices such as

A simple graphical representation of a graph is shown in Figure 4.2. The graph has 5 nodes labelled a, b, c, d and e, and 7 edges labelled e_{ij}., where the indexes i and j represent the vertices adjacent to each other.

Matrices offer an alternative way to describe graphs. Given a graph G with n vertices the adjacency matrix of G is an $n \times n$ table A_G whose rows and columns are indexed by the vertices of G and element of $a_{v_i v_j}$ of $A_G$will have a value of 1 if v_i and v_j are adjacent and 0 otherwise. The adjacency matrix of the graph shown in Figure 4.2, is shown in equation 4.1.

eq 4.1

$$A_G = \begin{array}{c} \\ A \\ B \\ C \\ D \\ E \end{array} \begin{array}{c} \begin{array}{ccccc} A & B & C & D & E \end{array} \\ \begin{bmatrix} 0 & 1 & 1 & 0 & 1 \\ 1 & 0 & 1 & 1 & 1 \\ 1 & 1 & 0 & 1 & 0 \\ 0 & 1 & 1 & 0 & 0 \\ 1 & 1 & 0 & 0 & 0 \end{bmatrix} \end{array}$$

A walk, defined as $W = v_0, e_0, v_1, \dots, v_{f-1}, e_f, v_f$ is an alternating list of vertices and edges, where v_0 and v_f are the endpoints of the walk W on graph G. A walk that has no repeated edges is called a trail, and a walk with no repeated vertex is a path. The only exception to this is if the endpoints are the same vertex, then its a closed path or cycle. Likewise, a trail whose endpoints are the same vertex is called a closed trail. If every two vertices in graph G, are the endpoints of a walk, then the graph G is connected, else the graph is disconnected and formed by two or more separate sub-graphs called components. When every vertex is adjacent to every other vertex, we have a complete graph, denoted by K_n, where n is the number of vertices.

A simple visual representation of a random geometric graph is shown in Figure 4.3A. Here the vertices are placed in a metric space, e.g., the plane, and are connected by an edge if and only if their Euclidian distance is less than a threshold, i.e., a radius r. A simple example is shown in Figure 4.3B.

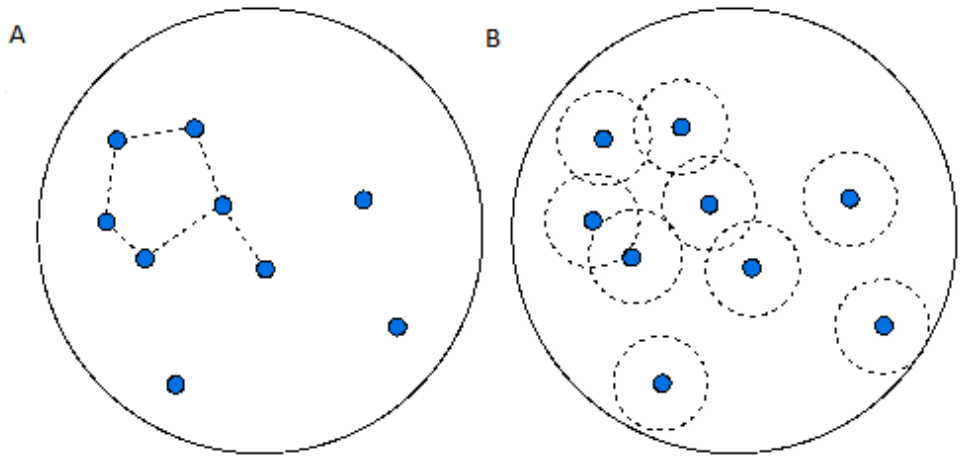

Figure 4.3: A small graph on nine vertices connected by a number of directed lines, describing a binary relationship on the set of vertices. Here position in the plane is irrelevant. I will focus on a special case of graphs (Random Geometric Graphs) in which connectivity is related to distance and edges are non-directional. Bottom: Comparison between the occupancy model and the graph theoretic approach. On the left the connecting edges are based on a distance threshold, whereas on the right it shows overlapping occupancy regions.

4.1.3 Graph theory and occupancy

Graphs and graph-theoretical measures provide ways to quantify the difference between two configurations. If the visual system is sensitive to these properties, these differences may explain perceived numerosity. A few studies have already employed some of these indices (e.g. Bertamini et al., 2016, 2018; Im et al., 2016), and more recent work has computed average edge length on a nearest neighbour graph as an alternative to occupancy (Allik & Raidvee, 2021). Unlike other measures such as size of the physical elements, measures based on graph properties are not based on arbitrary units (e.g., pixels, centimetres, inches).

For any 2D configuration, two vertices can be considered connected if their Euclidean distance is less than a given distance d, thus defining a random geometric graph G_d. Note that this distance is closely related to the region of influence hypothesised in the context of the occupancy model. The overlap between two neighbouring regions of influence occurs when the distance between the vertices is no larger than $2o_r$, where o_r is the occupancy radius; if we set $d = 2o_r$ then the edges of G_d describe exactly those elements whose regions of influence intersect. Figure 4.3B compares the two approaches for an example with only nine vertices.

As in the case of the occupancy model, the graph structure varies with the distance parameter, the larger the value of d the more edges there will be in G_d. Figure 4.4 shows a random 40-vertex configuration inside a circle C_R of radius R. In panel A, at a small connectivity distance of $d = R/4$, the graph is disconnected into ten components, the largest of which has 18 vertices. As the connectivity distance increases, eventually the graph connects (panel B). If the connectivity distance increases, more vertices will be connected, and the graph becomes denser. Finally, at $d = 2R$ all vertices are connected, and the last panel (D) describes the complete graph K_{40}.

The difference in graph structures between panels suggests that many properties of random geometric graphs change with connectivity distance. It is clear from the top left panel in Figure 4.4 that a small value of d, leads to G_d being split into two or more components. The other three panels represent a connected graph.

There is an important difference between the occupancy model and any index defined on graphs. Graphs are abstract entities defined on vertex configurations on the basis of adjacencies. Even when edges describe geometrical proximity between elements, the existence of the edges of G_d depends on the proximity of the vertices with a strict "all-or-none" criterion.

It is also important to say what aspects I did not consider in this study. I focus on the properties of the configuration, defined by the relationship between locations. The nature of the elements themselves is not relevant. I do acknowledge that numerosity perception is affected by properties of the elements. For example, twenty dots may have twice the surface area of ten dots. The correlation of these continuous measures with numerosity is a problem, recently discussed by (Salti et al., 2017). However, these physical properties of the elements are outside the scope of this thesis.

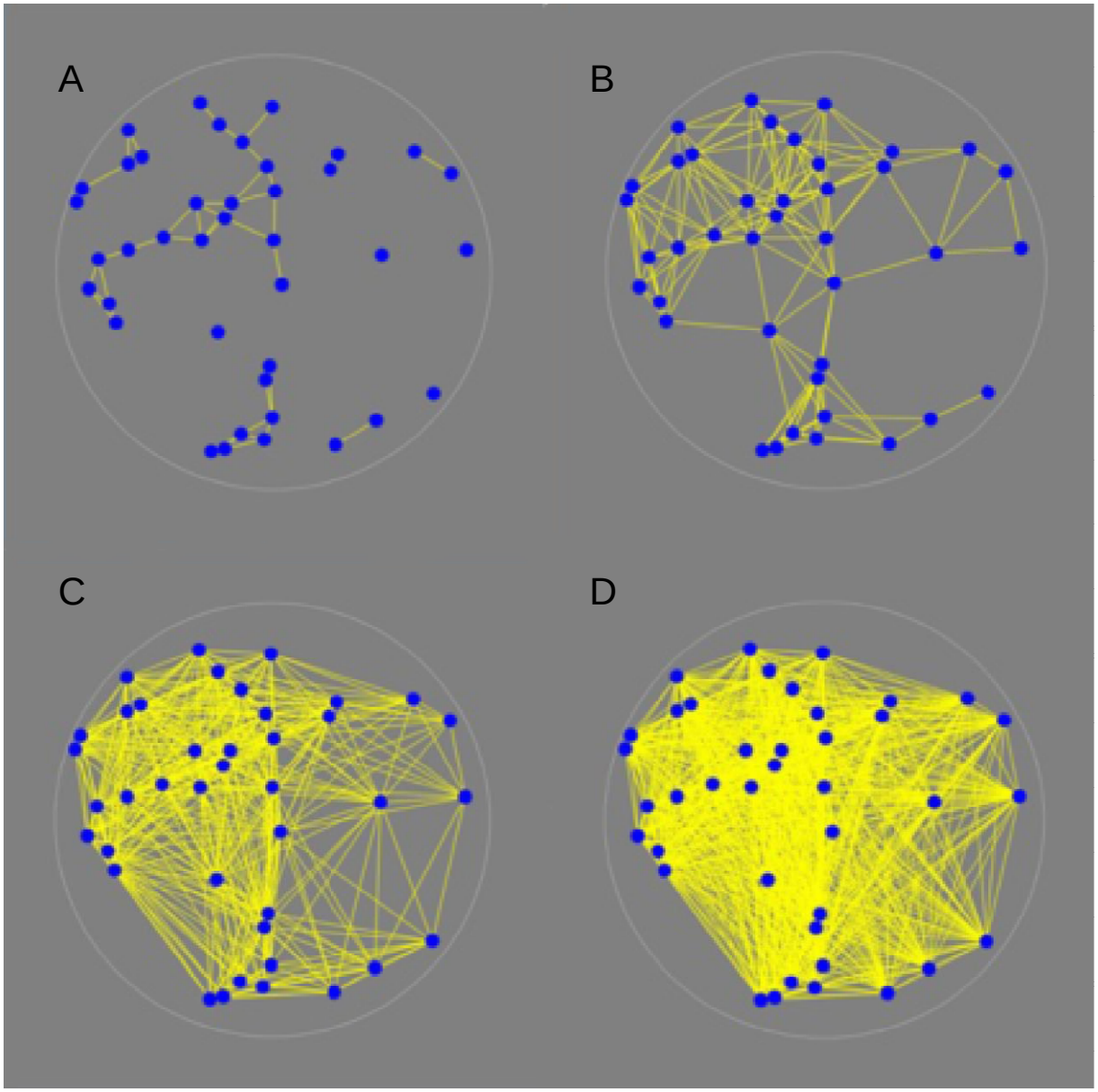

Figure 4.4: A: connectivity distance = $R/4$, number of edges 43, the graph is disconnected, B: connectivity distance = $R/2$, number of edges 171, the graph is now connected. C: connectivity distance R, number of edges 468, the graph is becoming denser. Finally, D, connectivity distance $2R$, number of edges 780, this is the complete graph K_{40}

Bertamini et al. (2016) used some graph indices in their study of numerosity. They considered three numerical measures of the configurations: the area of the convex hull, total degree, and (average) local clustering. They then compared these measures to predictions made by the occupancy model. The convex hull is a useful measure of overall dispersion. In 2D it can be defined as the closed curve with minimum perimeter containing all elements. Unlike the other indices discussed, it does not depend on the connectivity parameter d. The degree of a vertex

was defined earlier as the number of its edges, to get the total degree I sum this for all vertices. Because an edge always connects two vertices, total degree is twice the number of edges. Finally, the local clustering index will be defined in the next section. Bertamini et al. (2016) generated datasets for a limited range of connectivity distances d (approximately between $d = R/8$ and $d = 3R/4$, in steps of $R/16$), and then used correlational analysis to compare indices. However, the values of d did not cover the full range of possibilities (as shown in Figure 4.4, d can take on any positive value up to $2R$).

In this thesis I consider 10 graph indices along with the occupancy model and study their correlations for randomly generated vertex configurations. This list is not exhaustive, but it includes well-known indices developed to capture "clustering", as well as other properties. As argued in the introduction, there is evidence pointing to the importance of grouping and clustering (e.g. the Solitaire illusion). Also, for comparison I included the occupancy model.

I first investigate correlations between the indices for fixed values of the connectivity distance, across its full range. Certain correlations will depend on the connectivity distance, and in addition, some of the indices will only be valid for a limited range of d. I then describe a strategy that captures the key properties of the correlations between indices. I selected a specific connectivity distance for each index and then correlated the index values obtained at this distance. The correlation results obtained in this way capture the main correlations observed at fixed connectivity distances. Finally, a principal component analysis was performed in an attempt to isolate meaningful clusters of similar indices.

Correlation studies on graph indices have been attempted before on a smaller scale. For instance, Guzman et al. (2014) looked at different types of centrality and clustering measures, for a collection of 320 different graphs (or networks as these were called). In another study, Meghanathan (2016) concentrated on centrality measures and their correlation with maximal clique, with the aim of using correlational analysis to find computationally “light weight” alternatives to maximal clique. I will discuss the definition of clique in the next section.

A correlational analysis enables us to study certain (difficult) graph indices by working with related (simpler) ones. This has been done before, analytically, in several studies of random graph properties.

The remainder of the chapter is organized as follows. In the next section the selected indices are described. I then provide all the details of our tests. The last part of the chapter is devoted to an analysis of the results.

4.2 Description of the indices

Hundreds of different graph indices exist. In choosing the list of indices, I picked measures that are sensitive to connectivity distance, and indices that have been studied in other disciplines. I wanted to take advantage of the range of features that different graph indices can compute. For instance, information spread on graphs can be affected by only a small number of vertices (Karunakaran et al., 2017), and there exist centrality measures that are known to extract information about such vertices (Newman, 2018). I will work with Eigenvector Centrality as an example of such centrality measures. Eigenvector Centrality has been used in social network analysis, as well as clique finding and clustering (Wasserman & Faust, 1994). Both independent and dominating sets have been used in wireless sensor networks (Basagni, 2001; Fu et al., 2015). Lastly, I included connected components and total degree as these are particularly sensitive to groupings and density, which are known to be of importance in studying numerosity (Anobile et al., 2015; Frith & Frith, 1972).

Definitions in each case (except for occupancy) are given next. To avoid dealing with range heterogeneity, all indices were normalized by the maximum value for a given fixed number of vertices n. However occasionally the normalization factor depends on d.

4.2.1 Total Degree TD

The Total Degree in a graph is the sum of the degrees of its vertices. Each edge is adjacent to two vertices, and the sum of the degree is therefore also twice the number of edges, equation 4.2.

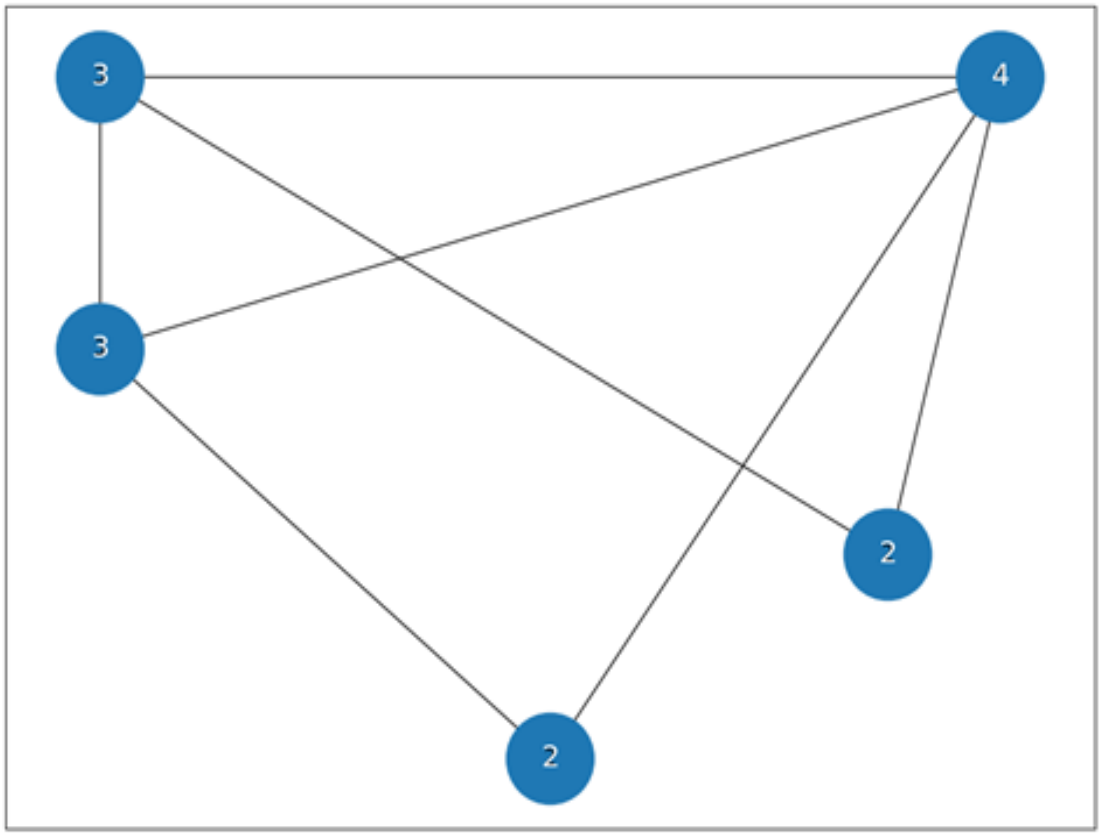

Figure 4.5: The degree of each vertices is used as the label of each vertices. The degree of a vertices is the number of edges incident to it.

eq 4.2

$$\sum_{v \in V} \deg v = 2|E|$$

Figure 4.5 shows the graph from Figure 4.2, except the degree of each vertex is used as its label. We see that the degree of a vertex is simple the number of edges incident on it.

Normalization: Division by the maximum number of edges possible, $n(n-1) \,/\, 2$, where n denotes numerosity.

4.2.2 Total Edge Length TL

The Total edge Length (TL) of a graph is the sum of the Euclidean distance between all pairs of vertices at a distance of at most d.

eq 4.3 $$TL = \sum_{\{u,v\} \in E(G)} dist(u, v)$$

Normalization: The quantity is normalized by dividing it by $2d|E(G)|$.

4.2.3 Random Walk RW

A random walk on a graph G is a process that, starting at an arbitrary vertex, hops around in discrete times steps following random edges. I am interested in the time needed for the walk to visit (at least once) all vertices of G. I only consider random walks for graphs that are connected. For each G_d I computed 1000 random walks and computed the mean of the number of steps taken. The measure RW is then obtained as the inverse of this number multiplied by its theoretical minimum, which is slightly less than $n \log n$, where n is the numbers of vertices, as proved by Kahn et al., (1989).

4.2.4 Eigenvector Centrality EG

Eigenvector centrality gives a value to each vertex, proportional to the sum of the values of its neighbours (Bonacich, 1987). Formally such vector can be obtained as solution of the equation

eq 4.4 $$\boldsymbol{Ax} = \lambda \boldsymbol{x}$$

where $\boldsymbol{A}$ is the adjacency matrix of the given graph, see eq 4.1 section 4.1.3 for an explanation on adjacency matrix. Also, λ is the eigenvalue. The vector $\boldsymbol{x}$ can be computed iteratively, starting by setting $\boldsymbol{x}$ to be the degree sequence of the given graph. The multiplication $\boldsymbol{Ax}$ generates a new vector. Matrix $\boldsymbol{A}$ can be multiplied by such vector and the whole process repeated until the product $\boldsymbol{Ax}$ stabilizes to satisfy the equation above.

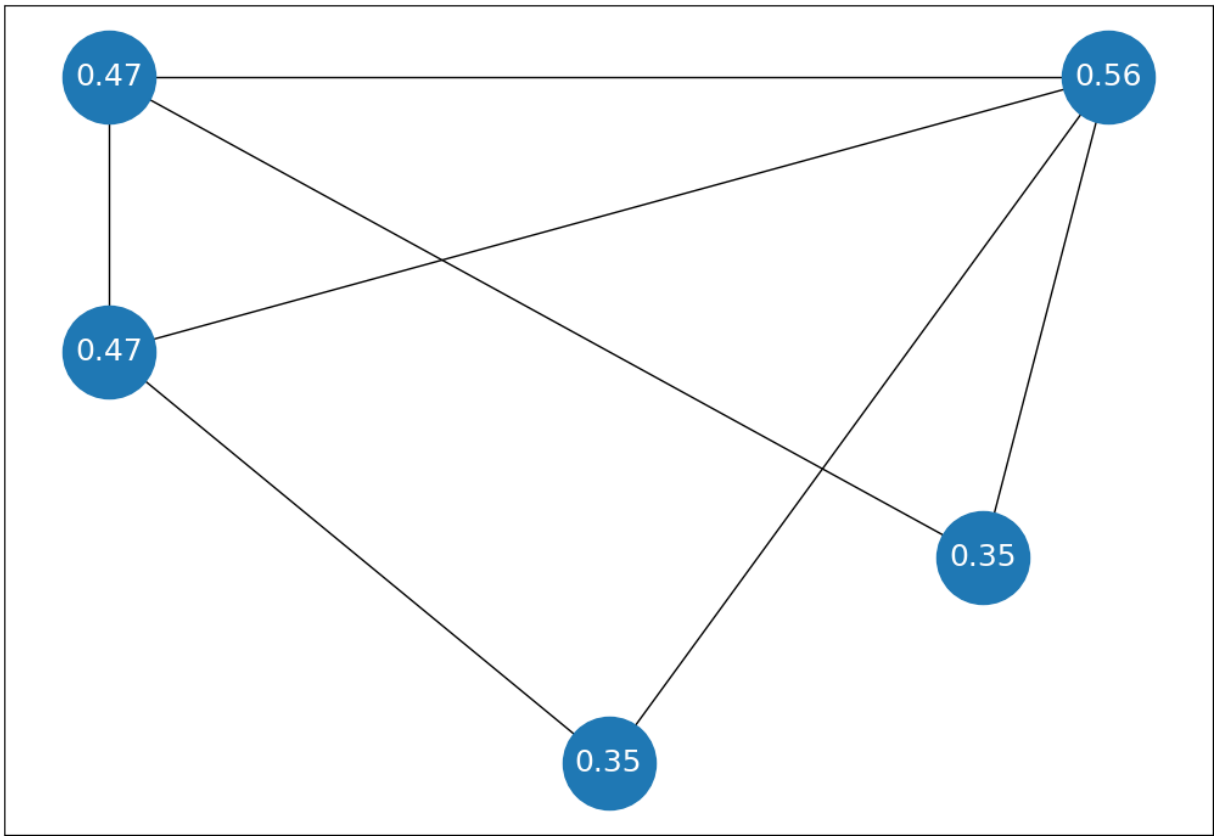

Figure 4.6: A simple graph where the eigenvalue for each vertex is used as its label. We see that the vertex with the highest degree has the highest eigenvalue. This due to eigenvector centrality as an indices being degree based,

If a convergence is achieved after n iterations, then real value λ is an eigenvalue of $\boldsymbol{A}$, and the average value of the components of the resulting $\boldsymbol{x}$ defines the eigenvector centrality of the given graph. If there is no convergence, then its value is zero.

Notice that the vertex with the highest degree, in Figure 4.6, also has the highest eigenvalue. This is because this particular index is degree based.

Normalization: This value is normalized by using the square root of the sum of each eigenvalue, on each iteration.

4.2.5 Connected Components CC

At low connectivity distance, graphs are typically not connected. They can be described as formed by a number of connected components, each containing at least one vertex. Single vertices are treated as one component, the maximum number of components that a graph can have is the cardinality of the set V. As the connectivity distance grows the number of components reduces and eventually d is so large that the graph becomes connected. CC is the number of connected components, divided by the number of vertices.

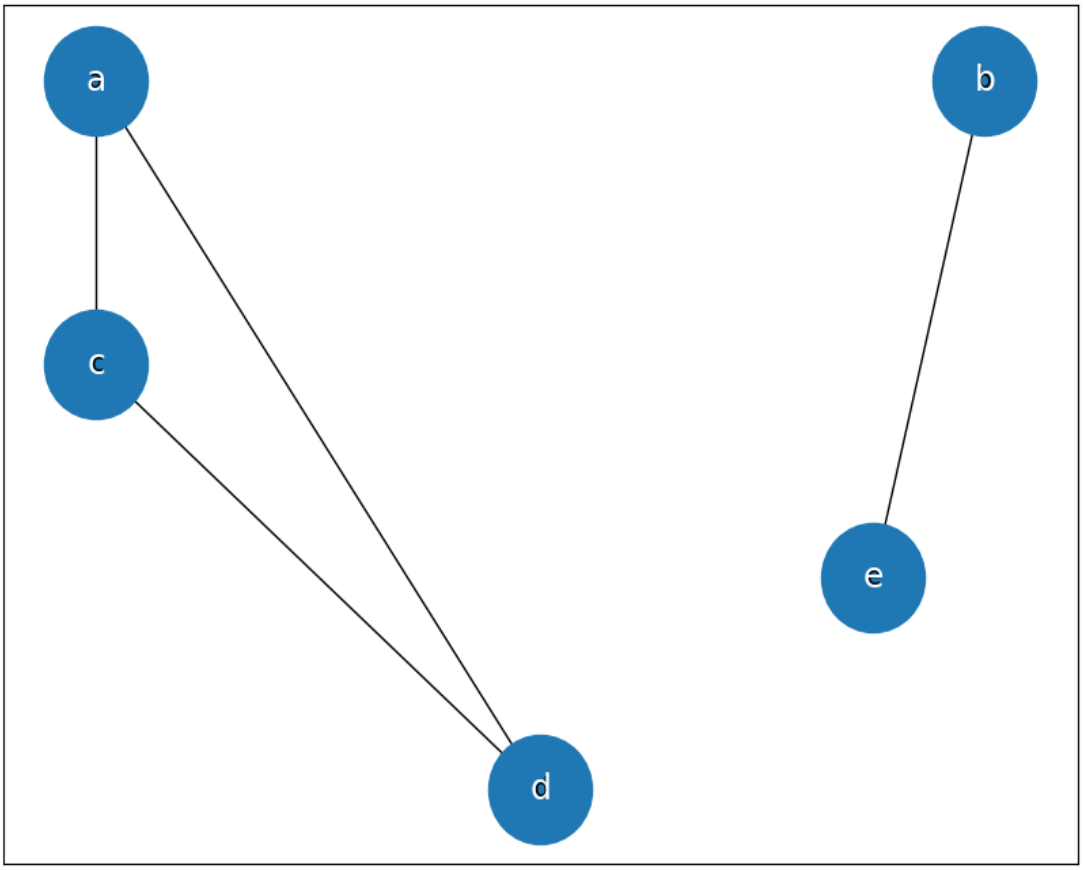

Figure 4.7: A split into two components. The two components consist of vertices (a, c, d) and (b, e). Having more then one connected component is typical when using a small connectivity distance.

We see from Figure 4.7, that the graph shown has two components, one component is vertices (a, c, d), the other is (b, e).

Normalization: The division of the number of vertices in the dot pattern, is used to normalize

4.2.6 Clique number CL

A clique, in a graph G, is a subgraph that is itself a complete graph. The size of the largest clique in a graph G is called the clique number of G. As an example, the largest clique in the graph shown in Figure 4.7 is (a, c, d), as all of these vertices are connected to each other, hence CL for this graph is 3.

Normalization: Division by the number of vertices $n = |V|$, as this is the maximum sized clique.

4.2.7 Domination Number DN

In a graph G, a dominating set D is a subset of the vertex set $V(G)$, such that every vertex in $V(G)$ is either a member of D, or is adjacent to a vertex in D. The set $V(G)$ is trivially a dominating set. The cardinality of the smallest dominating set for G, is called the domination number (DN) of graph G. The set that makes up the dominating set tends not to be unique, as an example, the domination number of the graph in Figure 4.7 is 2. The sets $(a, b),\ (a, e),\ (c, b),\ (c, e),\ (d, b),\ (d, e)$, are all valid dominating sets.

Normalization: Is the number of vertices $n = |V|$.

4.2.8 Independent Number IN

Two vertices in a graph are pairwise independent if they are not connected by an edge. This concept of pairwise independence enables us to study non-trivial, large dominating sets. An independent set in a graph G is a set of pairwise independent vertices. Trivially a set with one vertex is an independent set, and, in general, maximal independent sets are also dominating sets. A maximum independent set (IN) in G, is an independent set in G of largest cardinality, and its

cardinality is the independence number of G. IN is similar to DN, in that it is not necessarily a unique set that is the largest independent set.

Normalization: Is the number of vertices $n = |V|$.

4.2.9 Local Clustering Coefficient LC

The local clustering coefficient lc_v of a vertex in a graph G, calculates how close its neighbours are to form a complete graph (Watts & Strogatz, 1998). If we let number of edges induced by connectivity distance d, be $e(V)$ and the set of vertices connected to a v be $N(v)$, then the local clustering coefficient lc_v can be defined as:

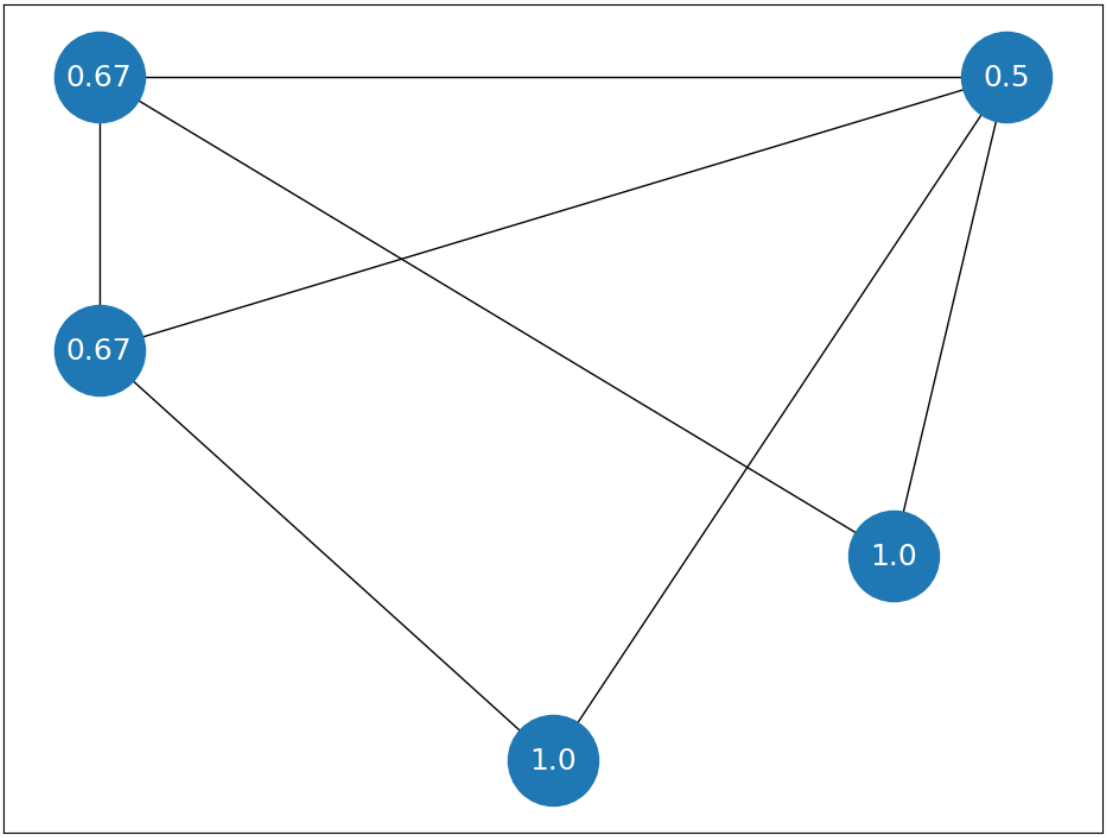

Figure 4.8: The simple graph of Figure 4.1, but with the local clustering coefficient used as vertex labels. The Vertex with the highest degree is not necessarily the most clustered vertex. This because this graph index computes how many neighbouring vertices are themselves neighbours.

eq 4.5

$$lc_v = \frac{2e\big(N(v)\big)}{\deg v(\deg v - 1)}$$

Notice, in Figure 4.8 how the vertex with the highest degree, only has a clustering coefficient of 0.5. This is because this index computes how many of a vertex's neighbours are

themselves neighbours. If we use a social network as an analogy, if a person has few friends but all of those friends are also friends, that that person must be part of a highly clustered community.

Normalization: This index produces a coefficient that is already normalized. The indices used in this chapter takes an average of the sum total of the coefficients.

4.2.10 Global Clustering Coefficient GC

The global clustering coefficient (GC) differs from the local version above, in that it attempts to capture the clustering in a graph as a whole, not just a local\neighbourhood level. The first attempt to formalize such notion dates back to Luce & Perry, (1949). The concept has had a revival of interest at the turn of the century (Wasserman & Faust, 1994) in the context of social network analysis. Its computation involves finding the ratio of closed triplets (3 vertices forming a triangle) and open triplets (two out of three vertices are connected) in G.

eq 4.6

$$gc = \frac{3 \times Number\ of\ triangles}{Number\ of\ connected\ triplets}$$

Normalization: Indices returns a normalized value

4.3 Methods

In this chapter I study configurations of elements with four different cardinalities $\{22, 28, 34, 40\}$, confined to a circular area of radius R. These numerosities are above the subitizing range, and unlikely to form a texture. To estimate the density for an observer, we must assume a viewing distance. On a typical computer display at 57 cm, R equals 160 pixels if we assume there are 32 pixel/cm. Therefore, densities would be: 0.28, 0.36, 0.43, 0.51 elements/deg2, respectively.

One thousand random patterns in the 2D plane were produced for each value of n. There are excellent tools for generating patterns (De Marco & Cutini, 2020; Gebuis & Reynvoet, 2011). I opted for a simple rejection sampling technique: select a random location in a rectangle

and keep it if it is inside the circle C_R and no other element is within distance δ from it. The first constraint limits the vertex spread to a finite circular region. This is useful because in the context of human vision a circular region has a specific level of eccentricity, i.e., distance from fixation. With respect to the second constraint, the parameter δ avoids overlap.

4.3.1 Implementation

An interesting feature of the indices considered in this study is their computational complexity. Some of them (e.g., local or global clustering, connected components, total degrees and total edge length) can be computed in a time that is proportional to the size of the input graph. However, some pose greater computational problems (eigenvalue centrality and occupancy), and others are slow to compute (clique, independent and dominating sets). I used Python 3.6 combined with libraries Networkx v2.5 (Hagberg et al., 2008) and an extension to Networkx; GrinPy v19.5a0 Amos, Davila, 2019) for most of the computations (including max cliques, dominating and independent sets). However, I resorted to a more ad-hoc method in the case of occupancy, which will be explained next.

To compute occupancy, one needs to find (the proportion of) the total area of interest that falls within at least one of the influence areas. This is an interesting computational problem which has been studied in the past (Edelsbrunner, 1993). Methods exist that compute the occupancy of a set of circles in a time proportional to the number of circles (Aurenhammer, 1988). Such methods are not always useful in practice. Bertamini et al. (2016) used an exhaustive process that calculated the occupancy by computing all possible circle intersections. The properties of those configurations meant that the process could be completed in a reasonable amount of time. In the current study I compute occupancy values for larger influence radii. When the influence radius becomes large most circles intersect, and the exhaustive process

becomes slow. I therefore resorted to an alternative approach. To calculate occupancy, the python library PsychoPy (Peirce, 2009), was used.

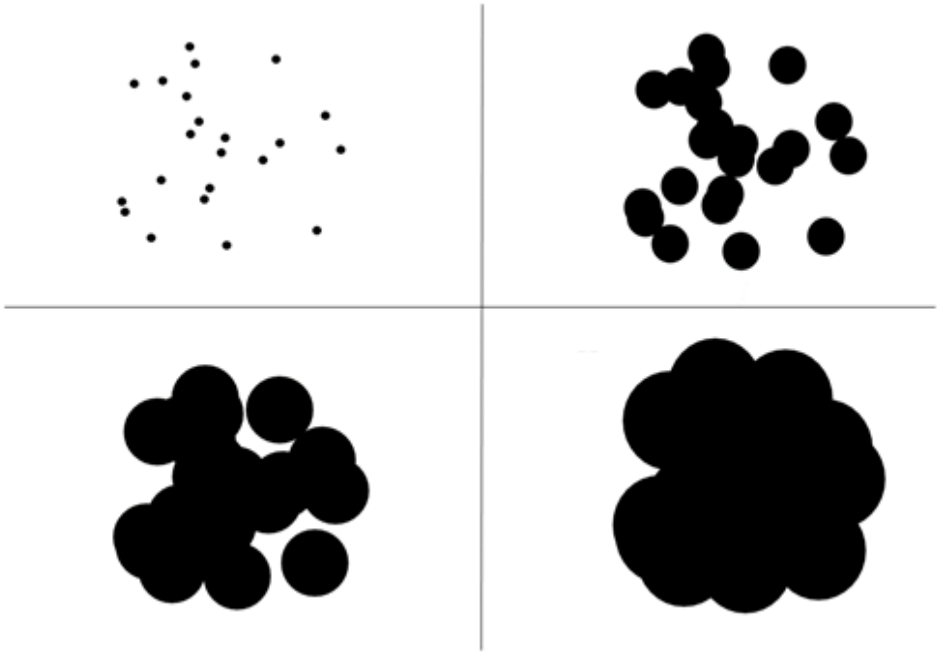

Figure 4.9: How occupancy value (OC) changes with an increase in the occupancy radius o_r. Top left $o_r = R/16$, top right $o_r = R/3$, bottom left $o_r = R/2$ and bottom right $o_r = R$. The amount of overlap increases with increasing o_r. For all patterns cardinality is 22.

For each point a black circle of radius r was drawn on a white background, see Figure 4.9 for example of a configuration for $n = 22$, for various occupancy radii. The PsychopPy function getMovieFrame() then captured the image of the screen, after which the number of black pixels counted. Hence the algorithm returns the total number of black pixels, normalized to the maximum possible value that the occupancy can take, which is $\mathrm{n}\pi(d/2)^2$, the area of n disjoint circles of radius $d/2$. The method was tested against the exact algorithm used by (Bertamini et al., 2016) and found to have correlations larger than 0.998 across $d = \delta$ to 12δ pixels, in steps of δ. Hence, although this algorithm is an approximation, it still produces a valid measure of occupancy. I used the library Networkx for finding the average eigenvector centrality (c.f. Guzman et al., 2014). To ensure convergence, I used 1000 iterations for each G_d.

Values for all indices are made available on Open Science Framework: https://osf.io/yxdvm/. In addition, I made available a full set of python functions that can analyse any set of coordinates; these functions are provided with documentation and examples.

Researchers can specify which index to compute and over what connectivity distance range. See the python script "run_me.py", on how to input any number of dot patterns, and subsequently compute either occupancy values, or one of the graph indices described in this work. When executed, the script returns an excel dataset consisting of the chosen index, computed over each value of d and for each dot pattern. This script also prints out the value of d that gives the maximum standard deviation.

It is possible to input just one pattern and use that to compute different indices over different values of d. See the script "run_me_toy_example.py", for ways to draw graphs, and visualize indices such as independence number, and local clustering coefficient, using the drawing package provided by the library Networkx. Using these scripts, researchers can input one dot pattern at a time and "play" with a graph index over any chosen range of d. There is an accompanying document, called "InstructionManual.pdf" that describes each of the steps taken in "run_me.py", and "run_me_toy_example.py". The document also demonstrates how to create visual illustrations and heatmaps similar to those used in this thesis.

4.4 Results

4.4.1 Correlational Analysis Results

I computed the correlation matrices between indices at each$d \in \delta, \delta + 5, \delta + 10, \delta + 15, \dots, 2R$. This in turn was repeated for each value of n. The resulting correlational matrices revealed the presence of transient correlations (i.e., correlations between pairs of indices that only existed at a particular connectivity distance, see Figure 4.10) and also pathological distributional patterns in the underlying data.

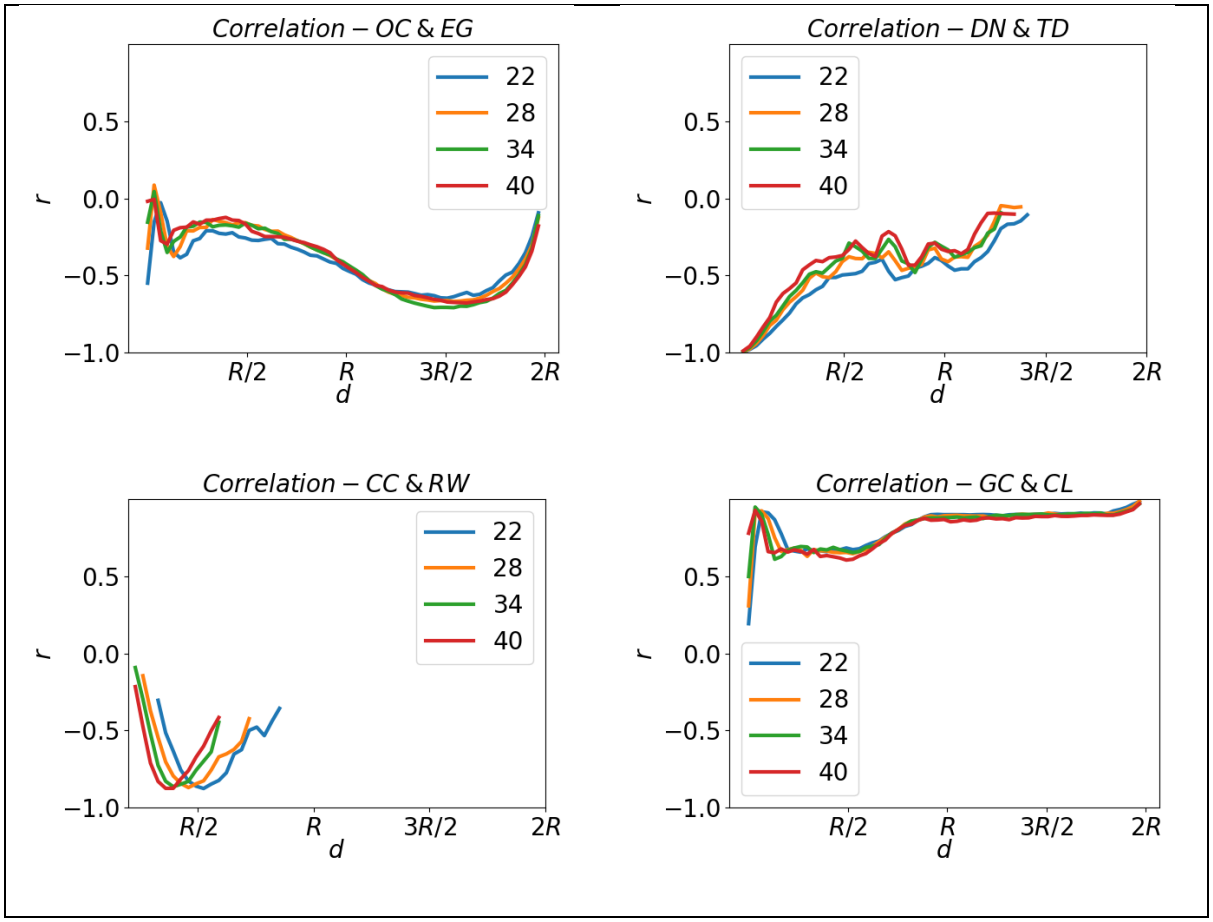

Figure 4.10: All correlations were computed using the Pearson coefficient, any with $p > 0.05$ were ignored. Top and bottom left show examples of transient correlations. Top left EG and OC are strongly correlated $r(998) > |0.6|$, at $3R/2$, but much lower for other d values. Also, CC and RW are strongly negatively correlated for $d = R/2$, but the correlation decreases rapidly elsewhere. Bottom right shows both CL and GC are strongly positively correlated, throughout the full range of d. Top right shows how some indices will have a threshold value, DN hits it minimum value across all n when $d = 3R/2$.

The top and bottom left panels of Figure 4.10 show how, over a small range of d, indices can be correlated, for instance CC and RW are strongly negatively correlated only in a range around $d = R/2$. In the bottom right panel, CL and GC formed strongly positive correlations across most of the range of d. It is also clear from the top right and bottom left panels of Figure 4.10, that indices may reach their respective limiting values at different d. As an example, the threshold values for CC (bottom left panel of Figure 4.10) are 22: 0.75R, 28: 0.625R, 34: 0.625R and 40: 0.56R. Values greater then this for d will guarantee all graphs are connected, and hence the variance in CC will be zero. Likewise, DN reached its threshold value for all n by $d = 3R/2$.

Indices approaching threshold values raise problems with computing correlations. For instance, when I investigated the maximum correlation for RW and CC, Figure 4.10 bottom left panel, the correlation between CC and the RW at $n = 40$ and $d = R/2$ was $r(998) = -0.816, p = 0.000$. Figure 4.11 shows a scatter plot of RW and CC at $n = 40$, and $d = R/2$. It is clear that the relationship between CC & RW is not linear.

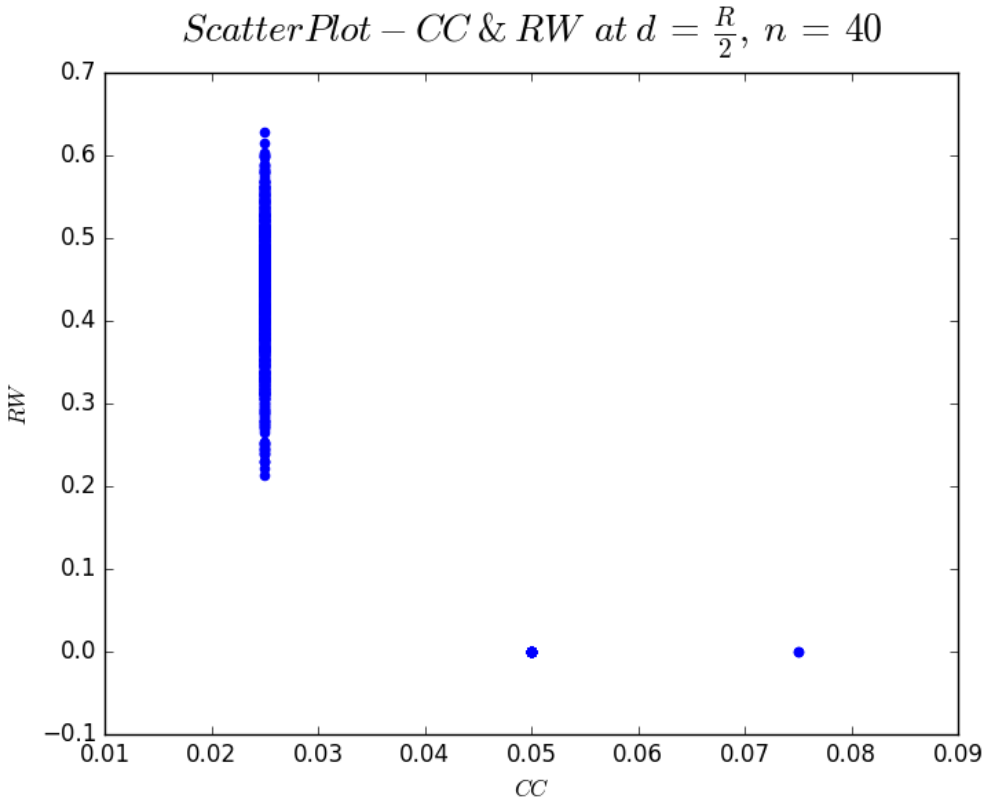

Figure 4.11: Scatter plot of connected components against random walk at connectivity distance $R/2$. This has a correlation of $r(998) = -0.849$, $p = 0.000$. The strength of the correlation is due to CC approaching its threshold value, and random walk becoming a computable index.

The root of the problem is that CC is getting close to its threshold value as most graphs start to connect, while RW is only just becoming a computable index for the same reason. When plotted, CC is oscillating between to two values, and RW has values that are zero and thus acting as outliers. Each correlation matrix requires 45 separate correlation computations, at each data point in d. Hence inspecting each correlation visually would not be feasible. The problem is compounded by a sample size of $N = 1000$. Tests for normality, for instance Kolmogorov–Smirnov and Shapiro-Wilk, are known not to be accurate for $N > 300$ (see Field, (2009), for

discussion). Nevertheless, Figure 4.11 does suggest that these cases do not contain enough variability at a specific value of d. The ability to filter out unreliable correlations will be the topic of the next section.

When interating through d two groups of strongly correlated indices, were found across all n. From now on I will refer to indices OC, DN, IN, and CC as belonging to the clustering group, and CL, TD, and TL as belonging to the spread group. Other correlations were found, however these were either expected, such LC and GC, or artificial correlations due to indices converging on the same threshold value when the graphs started to become dense.

Heat maps for connectivity distance $d = R/8$ are shown in Figure 4.12, for each n. It is clear the clustering group is present, coloured blue, top left. It would be expected that both DN and IN will correlate strongly with each other as both search for a dominating set, in the case of DN it searches for one with a minimum cardinality, whereas IN searches for one with a maximum cardinality. Of more interest is that they also cluster with CC and OC. In addition, TD and TL formed a strong negative correlation with the clustering group. This group does not persist across a wide range of d, as CC no longer varies after graphs become connected.

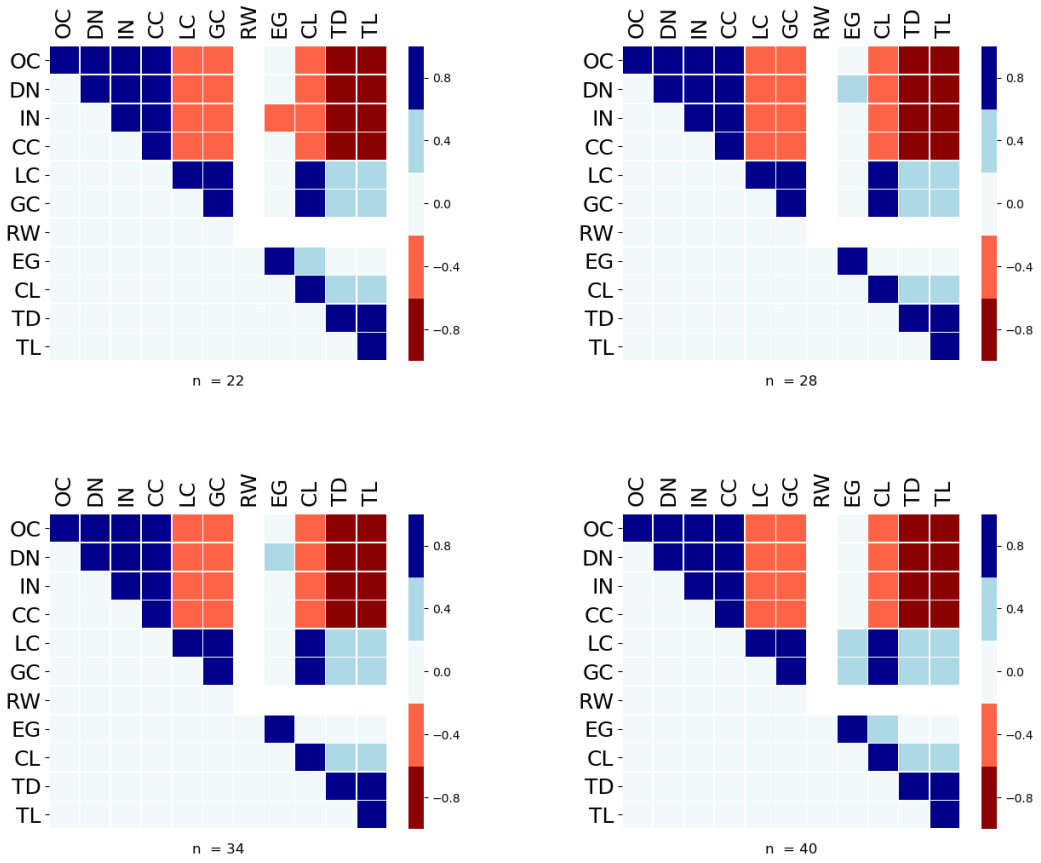

Figure 4.12: Heat maps for $d = R/8$ we see clear patterns emerging that are independent of n, for instance the positively correlated cluster of OC, DN, IN & CC. I termed this as the "cluster" group, as the graph indices are all sensitive to clustering. Notice that the OC is in this group.

Figure 4.13 shows the heat maps at $d = R$ for all n. As this is the radius of the enclosing circle R, all graphs will be connected with a high probability, consequently the index CC will have reached its threshold value, and its variance will be zero. Therefore, the clustering group has disappeared, but the spread group has formed for all n. Also, LC and GC have now strong correlations with the spread group.

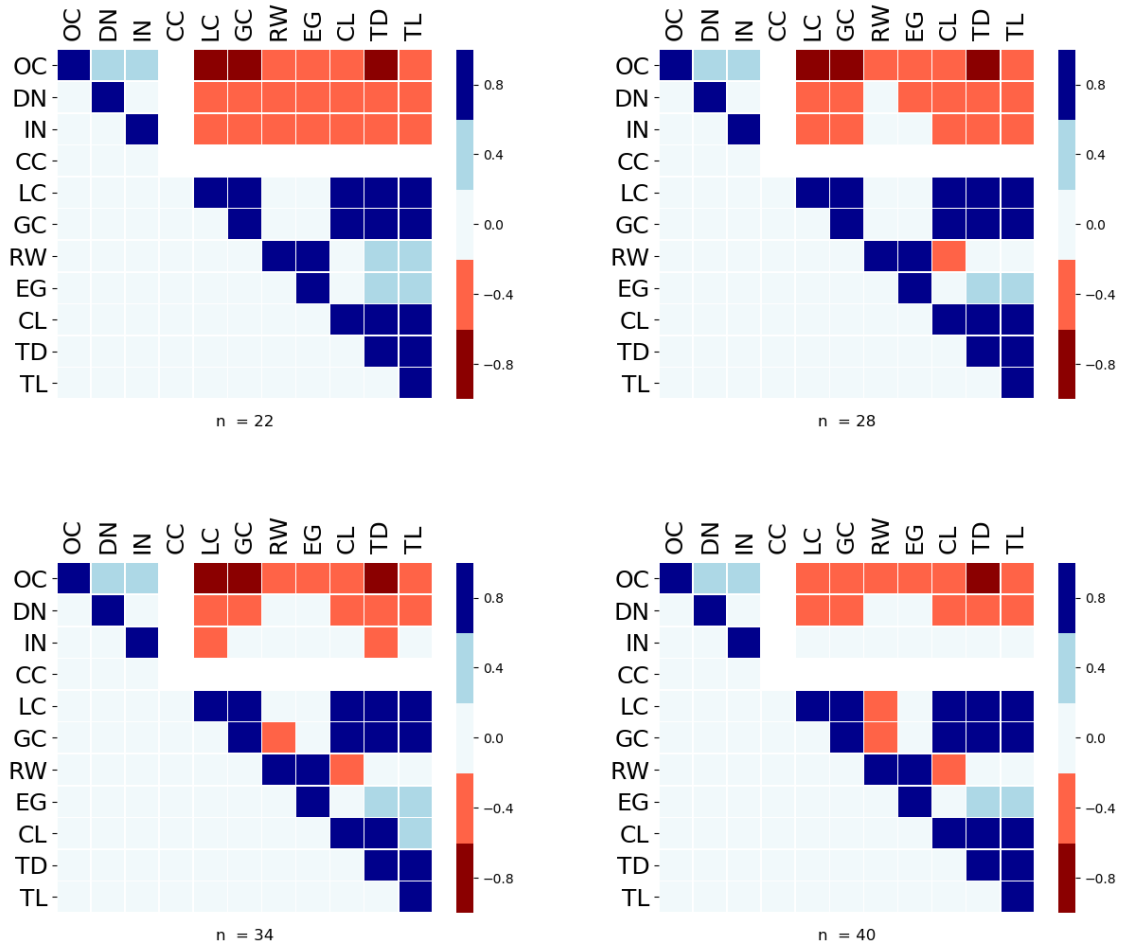

Figure 4.13: Heat maps for $d = R$. Again, clear patterns emerge that are independent of n, notably a cluster of highly positive correlations between TL, TD and CL.

4.4.2 Comparisons based on Maximum Standard Deviation

The analyses presented for each n, enable us to obtain correlation matrices at each $d \in \delta, \delta + 5, \delta + 10, \delta + 15, \dots, 2R$. I reasoned that it would be useful to find where indices are most informative, select only one value of d per index, and then show how indices relate to each other when computed on graphs obtained by using those particular values of d.

In an attempt to capture the most significant correlations, I computed, for each index m, the value $d_m(n)$ of the connectivity distance that maximizes the standard deviation $\sigma_m(n, d)$, and then studied the correlations between the values of the 11 indices computed in the graphs

$G_{d_m(n)}$. I call these the maximum standard deviation correlations. Table 4.1 shows the values of $d_m(n)$ for all indices.

Table 4.1: Each cell displays the numerical value computed for the maximum standard deviation for each index, and the same value in terms of R. The value of 160 for R was chosen because this would correspond to 5^0 of visual angle on a screen at distance 57cm (assuming 32 pixels/degree).

N	OC	DN	IN	CC	LC	GC	RW	EG	CL	TD	TL
22	60	30	35	35	55	55	125	70	220	180	155
	0.38R	0.19R	0.22R	0.22R	0.34R	0.34R	0.78R	0.43R	1.38R	1.13R	0.97R
28	55	30	30	35	50	45	115	65	230	170	155
	0.34R	0.19R	0.19R	0.22R	0.31R	0.28R	0.72R	0.41R	1.44R	1.06R	0.97R
34	50	30	25	30	45	40	105	65	235	170	160
	0.31R	0.19R	0.16R	0.19R	0.28R	0.25R	0.66R	0.41R	1.47R	1.06R	R
40	45	25	25	25	40	35	95	60	240	175	160
	0.28R	0.12R	0.16R	0.16R	0.25R	0.22R	0.59R	0.38R	1.5R	1.09R	R

This analysis for the maximum standard deviations was repeated for each index and the heat maps are shown in Figure 4.14. Notice that the two most interesting components seen in the correlational analysis between measures at fixed values of d are still present. We see a strong negative correlation between LC and occupancy. Also, EG is strongly correlated with the spread group, even though the computed value of $d_{EG}(n)$ is closer to the average value of d for the clustering group.

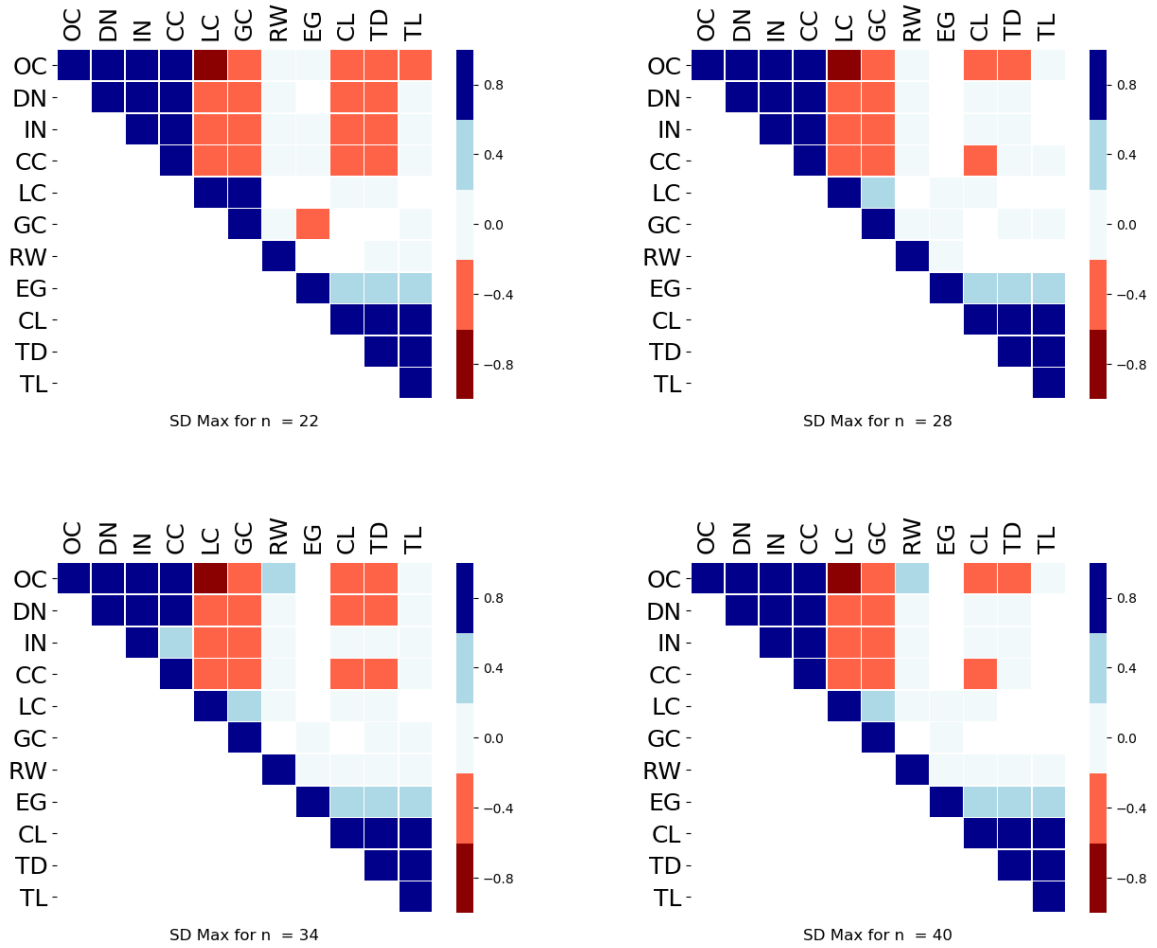

Figure 4.14: Heat maps with correlations between indices selected based on standard deviations. We see that the use of SD Max has captured the clustering and spread groups, regardless of cardinality. Thus, summarising the persistent groupings of highly correlated indices.

It might be argued that correlating the 11 indices using the values obtained in $G_{d_m(n)}$ in each case is artificial, as I am comparing measures obtained from different graphs, due to the different connectivity distances. However, the graphs used here are not totally unrelated. As pointed out in the introduction, the geometric graphs are such that if $d_1 \leq d_2$ then G_{d_1} is a subgraph of G_{d_2}. If $d_{m_1}(n) < d_{m_2}(n)$. comparing m_1 in $G_{d_{m_1}(n)}$ with index m_2 in (the denser) $G_{d_{m_2}(n)}$ may ignore irrelevant information about $G_{d_{m_2}(n)}$ when dealing with m_1. The goal is to find graph-theoretic indices that predict human numerosity judgements. These indices depend on the set of vertices but also on the value of d. Therefore, comparing indices using the same value of d might not be ideal.

4.4.3 Principal Component Analysis

I investigated the maximum standard deviation correlation matrices further, by performing a principal component analysis (PCA), with the purpose of extracting any uncorrelated\orthogonal features that are present in the data. The index RW was omitted, as it is clear from the previous section that it did not correlate with any other index. Please note that the term "component" as used in PCA is not the same as a "component" in graph theory. SPSS confirmed two strong eigenvalues, and a third just below 1, from the covariance matrix of $\sigma_m(n, d)$. The results are summarized in table 4.2.

Table 4.2: Summary of the first two eigenvalues found from the PCA analysis and cumulative variance explained from their components for each n. We see most of the variance is explained by these first two components

	n = 22		n = 28		n = 34		n = 40	
	Eigenvalue	Cumulative variance %	Eigenvalue	Cumulative variance %	Eigenvalue	Cumulative variance %	Eigenvalue	Cumulative variance %
Component 1	4.58	45.75	4.01	40.54	4.22	42.18	4.26	42.60
Component 2	2.8	73.44	2.9	69.53	2.72	69.34	2.90	71.56

The varimax matrix extracted two components, with the following members: component 1: OC, DN, IN, CC, LC, and GC, and component 2 containing EG, CL, TD, and TL. Largely confirming the two groups (clustering, spread) seen in the informal correlational analysis in the previous section. Also, the PCA placed LC inside PCA component 1 with a load factor ranging between -0.76 and -0.70 dependent on n. This was reflected in the correlational analysis at fixed distances, since it found negative correlation values < -0.3 between LC and OC until LC started reaching its threshold value as the graphs became dense. Using the same argument, GC was consistently moderately negatively correlated $\succ 0.6$and < -0.2 with OC, which is reflected in its load factor between -0.68 and -0.48 (see Table 4.3).

For completeness it should be noted that there are other pairwise features between indices that are not present in either correlational or principal component analysis. For instance,

GC and CL were strongly correlated through a wide range of values for d, as were OC and TD. This is not seen in either the correlational analysis or PCA of the maximum standard deviations (this could be due to their respective σ_{max} being far apart in terms of d, as seen in Table 4.1). In Figure 4.12 notice a strong correlation between the spread group and indices LC and GC. This also has not been extracted. However, correlations between the spread group and indices {LC, GC} were more transient and relied more heavily on connectivity distance d.

Table 4.3: Rotated matrices produced by a PCA. The two components contain all indices. Each component represents the cluster and spread group from the correlational analysis. Note that loadings below, values of .3 or less have been suppressed.

n = 22	Component		n=28	Component	
	1	2		1	2
OC	*0.90*		**OC**	*0.92*	
DN	*0.85*		**DN**	*0.90*	
IN	*0.83*		**IN**	*0.83*	
CC	*0.90*		**CC**	*0.83*	
LC	*-0.76*		**LC**	*-0.72*	
GC	*-0.68*		**GC**	*-0.53*	
EG		*0.75*	**EG**		*0.63*
CL		*0.86*	**CL**		*0.88*
TD		*0.94*	**TD**		*0.96*
TL		*0.91*	**TL**		*0.92*
n = 34	Component		n=40	Component	
	1	2		1	2
OC	*0.90*		**OC**	*0.90*	
DN	*0.90*		**DN**	*0.93*	
IN	*0.75*		**IN**	*0.86*	
CC	*0.90*		**CC**	*0.95*	
LC	*-0.73*		**LC**	*-0.70*	
GC	*-0.48*		**GC**	*-0.51*	
EG		*0.67*	**EG**		*0.67*
CL		*0.86*	**CL**		*0.87*
TD		*0.96*	**TD**		*0.96*
TL		*0.93*	**TL**		*0.94*

4.4.4 Discussion

This study had three goals. The first was finding useful graph indices for the study of numerosity. I wanted to expand on the approach taken by some researchers in the numerosity literature who used graph indices to predict human and animal numerosity perception (Bertamini et al., 2016; Im et al., 2016). For this reason, I selected a list of graph theoretic indices that might be useful in the study of numerosity estimation. Since many numerosity studies involve the use of random configurations of elements as stimuli, I focused on random geometric graphs for our analysis, as they are determined by the geometric distribution of a configuration, combined with a connectivity distance parameter. This approach enabled the more formal study of the combinatorial/geometric properties of this type of stimuli. It was important, in choosing indices, that the graph properties they measured were wide-ranging, in the sense that I would have indices sensitive to groupings/clustering, density, and other graph properties such as centrality and the cardinality of the independent/dominating set.

I analysed ten indices: number of connected components CC, domination number DN, independence number IN, average local clustering coefficient LC, global clustering coefficient GC, average eigenvector centrality EG, random walk RW, maximum clique size CL total edge length TL and total degree TD. Together these indices represent a broad range of properties found on graphs. The correlational analysis also enabled us to study certain (computationally intractable) graph indices by working with related (simpler) ones.

The second aim followed directly from the first one. I wanted to compare the graph theoretic approach with the occupancy model (Allik & Tuulmets, 1991). I therefore added this measure (denoted by the abbreviation OC) to the ten mentioned above, thus providing a total of eleven indices. Although there is a relationship between connectivity distance of random graphs and the occupancy radius, OC represents a fundamentally different way to capture clustering and grouping properties. Edges on graphs represent relationships between elements (an all-or-none relationship), whereas occupancy is based on the idea that each element has a region of influence, estimated by a circular area. The total area of influence is then taken as the predictor

of the overall perceived numerosity. There is a parallel between the connectivity distance used to construct a graph, and the size of the region of influence, and therefore I manipulated this factor in a similar way for all measures (that is, distance affects both edge creation between two vertices on a graph, and the overlap of each elements region of influence). The results indicate a strong correlation between occupancy and some other measures, highlighting a couple of important geometric features that affect the perception of numerosity.

Our third aim was to study the correlations between indices, and across a range of connectivity distances. In previous studies, only a subset of values was used (Bertamini et al., 2016). I wanted to see which indices grouped together, and whether these groups would persist across connectivity distances. Finally, I aimed to summarise these results, and draw conclusions about their implications for research in numerosity perception.

The correlational analysis identified many pairwise relationships between individual indices that were transient in nature. Nonetheless, some structures of the pairwise correlational patterns persisted across numerosity, and hence our attention turned towards the formation of persistent groups of indices (three or more highly correlated indices) over specific ranges of the connectivity parameter d. Two such groups were identified. The first of these (referred to as the clustering group) included OC; IN; DN; and CC. This group had connectivity values around $d = R/8$ for all n, as shown in Figure 4.12. As its connectivity distance was small, it is sensitive to how groups of elements cluster together. The second group (referred to as the spread group) included CL, TL, and TD. This group formed at a larger connectivity distance $d \geq R$, again this was independent of n. It is possible that at larger connectivity distances this group was picking up on the more global properties of the patterns, like areas of highest density. Of the two groups, the spread group persisted over a larger range of values of d. This was because the clustering group contained both CC and DN, two indices whose extreme values are reached well before the other indices.

In an attempt to filter out pathological and transient correlations, and summarise the main results found in the correlational data, four additional datasets were created, one for each value n. Each dataset consisted of the value of d that generated the maximum standard deviation for each index1. When the correlational analysis was repeated on the resulting four datasets, it had the advantage of ignoring trivial and transient correlations. Importantly, it found both groups of indices described in the previous paragraph (Figure 4.14).

The maximum standard deviation datasets were investigated further with a principal component analysis, which confirmed that the two groups were orthogonal. Within the first PCA component indices LC and GC joined the group with members OC, DN, IN, and CC. This confirmed our hypothesis that this group of indices is more sensitive to how groups of elements cluster together. The second PCA component included CL, TD, TL, and added EG. Again, the addition of EG makes sense as this index extracts the most influential vertices in graphs. RW was not a member of either components, which reflects the fact that it rarely formed any significant pairwise correlation with another index, other than EG and CL, across any value of d or n.

The connectivity distance for the clustering group had an average value of $d \approx R/4$, and from the correlational analysis that this is below the threshold value for CC. Therefore, the input graphs to the clustering group will be disconnected into discrete units. OC was also a member of this group, and this is consistent with finding that the region of influence operates over a small distance (Allïk & Tuulmets, 1991; Bertamini et al., 2016). Also, Allik and Tuulmet suggested that the optimum value for the occupancy radius may be a property of the type of stimulus. The value that gives the maximum variance could be that property. As an index OC is sensitive to patterns that manipulate the spacing between elements. However, when used on

[1] For two of the indices (RW and EG) the value of d that gave the maximum standard deviation was pathological, with most of the values in the data zero, and the remaining values close or equal to 1. Instead, that value of d was used that gave the maximum standard deviation, provided more than 99% of the data was non-zero.

purely random patterns, with no manipulation on spacing, it is also sensitive to groupings. This is confirmed by its strong correlation with CC, something that also became apparent from the PCA. This suggests that CC could be a computationally efficient alternative to OC for researchers in numerosity.

The spread group had a much larger connectivity distance that was above the threshold value for CC, thus ensuring that the input graphs are connected into one graph component, and hence this group is more sensitive to global structures such as areas of dense clustering (TD, CL), and influential vertices that are central to information spread - EG. It is known that, in enumeration studies, element saliency is important in predicting initial eye fixations and scanning strategies (Paul et al., 2017). Furthermore, in a recent study it was found that centroid measures were most useful in predicting the position of the first eye fixation (Paul et al., 2020). However, such centroid measures use centre of mass calculations that will not necessarily return the coordinates of an element. Centrality measures from graph theory, such as EG, can extract features in patterns such as the most influential or salient elements, and thus may provide a more precise method in predicting initial eye fixations. This has been done before: in eyetracking studies centrality has been shown to provide an effective method of distinguishing facial scan patterns between autistic and non-autistic children (Guillon et al., 2015; Sadria et al., 2019).

Our findings of two components (clustering, spread), is also related to work by Salti et al. (2017). They describe the existence of two categories of continuous magnitudes (intrinsic and extrinsic). Intrinsic relates to magnitudes that can be computed on individual dots, such as total circumference, total area, and average diameter. Extrinsic magnitudes are concerned with indices that are computed on the array, such as convex hull and density. In our work density sensitive indices such as total degree and maximum clique are members of the spread group, and the occupancy model (related to area of influence) is a member of the clustering group. However, for Salti et al. (2017) the location of the elements is only needed for the convex hull. All other indices strongly correlate with numerosity. Recently, De Marco and Cutini (2020) described a

novel way of computing density: the length of the shortest path connecting all elements n, divided by $n-1$. They note that this measure is negatively correlated with numerosity.

In contrast to these continuous measures, all indices in our approach operate on a discrete structure and are sensitive to the spatial relationships of the elements. A graph G has a finite number of vertices V and edges E, and this approach may have an advantage when representing the configuration of discrete elements, such as an array of dots. For instance, total degree TD was used as a measure of density, which is computationally efficient because it needs only the count of the edges present in a graph. Unlike average distance between elements, TD is positively correlated with numerosity.

4.5 Conclusion

In this chapter I describe random 2D configurations with indices based on graph theory, and compare them with the occupancy model. It was found that the indices have different properties and are sensitive to different aspects of clustering. Some may be interchangeable because they are highly correlated, potentially providing efficient alternatives to more computationally intensive methods such as the Occupancy index. The analysis of the pattern of correlations suggests two main groups of measures. The first is sensitive to presence of local clustering of elements, the second seems more sensitive to density and how information spreads in graphs. Empirical work on perception of numerosity may benefit from comparing, or controlling for, these properties.

4.6 Open practices statement

All data sets and coding are available in anonymized form on OSF (https://osf.io/yxdvm/).

5 The solitaire Illusion is an illusion of clustering, between interacting patterns.

5.1 Introduction

For far we have seen the importance of clustering in the perception of numerosity. We saw in the previous chapter how occupancy was firmly in the cluster group\component. I believe it to be informative to study the development of the occupancy model, as clustering is important simply because it is very sensitive to spacing between elements, this was seen in chapter 2.

5.1.1 The importance of Clustering

The effect of spacing was originally described as the random-regular numerosity illusion (Cousins & Ginsburg, 1983; Ginsburg, 1980). When elements are more evenly separated the configuration appears more numerous (Figure 5.1). It is likely that regularity has an effect on perceived numerosity because regularly spaced elements are not approaching each other (Vos et al., 1988).

One of the early attempts at explaining this phenomena concentrated on the concept of a filled area (Vos et al., 1988), which the authors defined as the "ensemble of parts of the stimulus field occupied by the dots". The CODE algorithm proposed by (van Oeffelen & Vos, 1983), used a monotonically decreasing spread function centred on each dot, with the amount of spread dictated by the distance to its nearest neighbour. For evenly spaced dots, the algorithm predicts the pattern will fill the entire stimulus field, left hand panel Figure 5.1. For more random patterns, the CODE algorithm could detect the concave hull of dot clusters, thus the filled area of the hulls could be computed. It is clear from Figure 5.1 bottom right hand panel, that the filled area of a random pattern is far less than that of a regularly spaced pattern.

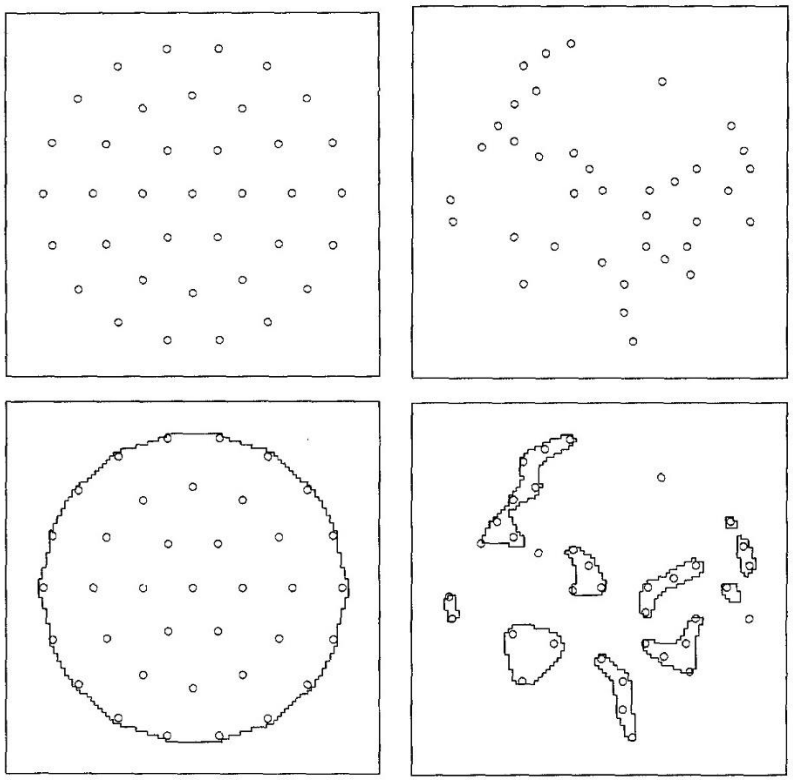

Figure 2.1. The concept of filled area. The ordered tiling of dots on the left, gives a filled area of the whole stimulus field. While the random pattern on the right is more clustered, and has a filled area that is much less. Taken from Vos et al. 1988.

Another early attempt was the cluster continuum (Ginsburg & Goldstein, 1987), which was a model taken from ecology as a measurement of how grouped together natural objects are in a scene. In this approach, the stimulus field was divided into a grid of n equally sized cells, where n was the number of dots in the pattern. A regularly spaced pattern would have one dot occupy one cell, and therefore have a value of 0 on the cluster continuum, that is no clustering. As spacing between dots decreased, more cells would contain more than one dot. Accordingly, the patterns cluster value on the cluster continuum would increase.

Possibly motivated by both the notion of a cluster continuum and filled area, (Allïk & Tuulmets, 1991) , proposed the occupancy model of numerosity (OC). In this approach the spread function of (Vos et al., 1988) is simplified to that of a fixed occupancy radius, and the amount of overlap of occupancy circles, is the measure of clustering in pattern, see section 4.1.3. Like in the cluster continuum (Ginsburg & Goldstein, 1987), no overlap would represent no clustering.

Therefore, OC measures clustering. However, in terms of filled area and cluster continuum, the aim is to measure how far away a random pattern is from being regularly spaced, that is zero clustering. Given an optimum occupancy radius, the OC most certainly measures this too. Hence, how far away a random pattern is from being regular and how clustered it has, is equivalent.

Although old, the cluster continuum is useful in that it serves two purposes. It not only gives insight to the origins of OC, but also the optimum value that the occupancy radius o_r should have. If the statement of equivalence of the previous paragraph is correct, then its optimum value will be the maximum spacing, between dots for them to be an ordered pattern. Hence, any deviance from this and overlap or clustering occurs, and will be measured by OC. This must be its most sensitive value to clustering.

We can test this assumption out on the data from the chapter 4. C_R had an area of $A(C_R) = 80{,}384 \text{ pixels}^2$. Also, the number of dots n was taken from $n \epsilon \{22, 28, 34, 40\}$. If we divide $A(C_R)$ by, π and n, then take the square root, will get an upper bound on the occupancy radius for each n. It is clearly an upper bound as, this assumes that n occupancy circles, can fit exactly inside the outer circle C_R, with no gaps, and clearly this can't happen in practise. Also, this approach would not allow dots to be on the circumference of C_R, which is a slightly harder problem. A slightly better method would be to note that circle packing algorithms, can be represented by planar graphs (Stephenson, 2003). For random geometric graphs, it is known that the threshold connectivity distance for planarity is $n^{-\frac{5}{8}}$, where n is the number of dots inside a unit square (Bose et al., 2015). Then we can scale this for a circle of R.

Table 5.1 Shows the computed upper bound for planarity compared to the σ_{OC}, computed in section 4.4.2.

Table 5.1: For n, we see the computed upper bound for the occupancy radius, to tile it evenly in the plane, compared to the maximum standard deviation found for OC.

n	Upper Bound (pixels)	SD Max (o_r) (pixels)
22	36.4	30
28	31.3	27.5
34	27.7	25
40	25.0	22.5

The value of o_r is close to the threshold value for planarity for n circles within an outer circle C_R. This no surprise, as o_r will be the widest detectable range for the occupancy value, given n occupancy circles fitted best inside a boundary, in this case a circle C_R. Hence, the slightest deviation from an ordered pattern will be measured by OC. If the o_r is smaller or bigger, it won't measure the full range of deviation away from a regular pattern, and therefore the full range of clustering available.

For far we have seen the importance of clustering in the perception of numerosity. From studying the development of the occupancy model, we see that clustering is measure of far away a random pattern is from being regular. This is certainly the case with earlier approaches such as "filled area" (van Oeffelen & Vos, 1983) and the cluster continuum (Ginsburg & Goldstein, 1987). Allike and Tuulmets (1991) argued that the optimum value of the occupancy radius o_r would depend on the properties of the patterns being analysed.

However, I believe that its optimum value is that which allows the occupancy circles to evenly tile the stimulus space, or zero clustering. This also coincides with the maximum standard deviation, see section 4.4.2. If we consider Figure 5.1, the left-hand pattern is hexagon tiling, which is the most efficient way of tiling circles inside other circles. This is easy to see, as the

pattern on the left in Figure 5.1 is an example of centred hexagon numbers, starting from the centre the sequence goes as follows 1, 6, 12 & 18, and the sum of these numbers is 37.

It can be seen that clustering is measure of far away a random pattern is from being regular. This is certainly the case with earlier approaches such as "filled area" (van Oeffelen & Vos, 1983) and the cluster continuum (Ginsburg & Goldstein, 1987). Allike and Tuulmets (1991) argued that the optimum value of the occupancy radius o_r would depend on the properties of the patterns being analysed.

However, I believe that its optimum value is that which allows the occupancy circles to evenly tile the stimulus space, or zero clustering. This also coincides with the maximum standard deviation, see section 4.4.2. If we consider Figure 5.1, the left-hand pattern is hexagon tiling, which is the most efficient way of tiling circles inside other circles. This is easy to see, as the pattern on the left in Figure 5.1 is an example of centred hexagon numbers, starting from the centre the sequence goes as follows 1, 6, 12 & 18, and the sum of these numbers is 37.

5.2 Occupancy Model Applied to the Solitaire Illusion and The Regular Random Illusion.

Although over 30 years old, the occupancy model has enjoyed support from recent empirical studies (Bertamini et al., 2016, 2018; Valsecchi et al., 2013). However, to date the author is not aware of the OC being applied to the SI. The OC should predict the inner pattern to have the greater occupancy value, as the bias for the inner is so strong.

To compute the occupancy value exactly is computationally hard. I therefore computed the occupancy value directly, by counting pixels, using the same method as (Guest et al., 2022).

5.2.1 Method

A SI pattern was constructed with the following dimensions, the radius of each dot r was 8 pixels, and the vertical and horizontal spacing between dots was also 8 pixels. Therefore, the

spacing between positions on the peg solitaire board was 24 pixels. For each point in each dot configuration, a grey circle of occupancy radius r_o was drawn on a white background, this represented the occupancy circle. After all the circles were drawn, the PIL library was used to capture an image of the screen and count the number of black and grey pixels. Figure 5.3 shows examples of the images created for different occupancy values. In this method, the maximum value of 1 denotes when there is not overlap, as overlapping increases with increasing r_o, the occupancy value will then diminish.

For comparison I also applied the occupancy model to the configurations of Figure 5.1. The left configuration is Regular, and the right configuration is Random. Dot radius was 8 pixels, and both configurations were confined to a circle of radius $20r$. The minimum spacing between dots for the random pattern is $2r$, meaning the only restriction is that the dots do not overlap. For the regular pattern, the minimum distance is $6r$. For both patterns, OC was computed using the same method as Guest et al. (2022).

.

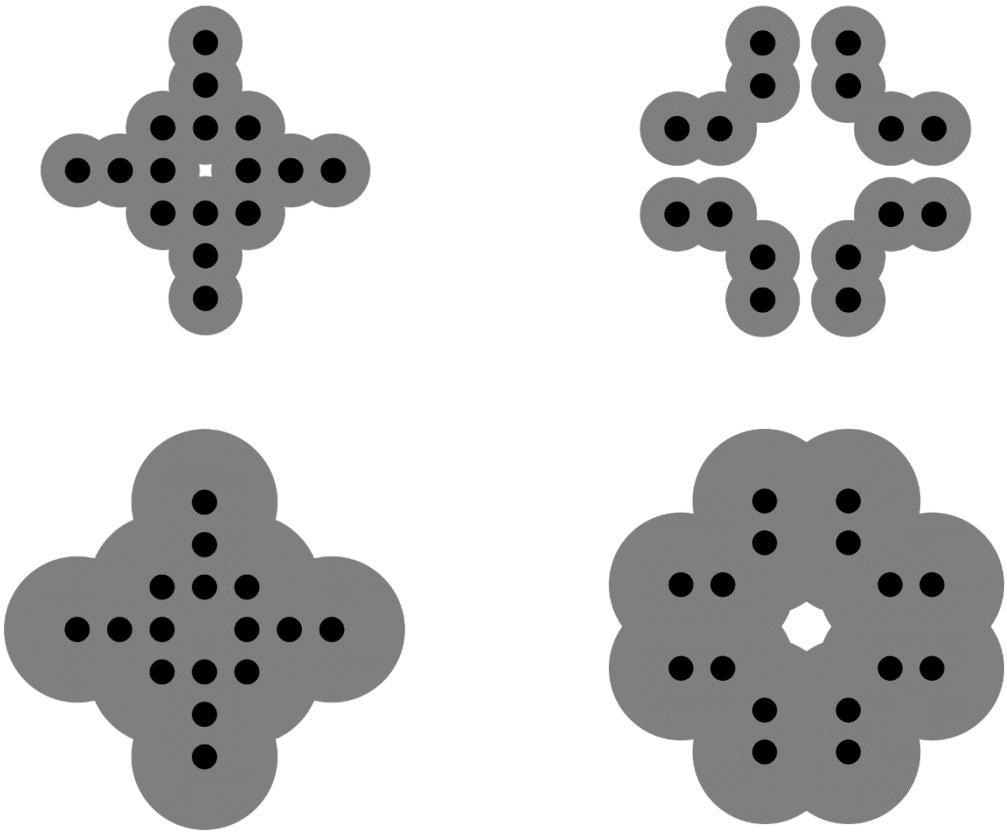

Figure 5.3: Shows screenshots of computing occupancy for the solitaire illusion, for both the inner (left column) and outer (right column) patterns. The top row shows the original illusion I call this radius = 1. The middle row shows inner and outer patterns for occupancy radius 3, and the bottom row is for occupancy radius of 6. We see as the occupancy radius grows, so does the amount of overlap.

5.2.2 Results

In figure 5.4 top panel, I plot the occupancy values for both inner and outer sets in units of the radii of the dots in the original illusion, hence the $r = 1$ is the original illusion separated top row of Figure 5.3, and $n = 16$. I then let r range from $1 - 22r$. As soon as overlap starts to occur, the outer pattern has the higher occupancy value over the inner pattern, Figure 5.4, and this is maintained up to $r = 22$.

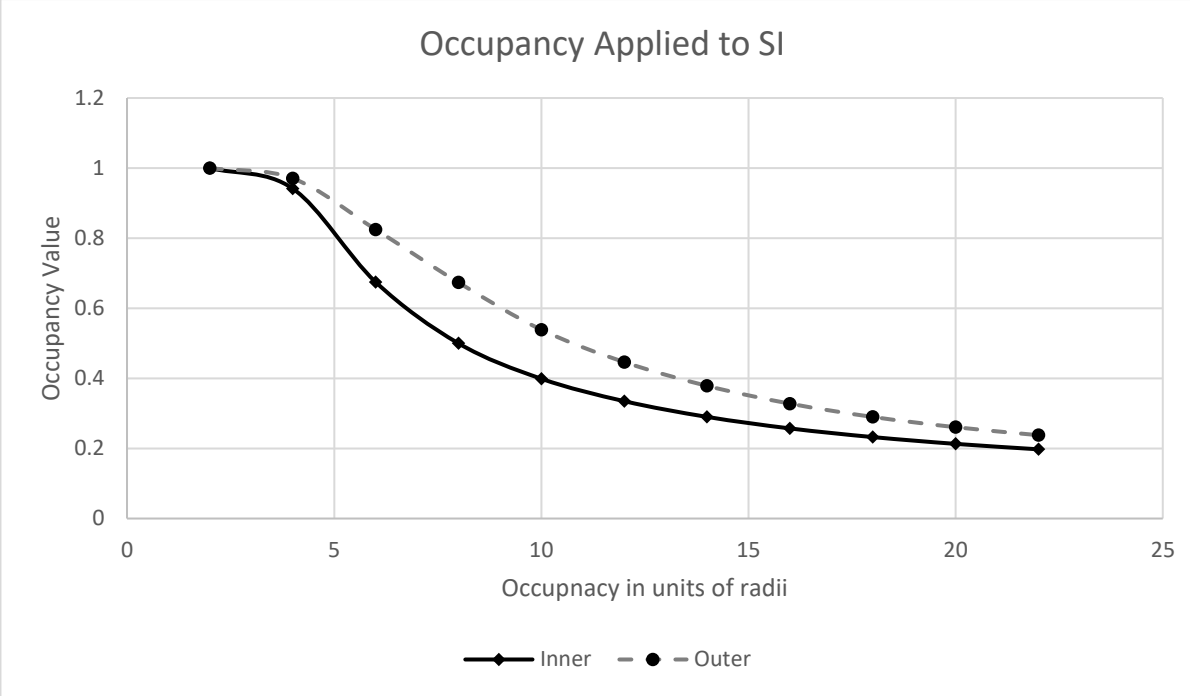

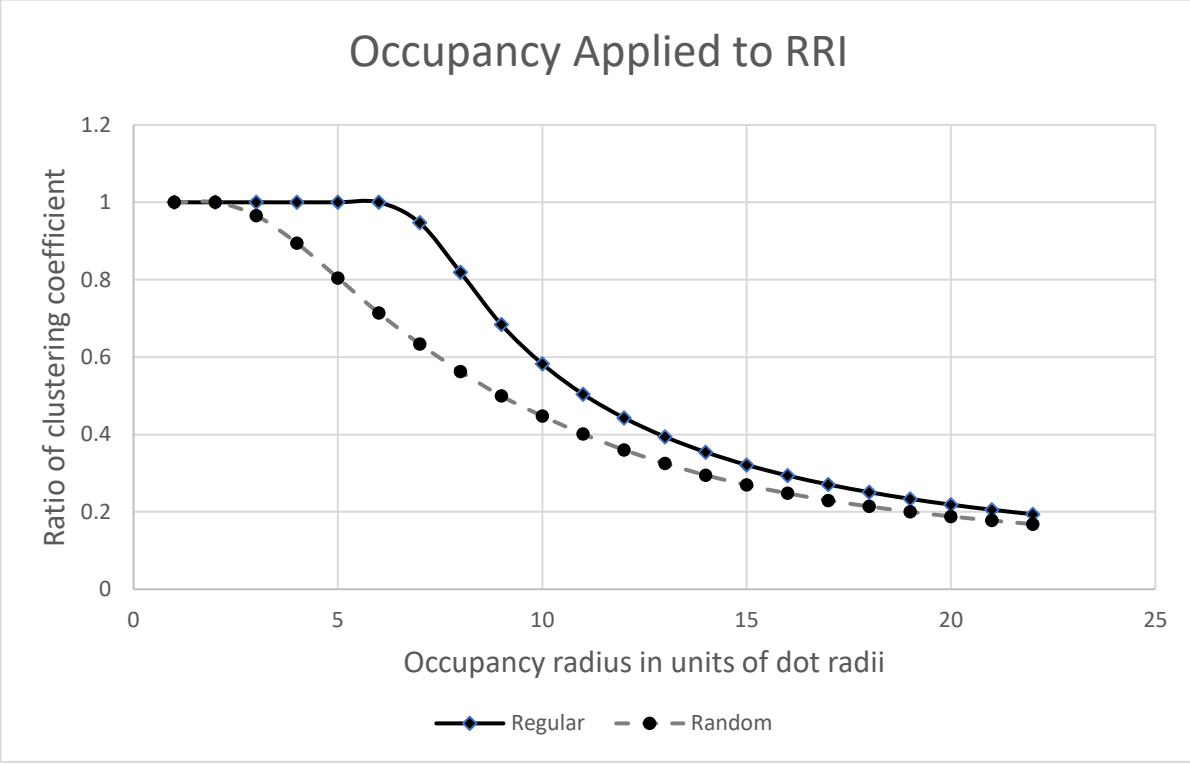

Figure 5.4: Top panel shows OC applied to SI, as soon as overlap starts to take place the inner pattern always has a lower occupancy value then the outer. Thus, should be perceived as less numerous by the occupancy model. In the bottom panel, we show data collected from the patterns used in Figure 5.1. It is the random pattern that starts to have overlap first. Both of these results are robust to changes in o_r. The way occupancy is computed, the closer to 1 a occupancy value is, the less clustered it is.

Figure 5.4 bottom panel, shows the occupancy model applied to the configurations of Figure 5.1.

Here n = 37, and computing occupancy was again done over occupancy radius $1 - 22r$. It is clear that OC it is sensitive to spacing, as it is the random configuration that starts to have occupancy circle overlap, and thus its occupancy value starts to decrease first, again due to its sensitivity to spacing between dots. This demonstrates that OC is effective at modelling clustering, and supports the findings of Guest et al (2022), that found OC was highly correlated with graph clustering indices.

5.2.3 Discussion and Outline for Chapter

As the RRI and SI are both illusions of numerosity that use the spatial arrangement of dots, it would be easy to think that they use the same underlying mechanism. As occupancy can explain RRI, then it should also predict the SI. However, from Figure 5.4 the occupancy value for the outer pattern is always larger than that of the inner, therefore it does not predict the SI.

This could be a result of spacing, which the occupancy model is sensitive to (Allik & Tuulmets, 1991a; Bertamini et al., 2018; Valsecchi et al., 2013) whereas the SI has regular spacing between elements on grid. However, as separate patterns the outer does not have this property, it has large spacing between "highly ordered groupings", and the decreased occupancy value of the inner could be the by-product of what Frith and Frith (1972) pointed to, that of the continuity of the inner.

Bertamini et al (2022) introduced a cell cardinality to increase the size of the SI, as well as a linear variant called Bar. This treated each dot in the original illusion as a cell, then replaced each cell with a square grid of dots, the cell cardinality ξ. After scaling the result is a new variant of the illusion, with increased cardinality. Their results showed both illusions were robust to changes in cardinality. Also, the variants of the illusion allowed for randomly sampling 50% and 10% of the elements in the configuration. This manipulation disrupts the continuity or connectedness of the inner pattern, a key property that Frith and Frith (1972) pointed to as

reason the inner was perceived as more numerous. However, even at 10% sampling of the illusion, there was a strong preference for the inner pattern, that was equal in magnitude to when sampling was absent. This result contradicts the claim that the continuity of the inner drives the illusion.

The illusion is not robust to separation, that is if you horizontally displace the inner and outer patterns, the preference for the inner diminishes. For instance, at 10% sampling the choice for the inner\outer patterns is no better than chance.

These results suggest that the SI cannot be understood by considering the inner and outer patterns separately, nor through the continuity of inner. It must be the case that something occurs when there is no separation, that is when the outer encloses the inner.

In this chapter I model the SI using graph theory. I will use a specific type of graph called a geometric graph see section 4.1.2, to represent interaction between the inner and outer patterns during enclosure. I will model this in a different way using graphs, and will show that this approach has more flexibility and will be able to extract features that other approaches cannot (Allïk & Tuulmets, 1991; Dakin et al., 2011).

I will use the local clustering coefficient with the aim to see what effect, if any, interaction (enclosure) has on this index, compared to when there is no interaction (separation). I chose this indices as it has been shown to correlate highly with OC (Guest et al., 2022), it is easier to compute and can be partitioned, I will discuss partitioning later. I do not believe that this approach of two interacting dot patterns has been fully investigated before. In the next section, I briefly outline the necessary graph terminology before describing how I will model the SI.

5.3 Modelling the Interaction between Inner and Outer Patterns

In this section I propose a novel way of modelling the SI (Frith & Frith, 1972). By using graph theory, I will show that it is possible to model interaction between the inner and outer patterns during enclosure.

5.3.1 Partitioning of the Illusion during Interaction

First, we start with the underlying pattern of the dots sown in Figure 5.5 top left panel. These are the peg positions of the game peg solitaire, that the illusion is based on. We then start to draw edges, based on the Euclidean distance d between all pair of dots, regardless of whether they will be eventually coloured as part of the inner or outer pattern, Figure 5.5 top right panel. This forms the underlying geometric host graph for the solitaire illusion $G_{d_{SI}}$.

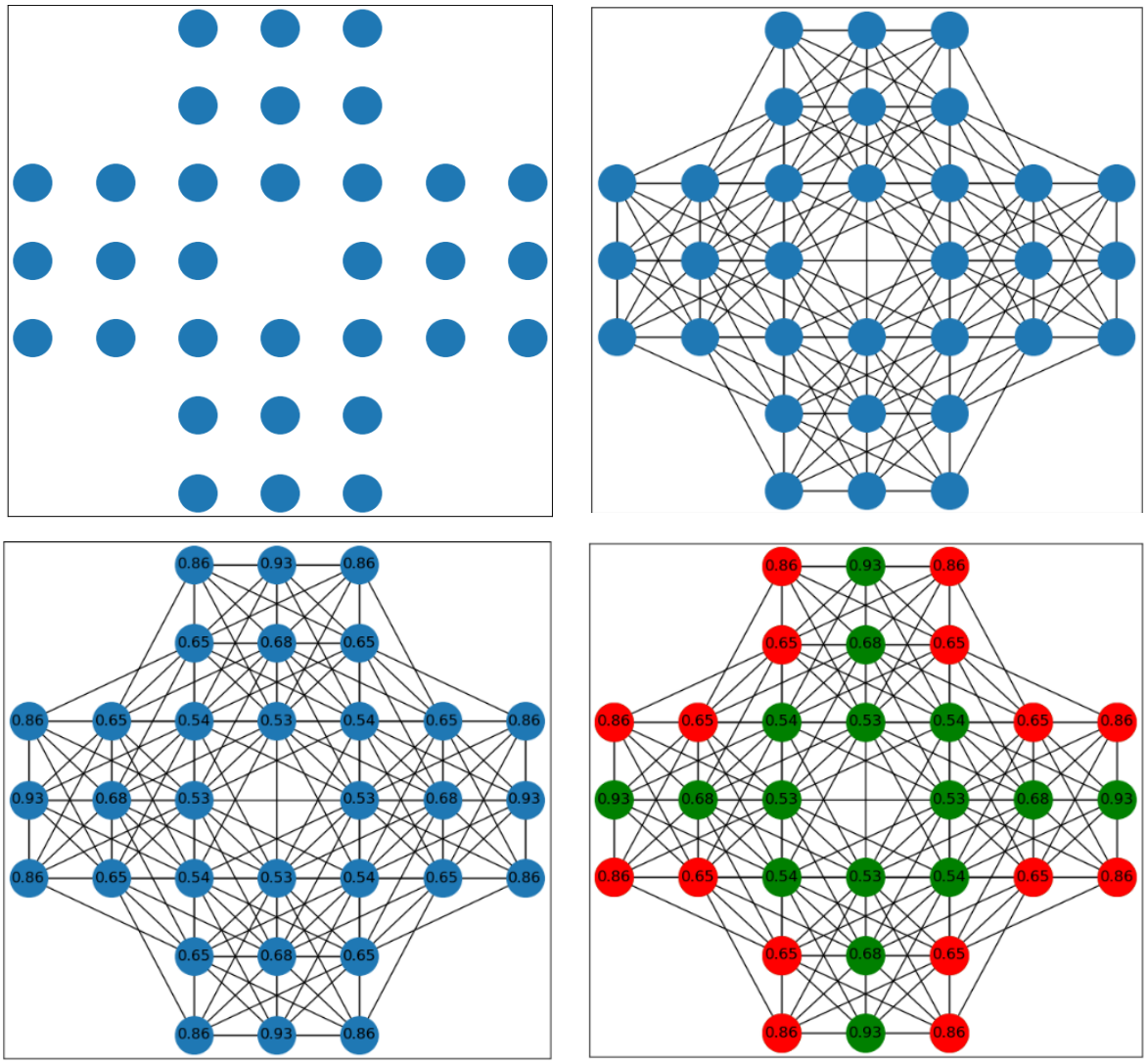

Figure 5.5: Top left panel shows the underlying dot pattern of the original solitaire illusion. The top right panel is the resultant geometric graph when a connectivity distance of 8 times the dot radii applied. The bottom left panel shows the lc computed for each node. Notes that for indices such as lc, it is possible to compute the coefficient down to vertex level. Because of this, can take an average of only the vertices of the inner, and likewise the outer. We see that with interaction the average clustering coefficient for the inner pattern is 0.67, while the average for the outer is 0.76. This different to when interaction is not allowed, see Figure 5.6.

Next, we compute an index, for this example we compute the clustering coefficient for each vertex, Figure 5.5 bottom left panel. We then colour the dots as per the solitaire illusion

Figure 5.5 bottom right panel. For visual convenience the clustering coefficient for each vertex is used as its label.

The final step is to partition the nodes into the inner and outer pattern and average node values for the graph index used. Let the average clustering coefficient for a shape be $\overline{lc}_{shape}$. Then in the example illustrated in Figure 5.5, $\overline{lc}_{inner} = 0.67$, whereas $\overline{lc}_{outer} = 0.76$. Let the ratio of $\overline{lc}_{outer}/\overline{lc}_{inner}$ in the enclosure condition be $\mathcal{R}_{enc_d}$, at any given d. If $\mathcal{R}_{enc_d} = 1$ this would indicate that both patterns are equally clustered. A ratio of $\mathcal{R}_{enc_d} < 1$, would indicate that the inner was clustered then the outer, and a ratio $\mathcal{R}_{enc_d} > 1$ would indicate the outer was more clustered then the inner. From the bottom right panel of Figure 5.5, we see $\mathcal{R}_{enc_{8r=}}1.13$, thus dictating the outer is 13% more clustered then the inner pattern, with interaction between dots allowed.

5.3.2 Interpretation of Partitioning During Interaction

The partitioning of $G_{d_{SI}}$, is a fundamental feature of this approach, as it computes indices while interaction occurs between patterns. This is important, as it extends analysing the inner and outer as just separate patterns. In the previous chapter we saw that the illusion is reduced or absent in the separate condition, that is presenting the inner and outer patterns separately. Although there is a strong preference for the inner, this diminishes with density. Interestingly, they found that the illusion remains, even at high cardinality and low density in the non-separate condition, that is when interaction occurs.

We can, however, compute an index while treating the inner and outer patterns as separate. In this approach we are using the inner and outer dot patterns to induce the respective subgraphs of $G_{d_{SI}}$. Figure 5.6 demonstrates this technique. The same value of $d = 8r$ was used as for $G_{d_{SI}}$ shown in Figure 5.5.

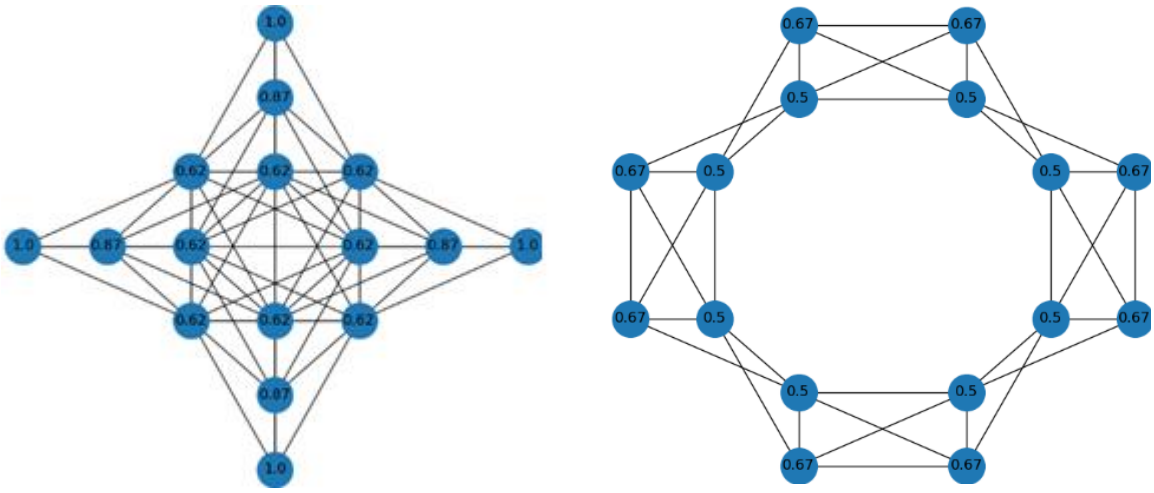

Figure 5.6: left panel shows the subgraph induced by the vertices that make up the inner pattern only, we see the average clustering coefficient is 0.78. Right panel is the subgraph induced by the vertices that make up the outer pattern only, its average clustering coefficient is 0.59.

Let $\overline{lc}_{outer}/\overline{lc}_{inner}$ in the separate condition be $\mathcal{R}_{sep_d}$, for any given value of d, then we see from Figure 5.6 $\mathcal{R}_{sep_{8r}} = 0.75$. Comparing the results from Figure 5.5 and Figure 5.6, it is clear that if one chooses to allow for interaction, this significantly increases the clustering of outer pattern compared to the inner.

This demonstrates the advantage of using graph theory to model dot patterns, in so far as we can drill down to the dot level and compute an index while simultaneously modelling or not, the interaction between patterns. This would not be possible with OC, as we compute on areas of overlap that would be hard to disentangle in terms of inner and outer patterns. Likewise, the method of Dakin et al (2011) produces a single number to represent perceived numerosity. neither approach is fine-tuned enough to partition into interacting patterns.

This also raises an intriguing question, could the placement of the dots in the SI be such, that when interaction occurs, the perceived clustering of the outer is increased?

5.4 Investigating the Solitaire Illusion, and its large Variants using Partitioning and Subgraphs

In the previous section we saw how allowing for interaction between the inner and outer patterns of the solitaire illusion, affected LC when compared to computing for inner and outer patterns separately. This raises an important question, that is to what extent is there a difference, when computing clustering between partitioning on $G_{d_{SI}}$, compared to inducing the subgraphs for the inner and outer pattern, over the whole range of the connectivity distance d? Also is this increase seen in the variants of the SI with more elements, as used in (Bertamini et al., 2022). In this section I investigate the stimuli used in experiment 1 of chapter 3.

5.4.1 Methods

Geometric graphs were created for the inner and outer patterns both in the separate and the non-separate condition, for $\xi: \{1, 4, 9\}$. These map to pattern cardinalities 32, 128 and 288. I chose a different range for d, for each ξ, to ensure I computed over the whole allowable range

At each d I computed the $\overline{lc}_{shape}$, in the enclosed and separate condition then calculated $\mathcal{R}_{enc_d}$ & $\mathcal{R}_{sep_d}$. Networkx (Hagberg et al., 2008) version 2.5.1, was used to compute LC.

5.5.2 Results

The results for $\mathcal{R}_{enc_d}$ & $\mathcal{R}_{sep_d}$ are shown in Figure 5.7, across the whole of d. The dotted line is $\mathcal{R}_{enc_d}$, whereas the solid line is $\mathcal{R}_{sep_d}$. I found that it was always the case that $\mathcal{R}_{enc_d} > 1$, regardless of what value of d used for the host graph Figure 5.7. This was not the case for $\mathcal{R}_{sep_d}$, we saw the opposite result except for very small ranges of d for $\xi \in \{4, 9\}$. This may be due to sparse graphs, that is graphs with few edges which can happen when using low values of d. In such conditions certain graphs can give large clustering values, see (Guest et al., 2022). The grid that the SI residues on may also exacerbate this.

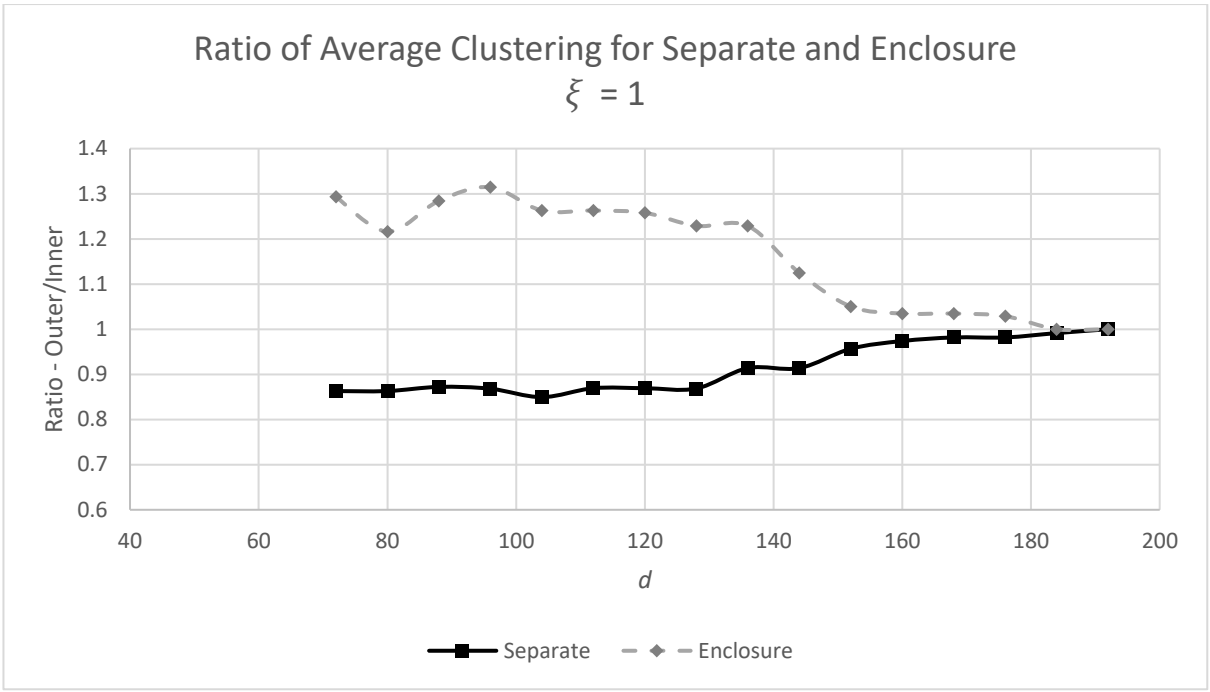
Ratio of Average Clustering for Separate and Enclosure
ξ = 1
Ratio - Outer/Inner
1.4
1.3
1.2
1.1
1
0.9
0.8
0.7
0.6
40
60
80
100
120
140
160
180
200
d
Separate
Enclosure

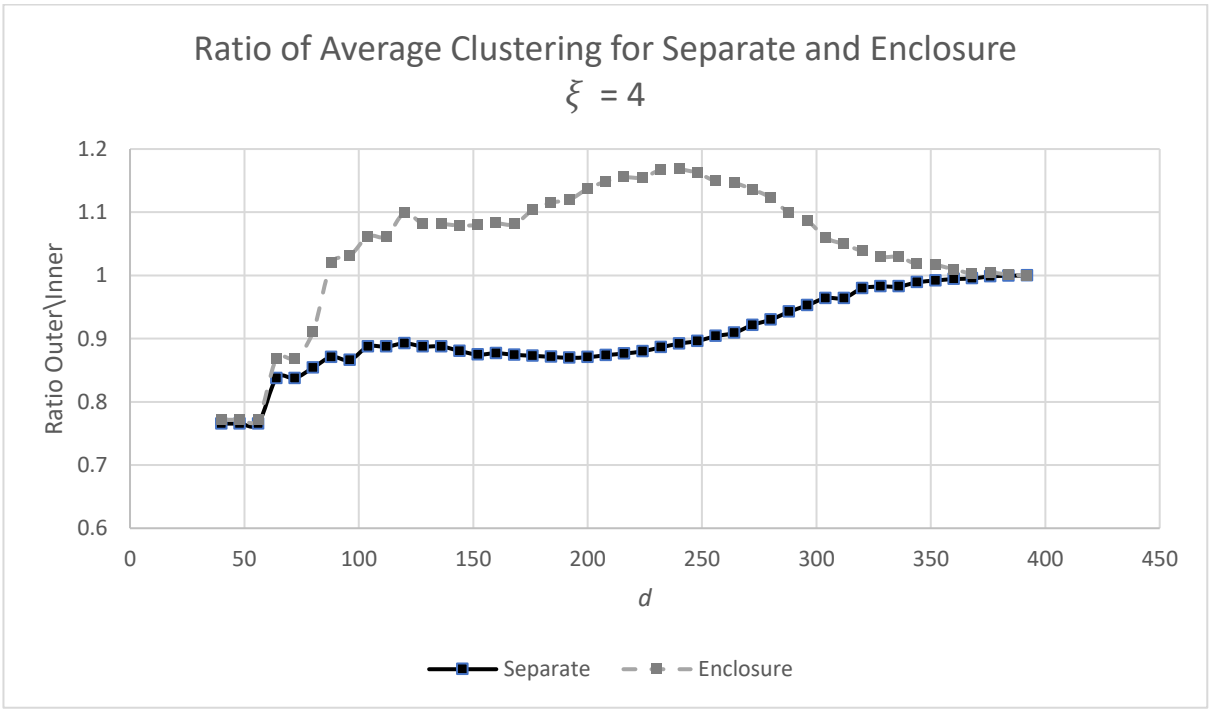
Ratio of Average Clustering for Separate and Enclosure
ξ = 4
Ratio Outer\Inner
1.2
1.1
1
0.9
0.8
0.7
0.6
0
50
100
150
200
250
300
350
400
450
d
Separate
Enclosure

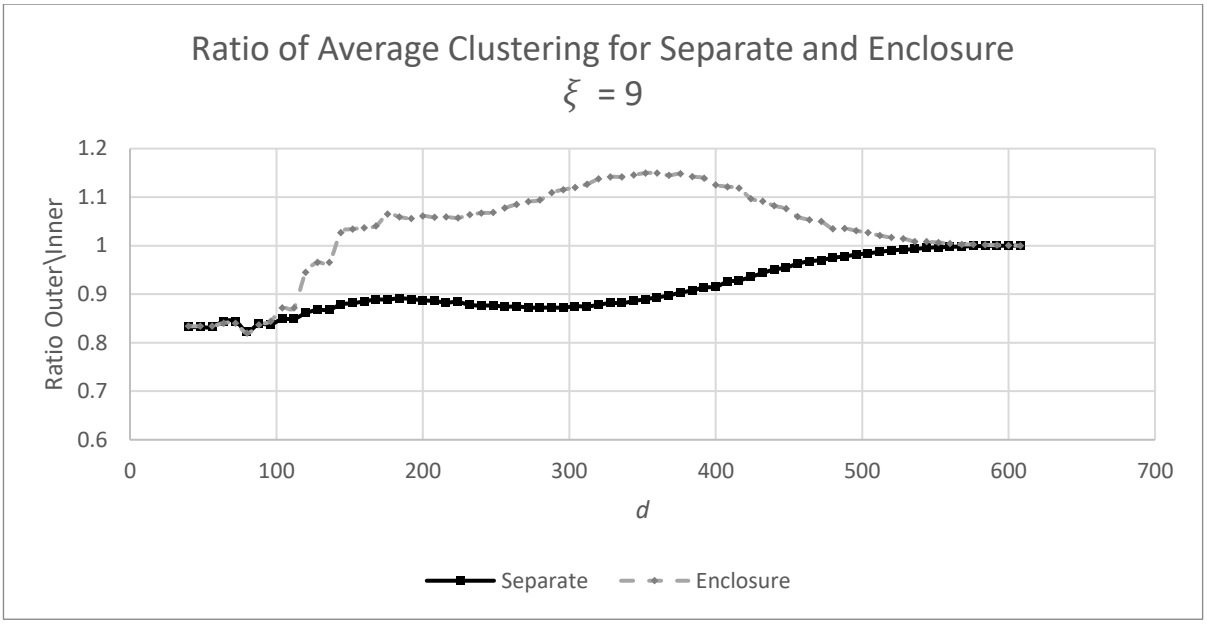

Figure 5.7: Comparison of $\mathcal{R}_{enc_d}$ when partitioning on $G_{d_{SI}}$ against $\mathcal{R}_{sep_d}$. We see that enclosure has the effect of, $\mathcal{R}_{enc_d} > 1$. While the opposite is true for the separate condition, $\mathcal{R}_{sep_d} < 1$. This was robust against changes in d except at very small values d, for $\xi \in \{4,9\}$.

Taken over the whole range of d, for $\xi = 1$ we saw a decrease in clustering of 4.1% for the inner pattern. This is in contrast to an increase of 16.1% clustering for the outer. The results for $\xi \in \{4, 9\}$ showed a similar pattern. This summarised in Table 5.1

Table 5.1: Table of changes in clustering for $\xi \in \{1,4,9\}$.

ξ	**Inner Change**	**Outer Change**
1	-4.1%	+16.1%
4	-8.7%	+4.6%
9	-8.2%	+3.3%

5.4.3 Discussion

The previous results of the inner having the greater clustering coefficient in the separate condition, seems counter-intuitive as Frith & Frith (1972) pointed to the highly ordered groupings of the outer pattern. However, it is the inner pattern that has the smaller convex hull , and density is proportional to the reciprocal of the convex hull (De Marco & Cutini, 2020) thus

it is the inner that is the denser pattern. Hence, a single dense pattern can be more clustered then a less dense pattern with more groupings.

In summary the inner pattern is the denser and least clustered pattern, when interaction occurs, both of which are positively correlated with increased cardinality.

5.5 Investigation of the Solitaire Illusion at Low Density

It is worth comparing frequency plots of the SI, at both high and low density from (Bertamini et al., 2022) Figure 5.8. Frequency bars above the x axis represent the proportion of responses for the inner as the more numerous pattern, below the x axis represents the proportion of responses for the outer as the more numerous pattern. The left-hand panel is the frequency plots for no sampling and $\xi \in \{1, 4, 9\}$, in both the separate and enclosure condition. The right-hand panel is frequency plots for 10% sampling at $\xi \in \{9,16,25\}$ in both the separate and enclosure condition. The most dramatic difference is in the separate condition, where responses start to favour the outer pattern, however statistical analysis showed there was no difference then chance. As a dataset I use the stimuli of experiment 4 in chapter 3.

Also, we see the strong preference both in the high and low density for in the inner pattern in the enclosure condition, in fact the preference for the inner pattern at 10% sampling and $\xi \in \{16, 25\}$ is equal to that of density 100% and $\xi = 9$. For the latter there is no variation in the patterns other than cardinality and separate, however for the former there is variation in the geometric placement of the inner and outer patterns. It is only at $\xi = 9$, that the 10% sampling has influenced the choice of pattern in the enclosure position. Thus, I ask the question, at 10% sampling (low density) what happens to the interaction between inner and outer in the enclosure condition?

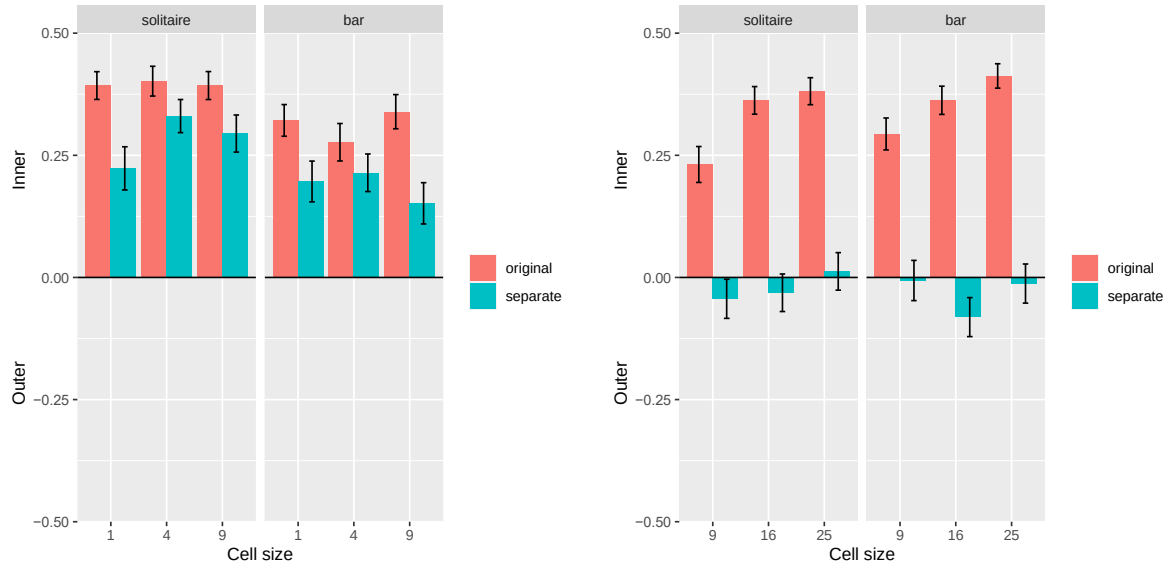

Figure 5.8: left-hand panel, is the frequency plots of the both the SI and Bar illusion at 100% density for $\xi \in \{1, 4, 9\}$, in the separate and enclosure conditions. The right-hand panel is the frequency plots for 10% density for $\xi \in \{9, 16, 25\}$ in the separate and enclosure condition. The Y axis is the ratio of participants selecting the inner, 1 is when everyone selects the inner. Original means enclosure.

5.5.1 Methods

I repeated the calculation of the previous section on the data from experiment 4 (Bertamini et al., 2022). To compute $\overline{lc}_{shape}$ at each value of d the average was taken over all patterns. This was also the case for computing clustering for the separate condition, , dataset size for each ξ was 160. Again the python library Networkx (Hagberg et al., 2008), version 2.5 to compute all indices.

5.5.2 Results

The results consistent with the pattern we saw in the previous section at $\xi \in \{1, 4, 9\}$ and no sampling Figure 5.9. Except for very small values and ranges of d, it was always the case that during enclosure that $\mathcal{R}_{enc_d} > 1$. However, this was not the case for $\mathcal{R}_{sep_d}$. In the separate condition the opposite was true, with $\mathcal{R}_{sep_d} < 1$ for large ranges of d.

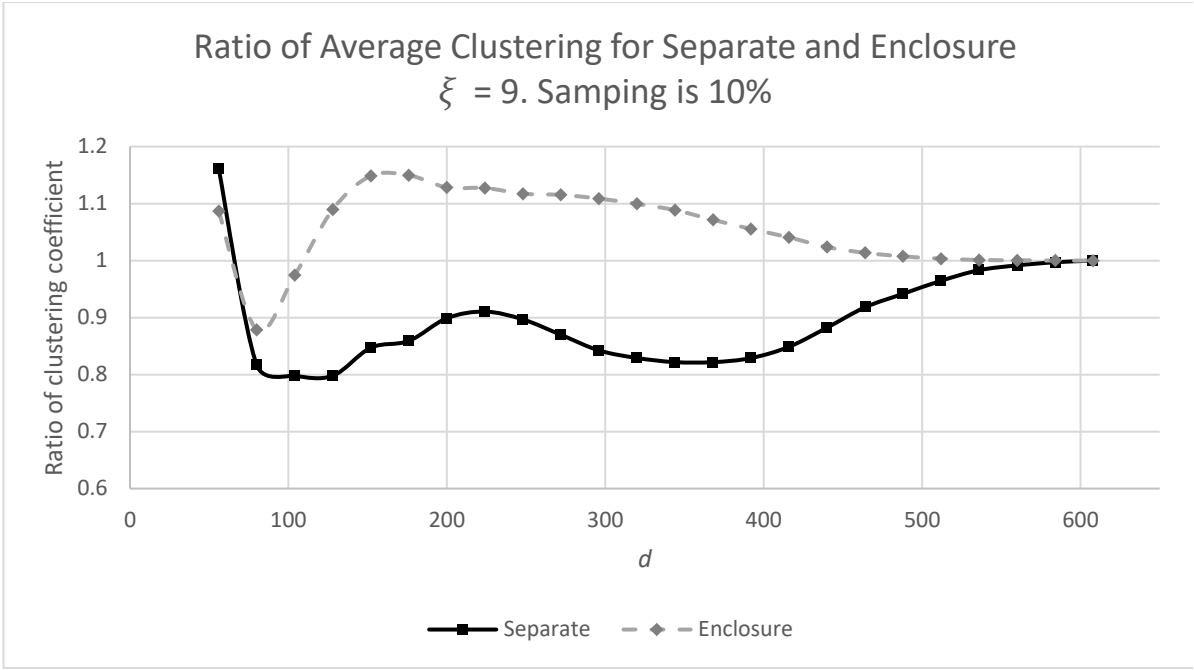
Ratio of Average Clustering for Separate and Enclosure
ξ = 9. Samping is 10%
Ratio of clustering coefficient
1.2
1.1
1
0.9
0.8
0.7
0.6
0
100
200
300
400
500
600
d
Separate
Enclosure

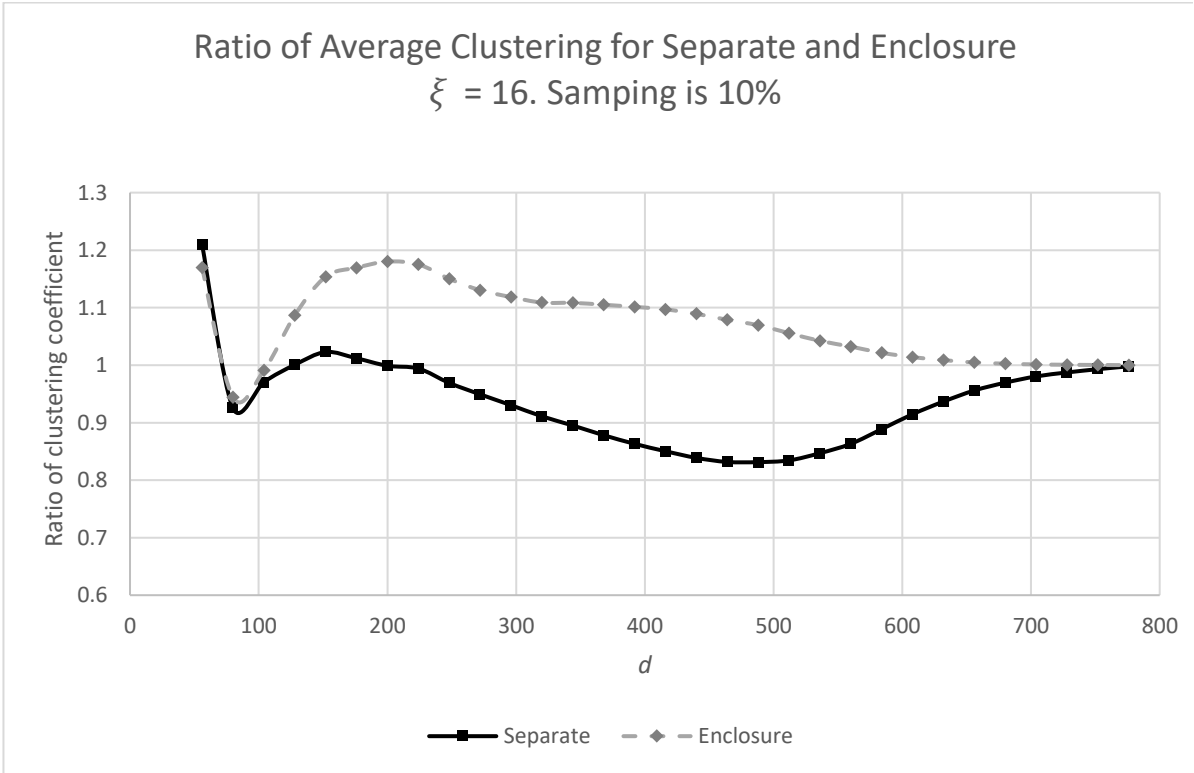
Ratio of Average Clustering for Separate and Enclosure
ξ = 16. Samping is 10%
Ratio of clustering coefficient
1.3
1.2
1.1
1
0.9
0.8
0.7
0.6
0
100
200
300
400
500
600
700
800
d
Separate
Enclosure

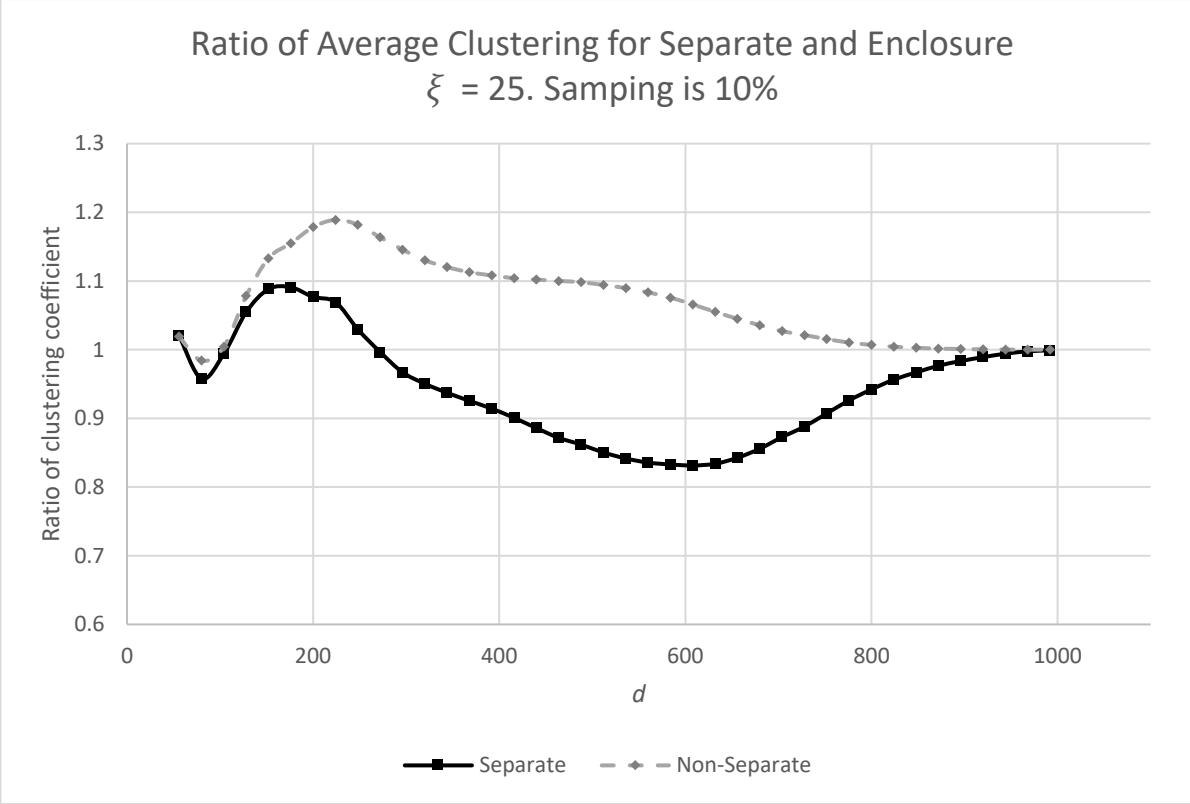

Figure 5.9: Ratio plots for $\xi \in \{9, 16, 25\}$ at 10% sampling. The dotted line is always the ratio between outer divided by inner in the enclosed condition, whereas the solid line is the same ratio except we treat inner and outer separate. The top row is $\xi = 9$, the middle row is $\xi = 16$ and the bottom row is $\xi = 25$. In all cases the pattern is clear, enclosure increases the clustering of outer.

Table 5.2 shows the change, with respect to the separate condition, in clustering of the inner and outer with enclosure. We see a consistent drop in clustering for the inner, while a simultaneous increase for the outer. Interestingly the decrease in clustering for inner strengthens with increasing

ξ, the opposite is the case the outer pattern.

Table 5.2: The change in clustering for both inner and outer during enclosure, with respect to the separate state.

ξ	**Inner Change**	**Outer Change**
9	-5.61%	+12.03%
16	-6.42%	+6.94%
25	-7.46%	+5.09%

5.5 Conclusions

I believe that SI can only be understood by modelling interaction between the inner and outer patterns. As opposed to treating each as separate. An example of the latter approach, is filled area (Vos et al., 1988), that argued the continuity of the inner pattern gives it the greater filled area of the stimulus field, and is therefore perceived as more numerous. However, this would be difficult to argue at high values of ξ and low random sampling, with the continuity of the inner gone. It also does not explain the differences in separate\enclosure states in experiments 3 and 4 (Bertamini et al., 2022).

It is known that clustering is negatively correlated with numerosity perception (Allik & Tuulmets, 1991a; Bertamini et al., 2016, 2018; Chakravarthi & Bertamini, 2020). If we define clustering in terms of the local clustering coefficient LC, in the separate condition the inner pattern is always more clustered independent of ξ or level of random sampling. However, during enclosure this flips and it is outer that is more clustered.

However, is the increase in clustering is just a by-product of the unusual shape of SI, and therefore an irrelevant feature? Although this is a valid question, the increase is present across either the vast majority or the whole range of d. Also, this argument can not apply for cell cardinalities of 9, 16 and 25, at low density. As these patterns adopt a far more quasi-random dot distribution and any resemblance of the original illusion is gone. The effect of enclosure on clustering, appears to be a robust finding, and therefore must be significant. Also, without the use of graph theory, this result would be difficult to find. I believe this underlies the importance of this approach to the study of numerosity.

Frith & Frith (1972) claimed that the Illusion is caused by the continuity of the inner forming a better gestalt then the highly ordered units of the outer. However, you do not need continuity in the inner pattern, nor do you need highly ordered sub units as an outer pattern. The results from experiments 3 and 4 (Bertamini et al., 2022) demonstrate this.

From my investigations, the solitaire illusion is a race to be the least clustered pattern when interaction occurs during enclosure. It is the increase in clustering of the outer, together with a corresponding decrease in clustering for the inner, that condemns the outer to be perceived as the least numerous.

6. Future Research and Conclusions

6.1 Future Research

The argument presented in the chapter, of an interaction between the inner and outer patterns driving the illusion, leads to an intriguing experiment. Using the large variants of the SI, and 10% sampling, it would be possible to generate stimuli, such that when the partitioning method of interacting patterns is computed, the outer is no longer the more clustered pattern. Consider Figure 5.10.

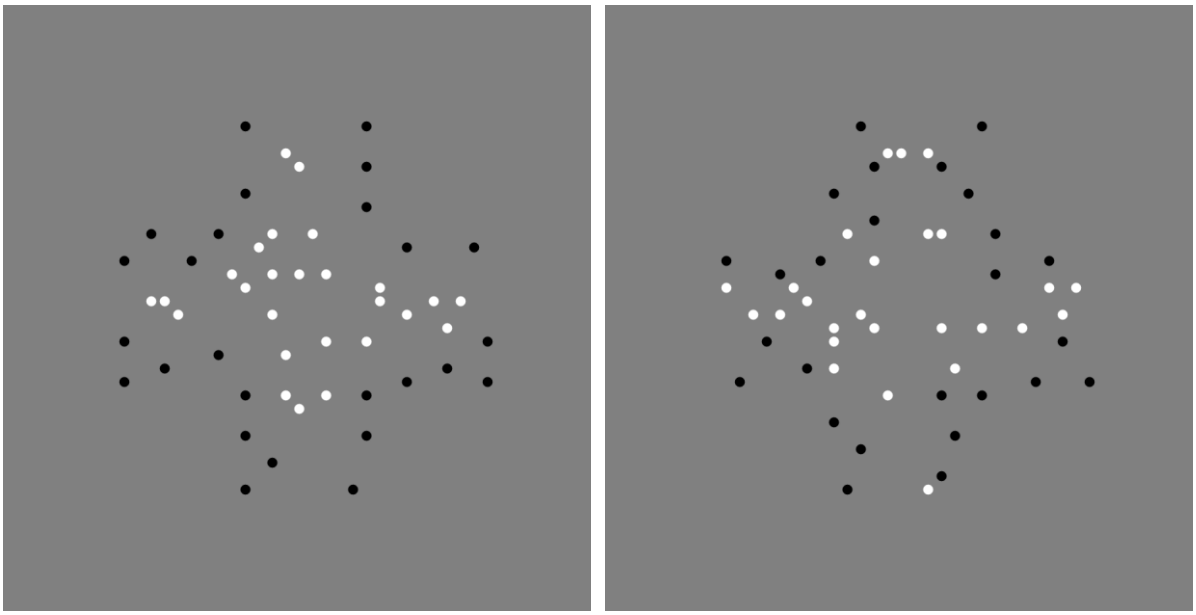

Figure 6.1: Both figures show the SI with $\xi = 16$, at 10% sampling. However, the picture on the left the outer pattern is not allowed to interact with the inner or any other dots in the outer pattern. The picture on the right has a minimum spacing between elements of the outer pattern, but is allowed to interact with the inner pattern. Both patterns would produce a $\mathcal{R}_{enc_d} < 1$

In the left-hand panel Figure 5.10, the outer pattern has a minimum spacing of 2 grid points between any other dot. This has the effect of spreading out of the outer, with no interaction with the inner. The right-hand panel the restriction on the outer dots only applies to the outer, not to the inner pattern. Here, there is interaction between inner outer. In both cases the $\mathcal{R}_{enc_d} < 1$, meaning it is the inner pattern that is more clustered during interaction. I predict that in both cases the illusion will be greatly diminished, or absent. Such an experiment, would pit the RRI against the SI, as from the RRI it is known an increase spacing has a positive

effect on numerosity perception. Also, would affect does interaction have? This could have profound consequences for the solitaire and Ponzo illusions.

6.2 Conclusions

In this thesis we investigated the potential uses of graph theory to the study of numerosity. Its main aim was to discover new methods that could shed light on the foundations of numerical cognition. Specifically, we looked at dot patterns, and how dot placement and the proximity to neighbouring dots can bias numerosity perception.

Numerosity is a branch of perception, that deals with the non-symbolic perception of number, termed the number sense (Dehaene, 2011). Typically, dot arrays are used to investigate this number sense, and in comparison studies it has been shown that dot placement, and the manipulation of distance between a dot and its neighbours can bias numerosity perception (Frith & Frith, 1972; Ginsburg, 1980; Valsecchi et al., 2013). The work of Ginsburg 1980, spurned the occupancy model of numerosity (OC) (Allïk & Tuulmets, 1991). In this approach, the proximity-based relationship between neighbouring dots is modelled by a fixed occupancy circle, of occupancy radius r_o, centred on each dot. Thus, the relations of proximity between neighbouring dots is modelled by the amount of overlap between neighbouring occupancy circles.

We found that graphs are discrete mathematical structures that model binary relationships, called edges E, between abstract objects, called vertices V. Edges can represent physical connections, like roads or bridges; the study of graph theory started with the paper the seven bridges of Konigsberg by Leonard Euler in 1736. Or they can be conceptual such as friendships on social networks. In this work the vertices were the position of dots, in dot stimuli. The edges were conceptual, that is we replaced the overlap of two occupancy circles with an edge.

If we denote proximity, as the Euclidean distance d between dots. Then the use of d as the criterion on whether two dots are connected by an edge, is termed a geometric graph $G_d(V, E)$. We found that the relationship between OC and $G_d(V, E)$, was $d = 2r_o$ which is

essentially the diameter of the occupancy circle. Thus, any neighbouring dot will be connected by an edge if the distance is equal or less then $2r_o$ or d. Therefore, each edge formed would model an overlap of two occupancy circles. This is the approach of Bertamini 2016, using $G_d(V, E)$ as the host graph, from which different indices can be computed. This thesis extended this method.

Other research has investigated proximity by the notion of connectedness between dots (Adriano et al., 2022; Allik & Raidvee, 2021), however these methods use either a nearest neighbour graph as the host graph, or Kanizsa illusion lines for form perceived connections between dots. However, both of these approaches tend to model the connectedness of only two dots at a time. The use of $G_d(V, E)$, allowed for all neighbouring dots with Euclidean distance d or less to be connected, thus host graphs were richer, or more connected.

We found that another advantage to this approach, is there are so many indices to compute on graphs. In this work we investigated 10 different graph indices. They were, connected components CC, local clustering coefficient LC, global clustering coefficient GC, independence number IN, domination number DN, eigenvector centrality EC, clique number CL, random walk RW, total edge length TL and total degree TD. They were chosen in order that a wide spectrum of graph features could be calculated. We computed the graph indices alongside OC. This was possible due to the relationship between the occupancy radius r_o and connectivity distance d.

In chapter 2, we produced 1000 dot patterns for each of the following numerosities 22, 28, 34 and 40, with each pattern confined to an outer radius R. Thus, the maximum range for the connectivity distance between any two dots was $\{0,\ 2R\}$. We computed each graph index, on all patterns at regular intervals on $G_d(V, E)$, where $d \in \{0,\ 2R\}$. At each d we used averages to compute correlation matrices. The resulting datasets were of high dimensionality, that is a correlation matrix for each d, multiplied by 4 different levels of numerosity. However, we represented the correlation matrices as discrete heatmaps. We grouped the correlations in the

following ranges ((1.0, 0.6), (0.59, 0.2), (0.19, -0.19), (-0.20, -0.59), (-0.6, -1)). Using discrete colours made easier the identification of groups of correlated indices at various points on d. We found a cluster of indices at short values of $d \sim R/4$, these were OC, CC, IN, DN, LC, GC, we called this the clustering group, as clear clustering indices of CC, LC and GC were members. At $d \sim R$ we found high correlations between TD, TL, EG & CL. We called this the spread group as EG is sensitive to how information spreads on graphs.

We found potential problems with approach, as graph indices have different threshold values, as graphs become denser and more connected, with increasing d. For instance, the index connected components CC will start to its threshold value as graphs become more connected. This is at the same point as random walk becomes a computable index. Thus, the small variance of both produces significant and high correlations between the two. This is a consequence of both indices having a pathological distribution, for the same d.

In an attempt to avoid such pitfalls, and to simplify the correlation datasets we only used the value of d_n that gave the maximum standard deviation for each index n. The resulting datasets σ_n thus had the advantage of cutting the number of datasets down from over 100 to 4. A drastic reduction in the dimensionality of the output. Secondly, we found that the spread and cluster group were also present on the same heatmap. Thus, summarising the main results of the correlation computation.

A principle component analysis was performed on σ_n, which seemed to confirm the results of the correlational analysis on σ_n. The PCA found two components, one being sensitive to clustering indices; this is the component OC was a member of. The members of this were identical to the cluster group of correlational analysis. The second component had as its members were the spread group of the correlational analysis. The load values of each index, of PCA, also represented the strength of each index's p value with other members of its group.

We found that the occupancy model is hard to compute, particularly as o_r grows. From our analysis OC seems to be novel method of measuring clustering. We suggest therefore that it may be useful for researchers to consider less computationally intensive indices, such as LC, GC and CC. More generally, researchers in the field of numerosity tend to control for factors such as convex hull and total dot surface area (Salti et al., 2017), however it may be useful to control for clustering and spread in dot stimuli.

In chapter 3 we investigated the concept of clustering, but in a different way. Would it be possible to use clustering or numerosity in order to learn a rule? As there is evidence of an ancient and shared number sense across the animal kingdom, could non-humans or baby chickens also use clustering in similar way? Baby chicks are interesting as to compare with as they are naïve with no learned behaviour.

To answer these questions, a joint study was performed with a team from the university of Padua. In the human study, participants were given a task of finding a rule based on spacing\clustering of dot patterns. The procedure was a between groups design, were one group was reinforced with smaller spacing between 40 dots, or high clustering. The second group was reinforced with large spacing between 20 dots, or low clustering. After learning the rule the main experiment contained random placed critical trials of 30 dots, with one pattern having a minimum restraint of 5.1 dot radii, and the other 2.1 dot radii. For the group that was trained on 40 dots, that is numerosity the assumption is that they would pick the pattern with minimum distance restraint of 5.1, as predicted by the occupancy model. Likewise, the group that was trained on 20 dots would pick the pattern with minimum distance 2.1 as this again is predicted to be have the lower perceived numerosity by the occupancy model.

However, a confounding variable is density. The test stimuli with minimum spacing 5.1 would resemble more the training patterns with 20 dots. Likewise, the training patterns with 40 dots would have a minimum spacing similar to that of the test stimuli with minimum distance of 2.1.

The results of the human study showed that the illusion, as predicted by OC was seen and participants went with numerosity, that is the group trained on 40 dots went with the 5.1 minimum distance pattern, the 20 dot group went with 2.1 minimum distance pattern. The results from the chick study was mixed. The researchers did two measurements. One was the first approach, the second was the stimuli that the baby chicken found chose by circumnavigating the board it was one for the food treat. For first approach, there was evidence that the baby chickens saw the illusion, that is went with numerosity\clustering, although the results were weaker then for the human study. For the second measurement, that is the test stimuli that was finally chosen, there was a strong preference for the highly clustered test pattern, regardless of what training group the chicken was in. The authors postulated that this could due to chicks prefer more natural distribution of random elements, consistent with a distribution of food in the environment. This is also consistent with the definition built for clustering in section 3.1.1, that clustering is a measure of far away a pattern is from being a regular pattern.

In chapter 4 we set out a series of experiments that we conducted, to investigate this illusion further. One the motivations for this work was that no one had ever applied the occupancy model to the SI. As an illusion, the SI consists of two patterns, one enclosed by the other (inner\outer). When applied, the OC predicts the outer as being perceived as the more numerous, however numerous studies have found that the opposite is true. Secondly, we wanted to investigate whether subitization had any effect on the illusion. We postulated this as the outer patterns has 8 ordered groupings of 2 dots. Thus, each group is well within the range of subitization ≤ 4.

We therefore we need to create versions of SI with increased numerosity. This was achieved by treating each dot in the original illusion as a cell. Then each cell was replaced by a square grid of dots of 4 or 9, then scaled accordingly. Thus, creating structurally similar versions of SI but with much increased numerosity. This meant that each group of the outer, taken out of the subitizing range.

The first experiment used the original and larger versions of SI and a linear variant called Bar. Bar was shape B in the original work of Frith & Frith 1972. We also split or displaced the inner and outer patterns, to test whether OC would predict a reversal of the illusion in this condition. We found that subitization had no effect on the illusion, a strong bias remained for the inner in the non-displaced state, regardless of numerosity. In the displaced condition, although reduced the strong bias for the inner pattern remained. Again, this result was robust against numerosity and illusion.

To emphasis the greater area of the outer, we repeated the 1st experiment except each pattern was enclosed by a set of lines that formed a concave hull around the inner and outer. The results mirrored the results of the 1st experiment. The concave hull had effect on the illusion in either the displaced or non-displaced condition.

The inability of OC to predict the results of the first two experiments, maybe due to as a method OC is sensitive to dot spacing. Whereas the SI is on a grid, where the spacing between neighbouring dots is equal. Also, he original authors of SI Frith and Frith 1972, suggested that it was the continuity of the inner that allowed it to form a better gestalt. Hence, it was this property that meant it was perceived as more numerous. We therefore introduced variability between dots by randomly sampling both illusions (SI, Bar) for numerosities 1, 4 and 9. Hence the 3rd experiment was a repeat of experiment 1, except each pattern was randomly sampled by 50%, thus producing quasi-random patterns for both inner and outer. In the non-displaced condition, variability in dot spacing had no effect on the illusion, there was a strong bias for the inner regardless of illusion or numerosity. The displaced condition was different. Although a bias for the inner remained, it was much reduced. This seemed to suggest that density effects the displaced condition but plays little or no part in the non-displaced condition.

In the 4th experiment, to avoid having numerosities in the subitization range, we used the following numerosity for SI and Bar, 9, 16 and 25. Then each pattern was randomly sampling down to only 10% of the original configurations. In this condition the continuity of the inner

was destroyed completely. Again in the non-displaced condition, the random sampling had no effect on the illusion, a strong bias was seen which grew with increased numerosity, and both illusions. In the displaced condition, the illusion was gone, binomial tests showed that the choice for either inner or outer was no different from random choice.

These results are quite profound. Density only has an effect in the displaced condition. However, it plays no part in either SI or Bar. Nor can the continuity of the inner be a factor, as stated by Frith and Frith 1972, as the illusion was strong at numerosity 25 randomly sampled down to 10%. The destruction of any bias for the illusion in displaced condition, also shows an important point, the solitaire illusion can not be understood as treating the inner and outer patterns as separate entities, whose properties when combined can explain the illusion. There must, in some sense be interaction between the two patterns, that produces the bias for the illusion. With this in mind, we decided to model the illusion as two patterns interacting. This possible using graph theory as it is built on binary relations between objects.

We computed clustering on both the inner and outer, as separate patterns and also as one pattern, the inner and outer combined, which we called the host graph. The host graph allowed for the modelling of interaction between the inner and outer, by the formation of edges between the two patterns. We chose clustering as it was closely correlated to OC, but computationally easier to compute. It is an important factor in both human and animal numerosity (Bertamini et al., 2016, 2018), and can computed at a node level. The latter property is important as this allowed for the partition of the host graph into the inner and outer pattern.

The analysis conducted showed that in the displaced condition, that is treating inner and outer as separate non-interacting patterns, it was the inner pattern that was computably the more clustered pattern. This was robust against either illusion, numerosity or level of random sampling. This was not expected as it is the outer that is the more grouped pattern. However, this changed when we allowed for interaction. When computed on the host graph and then partitioned into the inner and outer pattern, we found that the opposite was true. On the host

graph it was the outer pattern that was computably the more clustered pattern. We found this result was robust against illusion numerosity, level of random sampling and connectivity distance d.

In order to ensure that the above analysis was unique to clustering, we repeated the above with TD from the spread group. We found that the inner always has the higher TD regardless of whether the two patterns are separate or interact on a host graph. Thus, we believe the behaviour of clustering during interaction is an important feature of the illusion. We propose that clustering between interacting patterns is what drives the illusion. Further work is needed to investigate this further.

Appendix

Glossary

Approximate number system (ANS): Humans and other animals can estimate the size of a set of elements without relying on counting, language or symbols. The system that supports this estimation process has been called the approximate number system (ANS), and sensitivity to differences in numerosity follows Weber's law. It has also been found that ANS performance correlates with mathematics skill.

Clique: A (loop-less, simple) graph G is a clique (or a complete graph) if every pair of vertices in G forms an edge.

Convex hull: In the case of geometric elements in the 2D Euclidean plane, the boundary of the convex hull is the simple closed curve with minimum perimeter containing all elements. Visually, one may imagine stretching a rubber band so that it surrounds all the elements. Often what is computed is the total area of the convex hull.

Degree: (of a node v in a graph) is the number of edges containing v. This is usually denoted as $\deg_G v$ or simply $\deg v$ when the graph is clear from the context. The sum of all values of Degree is called Total Degree.

Edge: see Graph

Eigenvector: In linear algebra, an eigenvector $\boldsymbol{x}$ of a linear transformation A is a non-zero vector (a finite sequence of numbers) that changes at most by a scalar factor λ when the given linear transformation is applied to it. In symbols $A \cdot \boldsymbol{x} = \lambda \cdot \boldsymbol{x}$.

Global clustering coefficient: the global clustering coefficient in G is the ratio

$$\frac{3 \times \text{Number of triangles}}{\text{Number of connected triplets}}$$

where a triangle is a collection of three edges of the form: $(u,v),(v,w),(u,w)$, and a connected triple is a triplet of vertices u,v,w for which there exist two edges of the form $(u,v),(v,w)$.

Graph: In the context of graph theory, a graph is a formal structure defined by a set of points (or nodes, vertices) and a collection of unordered pairs of points called edges (or lines, links). The graph is loop-less if it contains no edge of the form (v,v). The graph is simple if it contains no repeated edge.

Graph theory: the study of graphs, which are mathematical structures used to model pairwise relations between elements. Graph theory is part of discrete mathematics.

Königsberg bridges problem: Königsberg (now Kaliningrad, Russia) is set on the Pregel River, and has two large island and seven bridges. The problem is to devise a walk that would cross all seven bridges once and only once. This problem has a place in the history of mathematics. In 1736 Leonhard Euler provided a solution (showing that it is not possible) that laid the foundations of graph theory.

Local clustering coefficient: The local clustering coefficient lc_v of a vertex v in a loopless, simple graph G is the ratio

$$lc_v = \frac{2e\big(N(v)\big)}{\deg v(\deg v - 1)}$$

where $N(V)$ and the set of vertices connected to a v through an edge, and $e(X)$ is the number of edges connecting two elements of the vertex set X. The average value of lc_v defines the local clustering coefficient of G.

Loop: In graph theory, a loop is an edge that connects a vertex to itself, (v,v).
Node: see Graph

Numerosity: although in English this noun can also mean the state of being numerous, i.e., numerousness, in the scientific study of numerosity it is used to refer to the quantity itself. Therefore, in this sense it is synonymous with what in mathematics is called the Cardinality of a set: a measure of the number of elements of the set.

Principal Component Analysis (PCA): a multivariate data analysis technique that allows to summarize information by means of a small set of summary indices. Statistically, PCA finds hyper-planes in the n-dimensional space that approximate the data as well as possible in the least squares sense.

Random Geometric Graph: a particular type of graph. It is an undirected graph constructed by randomly placing vertices in a metric space, i.e. 2D space. The placement is typically random, but the probability distribution can vary. Vertices are connected by an edge if and only if their Euclidian distance is less than a threshold, i.e., a radius r.

Random walk: in the mathematical sense, a random walk is a random process that generates a path between elements or locations in some mathematical space. The random walk is a sequence of random steps. We are interested in random walks within graphs.

Subgraph: (of a graph G) is a graph having all its vertices and edges in G.

Subitization: a rapid and accurate judgment of numerosity performed for small numbers. The term was coined by Kaufman et al. (1949) from the Latin adjective subitus (meaning "sudden"). The term captures a sense of immediately knowing how many items are present in the visual scene. The subtilization range does not exceed 4 or 5 items.

References

Adachi, I. (2014). Spontaneous spatial mapping of learned sequence in chimpanzees: Evidence for a SNARC-like effect. *PloS One*, *9*(3), e90373. https://doi.org/10.1371/journal.pone.0090373

Adriano, A., Girelli, L., & Rinaldi, L. (2022). Number is not just an illusion: Discrete numerosity is encoded independently from perceived size. *Psychonomic Bulletin & Review*, *29*(1), 123–133. https://doi.org/10.3758/s13423-021-01979-w

Agrillo, C., Dadda, M., Serena, G., & Bisazza, A. (2008). Do fish count? Spontaneous discrimination of quantity in female mosquitofish. *Animal Cognition*, *11*(3), 495–503. https://doi.org/10.1007/s10071-008-0140-9

Agrillo, C., Parrish, A. E., & Beran, M. J. (2014). Do primates see the solitaire illusion differently? A comparative assessment of humans (Homo sapiens), chimpanzees (Pan troglodytes), rhesus monkeys (Macaca mulatta), and capuchin monkeys (Cebus apella). *Journal of Comparative Psychology*, *128*(4), 402–413. https://doi.org/10.1037/a0037499

Agrillo, C., Parrish, Audrey E, & Beran, Michael. (2016). How illusory is the solitaire illusion? Assessing the degree of misperception of numerosity in adult humans. *Frontiers in Psychology*, *7*. https://doi.org/10.3389/fpsyg.2016.01663

Agrillo, C., Piffer, L., Bisazza, A., & Butterworth, B. (2012). Evidence for two numerical systems that are similar in humans and guppies. *PloS One*, *7*(2), e31923. https://doi.org/10.1371/journal.pone.0031923

Allik, J., & Raidvee, A. (2021). Proximity model of perceived numerosity. *Attention, Perception, & Psychophysics*. https://doi.org/10.3758/s13414-021-02252-x

Allïk, J., & Tuulmets, T. (1991). Occupancy model of perceived numerosity. *Perception & Psychophysics*, *49*(4), 303–314. https://doi.org/10.3758/BF03205986

Allik, J., Tuulmets, T., & Vos, P. G. (1991). Size invariance in visual number discrimination. *Psychological Research: An International Journal of Perception, Attention, Memory and Action*, *53*(4), 290. https://doi.org/10.1007/bf00920482

Anobile, G., Cicchini, G. M., & Burr, D. C. (2014). Separate Mechanisms for Perception of Numerosity and Density. *Psychological Science*, *25*(1), 265–270.

Anobile, G., Turi, M., Cicchini, G. M., & Burr, D. C. (2015). Mechanisms for perception of numerosity or texture-density are governed by crowding-like effects. *Journal of Vision*, *15*(5), 4. https://doi.org/10.1167/15.5.4

Aurenhammer, F. (1988). Improved algorithms for discs and balls using power diagrams. *Journal of Algorithms*, *9*(2), 151–161. https://doi.org/10.1016/0196-6774(88)90035-1

Barnard, A. M., Hughes, K. D., Gerhardt, R. R., eDiVincenti, L., Bovee, J. M., & Cantlon, J. F. (2013). Inherently analog quantity representations in olive baboons (Papio anubis). *Frontiers in Psychology*, *4*. https://doi.org/10.3389/fpsyg.2013.00253

Basagni, S. (2001). Finding a Maximal Weighted Independent Set in Wireless Networks. *Telecommunication Systems*, *18*(1), 155–168. https://doi.org/10.1023/A:1016747704458

Beran, M. J. (2006). Quantity Perception by Adult Humans (Homo sapiens), Chimpanzees (Pan troglodytes), and Rhesus Macaques (Macaca mulatta) as a Function of Stimulus Organization. *International Journal of Comparative Psychology*, *19*(4). https://doi.org/10.46867/IJCP.2006.19.04.05

Bertamini, M. (1), Guest, M. (1), Vallortigara, G. (2), Rugani, R. (3), & Regolin, L. (3). (2018). The effect of clustering on perceived quantity in humans (Homo sapiens) and in chicks (Gallus gallus). *Journal of Comparative Psychology*, *132*(3), 280–293. Scopus®. https://doi.org/10.1037/com0000114

Bertamini, M., Guest, M., Contemori, G., & Zito, M. (2022). What the Solitaire illusion tells us about perception of numerosity. *British Journal of Psychology (London, England : 1953)*. https://doi.org/10.1111/bjop.12627

Bertamini, M., Zito, M., Scott-Samuel, N. E., & Hulleman, J. (2016). Spatial clustering and its effect on perceived clustering, numerosity, and dispersion. *Attention, Perception, & Psychophysics*, *78*(5), 1460–1471. https://doi.org/10.3758/s13414-016-1100-0

Bolker, B. M., Brooks, M. E., Clark, C. J., Geange, S. W., Poulsen, J. R., Stevens, M. H. H., & White, J.-S. S. (2009). Generalized linear mixed models: A practical guide for ecology and evolution. *Trends in Ecology & Evolution (Amsterdam)*, *24*(3), 127–135. https://doi.org/10.1016/j.tree.2008.10.008

Bonacich, P. (1987). Power and Centrality: A Family of Measures. *American Journal of Sociology*, *92*(5), 1170–1182.

Bose, P., Gsieniec, L. A., Römer, K., & Wattenhofer, R. (2015). *Plane and Planarity Thresholds for Random Geometric Graphs* (Vol. 9536, pp. 1–12). Springer International Publishing AG. https://doi.org/10.1007/978-3-319-28472-9_1

Brannon, E. M., & Terrace, H. S. (1998). Ordering of the Numerosities 1 to 9 by Monkeys. *Science*, *282*(5389), 746. Gale OneFile: Health and Medicine.

Burgess, A., & Barlow, H. b. (1983). The precision of numerosity discrimination in arrays of random dots. *Vision Research*, *23*(8), 811–820. https://doi.org/10.1016/0042-6989(83)90204-3

Burr, D., & Ross, J. (2008). A Visual Sense of Number. *Current Biology*, *6*, 425–428.

Cantlon, J. F., & Brannon, E. M. (2006). Shared System for Ordering Small and Large Numbers in Monkeys and Humans. *Psychological Science*, *17*(5), 401–406. https://doi.org/10.1111/j.1467-9280.2006.01719.x

Cantlon, J. F., & Brannon, E. M. (2007a). How much does number matter to a monkey (Macaca mulatta)? *Journal of Experimental Psychology. Animal Behavior Processes*, *33 1*, 32–41.

Cantlon, J. F., & Brannon, E. M. (2007b). Basic Math in Monkeys and College Students. *PLOS Biology*, *5*(12), e328. https://doi.org/10.1371/journal.pbio.0050328

Chakravarthi, R., & Bertamini, M. (2020). Clustering leads to underestimation of numerosity, but crowding is not the cause. *Cognition*, *198*, 104195. https://doi.org/10.1016/j.cognition.2020.104195

Cicchini, G. M., Anobile, G., & Burr, D. C. (2016). Spontaneous perception of numerosity in humans. *Nature Communications*, *7*(1), 12536–12536. https://doi.org/10.1038/ncomms12536

Clark, A. (2015). *Pillow (PIL Fork) Documentation*. readthedocs. https://buildmedia.readthedocs.org/media/pdf/pillow/latest/pillow.pdf

Cordes, S., & Brannon, E. M. (2009). Crossing the Divide: Infants Discriminate Small From Large Numerosities. *Developmental Psychology*, *45*(6), 1583–1594. https://doi.org/10.1037/a0015666

Cordes, S., Gelman, R., Gallistel, C. R., & Whalen, J. (2001). Variability signatures distinguish verbal from nonverbal counting for both large and small numbers. *Psychonomic Bulletin & Review*, *8*(4), 698–707. https://doi.org/10.3758/BF03196206

Cousins, J. B., & Ginsburg, N. (1983). Subjective Correlation and the Regular-Random Numerosity Illusion. *The Journal of General Psychology*, *108*(1), 3–10. https://doi.org/10.1080/00221309.1983.9711472

Dakin, S. C., Tibber, M. S., Greenwood, J. A., Kingdom, F. A. A., & Morgan, M. J. (2011). A common visual metric for approximate number and density. *Proceedings of the National Academy of Sciences of the United States of America*, *108*(49), 19552–19557. https://doi.org/10.1073/pnas.1113195108

de Hevia, M. D., Izard, V., Coubart, A., Spelke, E. S., & Streri, A. (2014). Representations of space, time, and number in neonates. *Proceedings of the National Academy of Sciences - PNAS*, *111*(13), 4809–4813. https://doi.org/10.1073/pnas.1323628111

De Marco, D., & Cutini, S. (2020). Introducing CUSTOM: A customized, ultraprecise, standardization-oriented, multipurpose algorithm for generating nonsymbolic number stimuli. *Behavior Research Methods*, *52*(4), 1528–1537. https://doi.org/10.3758/s13428-019-01332-z

Dehaene, S. (1992). Varieties of Numerical Abilities. *Cognition: International Journal of Cognitive Science*, *44*(1–2), 1–42. https://doi.org/10.1016/0010-0277(92)90049-N

Dehaene, S. (2003). The neural basis of the Weber–Fechner law: A logarithmic mental number line. *Trends in Cognitive Sciences*, *7*(4), 145–147. https://doi.org/10.1016/S1364-6613(03)00055-X

Dehaene, S. (2011). *The Number Sense: How the Mind Creates Mathematics, Revised and Updated Edition* (Updated Edition). Oxford University Press.

Dehaene, S., Bossini, S., & Giraux, P. (1993). The Mental Representation of Parity and Number Magnitude. *Journal of Experimental Psychology. General*, *122*(3), 371–396. https://doi.org/10.1037/0096-3445.122.3.371

Ditz, H. M. & Andreas Nieder. (2015). Neurons selective to the number of visual items in the corvid songbird endbrain. *Proceedings of the National Academy of Sciences - PNAS*, *112*(25), 7827–7832. https://doi.org/10.1073/pnas.1504245112

Edelsbrunner, H. (1993). The union of balls and its dual shape. *Computational Geometry*, 218–231. https://doi.org/10.1145/160985.161139

Eger, E., Michel, V., Thirion, B., Amadon, A., Dehaene, S., & Kleinschmidt, A. (2009). Deciphering Cortical Number Coding from Human Brain Activity Patterns. *Current Biology*, *19*(19), 1608–1615. https://doi.org/10.1016/j.cub.2009.08.047

Feigenson, L., Dehaene, S., & Spelke, E. (2004). Core systems of number. *Trends in Cognitive Sciences*, *8*(7), 307–314. https://doi.org/10.1016/j.tics.2004.05.002

Ferrigno, S., & Cantlon, J. F. (2017). Evolutionary Constraints on the Emergence of Human Mathematical Concepts. *Evolution of Nervous Systems*, *3*, 511–521.

Field, A. (2009). *Discovering Statistics Using SPSS* (3rd ed.). SAGE Publications.

Franconeri, S. L., Bemis, D. K., & Alvarez, G. A. (2009). Number estimation relies on a set of segmented objects. *Cognition*, *113*(1), 1–13. https://doi.org/10.1016/j.cognition.2009.07.002

Frith, C. D., & Frith, U. (1972). The solitaire illusion: An illusion of numerosity. *Perception & Psychophysics*, *11*(6), 409–410. https://doi.org/10.3758/BF03206279

Fu, D., Han, L., Liu, L., Gao, Q., & Feng, Z. (2015). An Efficient Centralized Algorithm for Connected Dominating Set on Wireless Networks. *Procedia Computer Science*, *56*, 162–167. https://doi.org/10.1016/j.procs.2015.07.190

Gebuis, T., Cohen Kadosh, R., & Gevers, W. (2016). Sensory-integration system rather than approximate number system underlies numerosity processing: A critical review. *Acta Psychologica*, *171*, 17–35. https://doi.org/10.1016/j.actpsy.2016.09.003

Gebuis, T., & Reynvoet, B. (2011). Generating nonsymbolic number stimuli. *Behavior Research Methods*, *43*(4), 981–986. https://doi.org/10.3758/s13428-011-0097-5

Ginsburg, N. (1976). Effect of Item Arrangement on Perceived Numerosity: Randomness vs Regularity. *Perceptual and Motor Skills*, *43*(2), 663–668. https://doi.org/10.2466/pms.1976.43.2.663

Ginsburg, N. (1980). The regular-random numerosity illusion: Rectangular patterns. *The Journal of General Psychology*, *103*(2d Half), 211–216. https://doi.org/10.1080/00221309.1980.9921000

Ginsburg, N. (1991). Numerosity Estimation as a Function of Stimulus Organization. *Perception*, *20*(5), 681–686. https://doi.org/10.1068/p200681

Ginsburg, N., & Goldstein, S. R. (1987). Measurement of Visual Cluster. *The American Journal of Psychology*, *100*(2), 193–203. https://doi.org/10.2307/1422403

Ginsburg, N., & Nicholls, A. (1988). Perceived Numerosity as a Function of Item Size. *Perceptual and Motor Skills*, *67*(2), 656–658. https://doi.org/10.2466/pms.1988.67.2.656

Green, P., MacLeod, C. J., & Nakagawa, S. (2016). SIMR: an R package for power analysis of generalized linear mixed models by simulation. *Methods in Ecology and Evolution*, *7*(4), 493–498. https://doi.org/10.1111/2041-210X.12504

Guest, M., Zito, M., Hulleman, J., & Bertamini, M. (2022). On the usefulness of graph-theoretic properties in the study of perceived numerosity. *Behavior Research Methods*. https://doi.org/10.3758/s13428-021-01733-z

Guillon, Q., Afzali, M. H., Rogé, B., Baduel, S., Kruck, J., & Hadjikhani, N. (2015). The Importance of Networking in Autism Gaze Analysis. *PLoS ONE*, *10*(10), 1–14. https://doi.org/10.1371/journal.pone.0141191

Hagberg, A., Swart, P., & Chult, D. (2008). Exploring Network Structure, Dynamics, and Function Using NetworkX. In *Proceedings of the 7th Python in Science Conference*.

Hagbery, A., Schult, D., & Swart, P. (2008). Exploring network structure, dynamics, and function using networkx. *Proceedings of the 7th Python in Science Conference*.

Halberda, J., & Feigenson, L. (2008). Developmental Change in the Acuity of the 'Number Sense': The Approximate Number System in 3-, 4-, 5-, and 6-Year-Olds and Adults. *Developmental Psychology*, *44*(5), 1457–1465. https://doi.org/10.1037/a0012682

Hurewitz, F., Gelman, R., & Schnitzer, B. (2006). Sometimes area counts more than number. *Proceedings of the National Academy of Sciences - PNAS*, *103*(51), 19599–19604. https://doi.org/10.1073/pnas.0609485103

Im, H. Y., Zhong, S., & Halberda, J. (2016). Grouping by proximity and the visual impression of approximate number in random dot arrays. *Vision Research*, *126*, 291–307. https://doi.org/10.1016/j.visres.2015.08.013

Inglis, M., & Gilmore, C. (2013). Sampling from the mental number line: How are approximate number system representations formed? *Cognition*, *129*(1), 63–69. https://doi.org/10.1016/j.cognition.2013.06.003

Jordan, K. E., & Brannon, E. M. (2006). Weber's Law influences numerical representations in rhesus macaques (Macaca mulatta). *Animal Cognition*, *9*(3), 159–172. https://doi.org/10.1007/s10071-006-0017-8

Kahn, J. D., Linial, N., Nisan, N., & Saks, M. E. (1989). On the cover time of random walks on graphs. *Journal of Theoretical Probability*, *2*(1), 121–128. https://doi.org/10.1007/bf01048274

Karunakaran, R. K., Manuel, S., & Narayanan, S. (2017). Spreading Information in Complex Networks: An Overview and Some Modified Methods. *Graph Theory - Advanced Algorithms and Applications*. https://doi.org/10.5772/intechopen.69204

Kaufman, E. L., Lord, M. W., Reese, T. W., & Volkmann, J. (1949). The Discrimination of Visual Number. *The American Journal of Psychology*, *62*(4), 498–525. JSTOR. https://doi.org/10.2307/1418556

Kumle, L., Võ, M. L.-H., & Draschkow, D. (2021). Estimating power in (generalized) linear mixed models: An open introduction and tutorial in R. *Behavior Research Methods*, *53*(6), 2528–2543. https://doi.org/10.3758/s13428-021-01546-0

Lei, Q., & Reeves, A. (2018). When the weaker conquer: A contrast-dependent illusion of visual numerosity. *Journal of Vision (Charlottesville, Va.)*, *18*(7), 8–8. https://doi.org/10.1167/18.7.8

Looke, M., Marinelli, L., Eatherington, C. J., Agrillo, C., & Mongillo, P. (2020). Do Domestic Dogs (Canis lupus familiaris) Perceive Numerosity Illusions? *ANIMALS*, *10*(12). https://doi.org/10.3390/ani10122304

Luce, R. D., & Perry, A. D. (1949). A method of matrix analysis of group structure. *Psychometrika*, *14*(2), 95–116. https://doi.org/10.1007/BF02289146

MacDonald, S. E., & Agnes, M. M. (1999). Orangutan (Pongo pygmaeus abelii) Spatial Memory and Behavior in a Foraging Task. *Journal of Comparative Psychology (1983)*, *113*(2), 213–217. https://doi.org/10.1037/0735-7036.113.2.213

Miletto Petrazzini, M. E., Parrish, A. E., Beran, M. J., & Agrillo, C. (2018). Exploring the solitaire illusion in guppies (Poecilia reticulata). *Journal of Comparative Psychology*, *132*(1), 48–57. https://doi.org/10.1037/com0000092

Mitchell, K. G., Calton, J. L., Threlkeld, R. C., & Schachtman, T. R. (1996). Attenuation and reacquisition of foraging behavior in a patchy environment. *Behavioural Processes*, *36*(3), 239–252. https://doi.org/10.1016/0376-6357(95)00034-8

Moyer, R. S., & Landaeuer, T. K. (1967). Time required for Judgements of Numerical Inequality. *Nature*, *215*(5109), 1519–1520. https://doi.org/10.1038/2151519a0

Newman, M. E. J. (Mark E. J.). (2018). *Networks* (Second edition.). Oxford University Press.

Parrish, A. E., Agrillo, C., Perdue, B. M., & Beran, M. J. (2016). The elusive illusion: Do children (Homo sapiens) and capuchin monkeys (Cebus apella) see the Solitaire illusion? *Journal of Experimental Child Psychology*, *142*, 83–95. https://doi.org/10.1016/j.jecp.2015.09.021

Parrish, A. E., Beran, M. J., & Agrillo, C. (2019). Linear numerosity illusions in capuchin monkeys , and humans (Homo sapiens). *Animal Cognition*, *22*(5), 883. https://doi.org/10.1007/s10071-019-01288-9

Parrish, A. E., James, B. T., & Beran, M. J. (2017). Exploring Whether Nonhuman Primates Show a Bias to Overestimate Dense Quantities. *Journal of Comparative Psychology (1983)*, *131*(1), 59–68. https://doi.org/10.1037/com0000058

Paul, J. M., Reeve, R. A., & Forte, J. D. (2017). Taking a(c)count of eye movements: Multiple mechanisms underlie fixations during enumeration. *Journal of Vision*, *17*(3), 16–16. https://doi.org/10.1167/17.3.16

Paul, J. M., Reeve, R. A., & Forte, J. D. (2020). Enumeration strategy differences revealed by saccade-terminated eye tracking. *Cognition*, *198*, 104204. https://doi.org/10.1016/j.cognition.2020.104204

Pearson, J. M., Hayden, B. Y., Raghavachari, S., & Platt, M. L. (2009). Neurons in Posterior Cingulate Cortex Signal Exploratory Decisions in a Dynamic Multioption Choice Task. *Current Biology*, *19*(18), 1532–1537. https://doi.org/10.1016/j.cub.2009.07.048

Pecunioso, A., & Agrillo, C. (2021). Do professional musicians perceive numerosity illusions differently? *Psychology of Music*, *49*(3), 631–648. https://doi.org/10.1177/0305735619888804

Pecunioso, A., Miletto Petrazzini, M. E., & Agrillo, C. (2020). Anisotropy of perceived numerosity: Evidence for a horizontal–vertical numerosity illusion. *Acta Psychologica*, *205*, 103053. https://doi.org/10.1016/j.actpsy.2020.103053

Peirce, J. W. (2009). Generating stimuli for neuroscience using PsychoPy. *Frontiers in Neuroinformatics*, *2*. https://doi.org/10.3389/neuro.11.010.2008

Pelli, D. G., & Tillman, K. A. (2008). The uncrowded window of object recognition. *Nature Neuroscience*, *11*(10), 1129–1135. https://doi.org/10.1038/nn.2187

Piazza, M., Izard, V., Pinel, P., Le Bihan, D., & Dehaene, S. (2004). Tuning Curves for Approximate Numerosity in the Human Intraparietal Sulcus. *Neuron (Cambridge, Mass.)*, *44*(3), 547–555. https://doi.org/10.1016/j.neuron.2004.10.014

Ponzo, M. (1928). Urteilstauschungen über Mengen. [Misperceptions of quantities]. *Archiv Far Die Gesamte Psychologie*, *65*, 129–162.

Poom, L., Lindskog, M., Winman, A., & van den Berg, R. (2019). Grouping effects in numerosity perception under prolonged viewing conditions. *PloS One*, *14*(2), e0207502–e0207502. https://doi.org/10.1371/journal.pone.0207502

R Core Team. (2021). *R: A Language and Environment for Statistical Computing*. R Foundation for Statistical Computing. https://www.R-project.org/

Ross, J., & Burr, D. C. (2010). Vision senses number directly. *Journal of Vision (Charlottesville, Va.)*, *10*(2), 10.1-8. https://doi.org/10.1167/10.2.10

Rugani, R., Cavazzana, A., Vallortigara, G., & Regolin, L. (2013). One, two, three, four, or is there something more? Numerical discrimination in day-old domestic chicks. *Animal Cognition*, *16*(4), 557–564. https://doi.org/10.1007/s10071-012-0593-8

Rugani, R., Fontanari, L., Simoni, E., Regolin, L., & Vallortigara, G. (2009). Arithmetic in newborn chicks. *Proceedings of the Royal Society. B, Biological Sciences*, *276*(1666), 2451–2460. https://doi.org/10.1098/rspb.2009.0044

Rugani, R., Vallortigara, G., Priftis, K., & Regolin, L. (2015). Animal cognition. Number-space mapping in the newborn chick resembles humans' mental number line. *Science (New York, N.Y.)*, *347*(6221), 534–536. https://doi.org/10.1126/science.aaa1379

Sadria, M., Karimi, S., & Layton, A. T. (2019). Network centrality analysis of eye-gaze data in autism spectrum disorder. *Computers in Biology and Medicine*, *111*. https://doi.org/10.1016/j.compbiomed.2019.103332

Salti, M., Katzin, N., Katzin, D., Leibovich, T., & Henik, A. (2017). One tamed at a time: A new approach for controlling continuous magnitudes in numerical comparison tasks. *Behavior Research Methods*, *49*(3), 1120–1127. https://doi.org/10.3758/s13428-016-0772-7

Sayim, B., Westheimer, G., & Herzog, M. H. (2010). Gestalt Factors Modulate Basic Spatial Vision. *Psychological Science*, *21*(5), 641–644. https://doi.org/10.1177/0956797610368811

Scarf, D., Hayne, H., & Colombo, M. (2011). Pigeons on Par with Primates in Numerical Competence. *Science (American Association for the Advancement of Science)*, *334*(6063), 1664–1664. https://doi.org/10.1126/science.1213357

Schielzeth, H., Dingemanse, N. J., Nakagawa, S., Westneat, D. F., Allegue, H., Teplitsky, C., Réale, D., Dochtermann, N. A., Garamszegi, L. Z., Araya-Ajoy, Y. G., & Sutherland, C. (2020). Robustness of linear mixed-effects models to violations of distributional assumptions. *Methods in Ecology and Evolution*, *11*(9), 1141–1152. https://doi.org/10.1111/2041-210X.13434

Shuman, M., & Spelke, E. (2006). Area and element size bias numerosity perception. *Journal of Vision*, *6*(6), 777–777. https://doi.org/10.1167/6.6.777

Stephens, D. W., & Krebs, J. R. (John R.). (1986). *Foraging Theory David W. Stephens and John R. Krebs.* Princeton University Press. https://doi.org/10.1515/9780691206790

Stevens, J. R., Wood, J. N., & Hauser, M. D. (2007). When quantity trumps number: Discrimination experiments in cotton-top tamarins (Saguinus oedipus) and common marmosets (Callithrix jacchus). *Animal Cognition*, *10*(4), 429–437. https://doi.org/10.1007/s10071-007-0081-8

Stoffel, M. A., Nakagawa, S., & Schielzeth, H. (2021). partR2: Partitioning R(2) in generalized linear mixed models. *PeerJ*, *9*, e11414. https://doi.org/10.7717/peerj.11414

Tibber, M. S., Greenwood, J. A., & Dakin, S. C. (2012). Number and density discrimination rely on a common metric: Similar psychophysical effects of size, contrast, and divided attention. *Journal of Vision (Charlottesville, Va.)*, *12*(6), 8–8. https://doi.org/10.1167/12.6.8

Tokita, M., & Ishiguchi, A. (2010). How might the discrepancy in the effects of perceptual variables on numerosity judgment be reconciled? *Attention, Perception & Psychophysics*, *72*(7), 1839–1853. https://doi.org/10.3758/APP.72.7.1839

Trick, L. m. (1, 3), & Pylyshyn, Z. w. (2). (1994). Why are small and large numbers enumerated differently? A limited-capacity preattentive stage in vision. *Psychological Review*, *101*(1), 80–102. https://doi.org/10.1037/0033-295X.101.1.80

Uller, C., Urquhart, C., Lewis, J., & Berntsen, M. (2013). Ten-Month-Old Infants' Reaching Choices for 'more': The Relationship between Inter-Stimulus Distance and Number. *Frontiers in Psychology*, *4*, 84–84. https://doi.org/10.3389/fpsyg.2013.00084

Vallortigara, G. (2017). An animal's sense of number. *The Nature and Development of Mathematics: Cross Disciplinary Perspectives on Cognition, Learning and Culture*, 43–65.

Valsecchi, M., Toscani, M., & Gegenfurtner, K. R. (2013). Perceived numerosity is reduced in peripheral vision. *Journal of Vision*, *13*(13), 7. https://doi.org/10.1167/13.13.7

van den Berg, R., Lindskog, M., Poom, L., & Winman, A. (2017). Recent Is More: A Negative Time-Order Effect in Nonsymbolic Numerical Judgment. *Journal of Experimental Psychology. Human Perception and Performance*, *43*(6), 1084–1097. https://doi.org/10.1037/xhp0000387

van Oeffelen, M. P., & Vos, P. G. (1983). An algorithm for pattern description on the level of relative proximity. *Pattern Recognition*, *16*(3), 341–348. https://doi.org/10.1016/0031-3203(83)90040-7

Vos, P. G., van Oeffelen, M. P., Tibosch, H. J., & Allik, J. (1988). Interactions between area and numerosity. *Psychological Research*, *50*(3), 148–154. https://doi.org/10.1007/BF00310175

Wasserman, S., & Faust, K. (1994). *Social network analysis: Methods and applications* (Sydney Jones Library Grove Wing Ground Floor 14). Cambridge University Press.

Watts, D. J., & Strogatz, S. H. (1998). Collective dynamics of `small-world' networks. *Nature*, *393*(6684), 440. https://doi.org/10.1038/30918

Weisberg, S., & Fox, J. (2011). *An R companion to applied regression / John Fox, Sanford Weisberg.* (2nd ed.). SAGE Publications.

Zimmermann, E., & Fink, G. R. (2016). Numerosity perception after size adaptation. *Scientific Reports*, *6*(1), 32810–32810. https://doi.org/10.1038/srep32810